ATOMIC PROCESSES IN STRONG LASER FIELDS

DEJAN B. MILOŠEVIĆ

Faculty of Science
Department of Physics
University of Sarajevo
Bosnia and Herzegovina

Attosecond Science Workshop, KITP, UCSB, August 16, 2006

- Laser-assisted vs. laser-induced processes
- Theory:

S-matrix formalism – Feynman’s path integral – Strong-field approximation – Quantum-orbit theory

- Examples
- ATI by few-cycle pulses
- Numerical simulations
- ATI of diatomic molecules

Collaboration

- B. Piraux, Ph. Antoine, A. de Bohan, UCL, LLN, Belgium (1995-1998)
- Fritz Ehlotzky, University of Innsbruck, Austria (1996-)
- Anthony Starace, The University of Nebraska, Lincoln, USA (1998-)
- Wilhelm Becker, Max-Born-Institute, Berlin (1999-):
  Alexander von Humboldt, Volkswagenstiftung
- Gerhard Paulus,Texas A&M University, MPI Garching (2000-)
- Dieter Bauer, MPI, Heilderberg (2004-)
- Misha Ivanov (Canada) NSERC
- Marc Vrakking (AMOLF, Amsterdam)

- Since 2000: Research group in Sarajevo

M.Sc.	Postgraduate students
Azra Gazibegović-Busuladžić	Elvedin Hasović
Aner Čerkić	Adnan Mašić
Senad Odžak	Aida Kramo
Mustafa Busuladžić	

- W. Becker, F. Grasbon, R. Kopold, D.B. Milošević, G.G. Paulus, and H. Walther
  Above-threshold ionization: from classical features to quantum effects
  Adv. At. Mol. Opt. Phys. 48, 35-98 (2002)
- D.B. Milošević and F. Ehlotzky
  Scattering and reaction processes in powerful laser fields
  Adv. At. Mol. Opt. Phys. 49, 373-532 (2003)
- D.B. Milošević, G.G. Paulus, D. Bauer, and W. Becker
  Above-threshold ionization by few-cycle pulses
  J. Phys. B 39, R203-R262 (2006)

ATOMIC PROCESSES IN A STRONG LASER FIELD

- **Laser-assisted processes**
- Electron-atom scattering (Weingartshofer et al. 1977)
- X-ray-atom scattering
- Electron-ion recombination

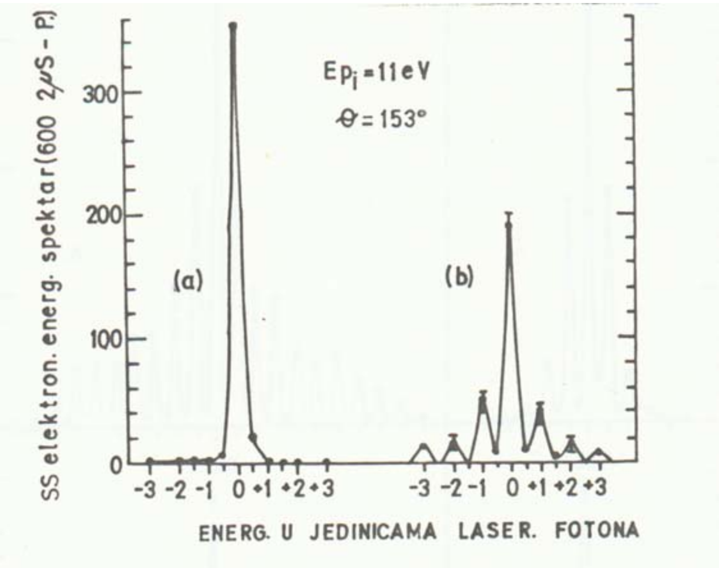

- **Laser-induced processes**
- Above-threshold ionization (ATI) (Agostini et al. 1979)
- Above-threshold detachment
- High-order harmonic generation

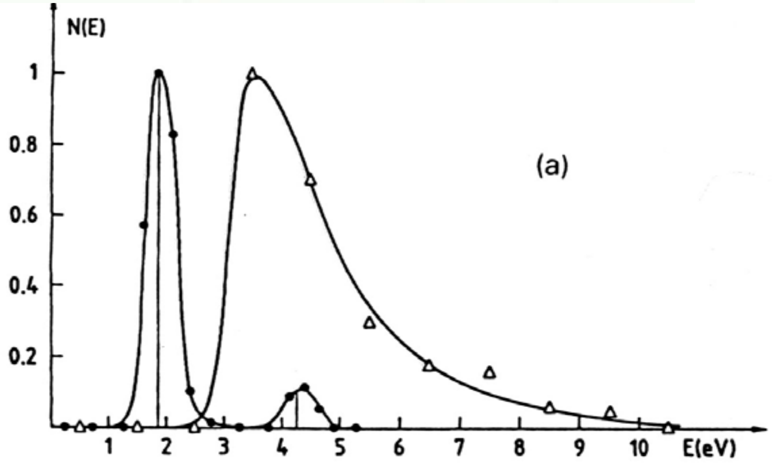

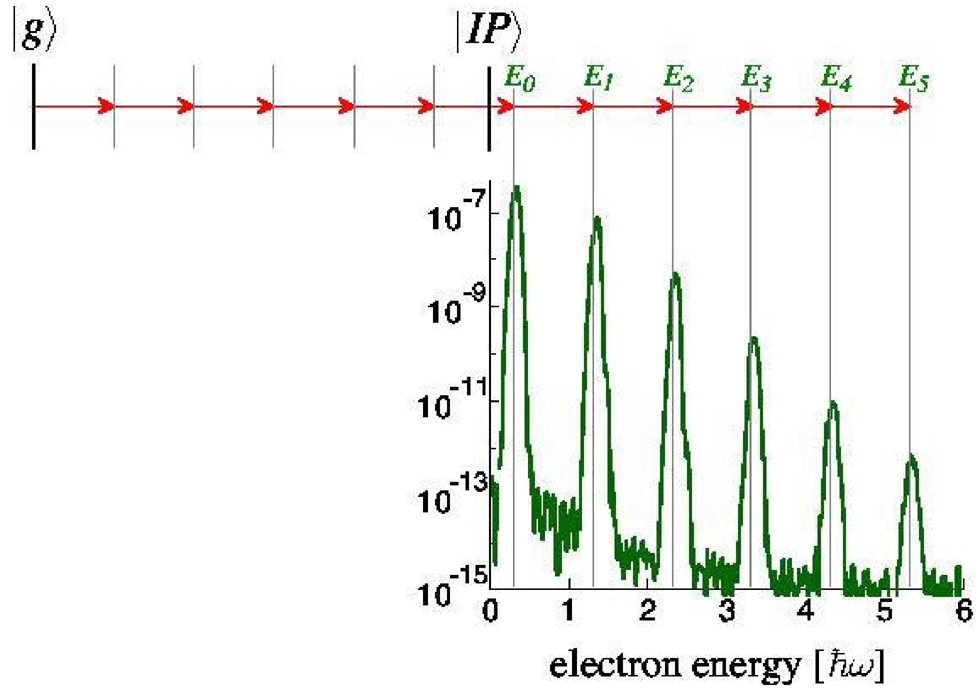

High-order ATI

(Paulus et al 1994)

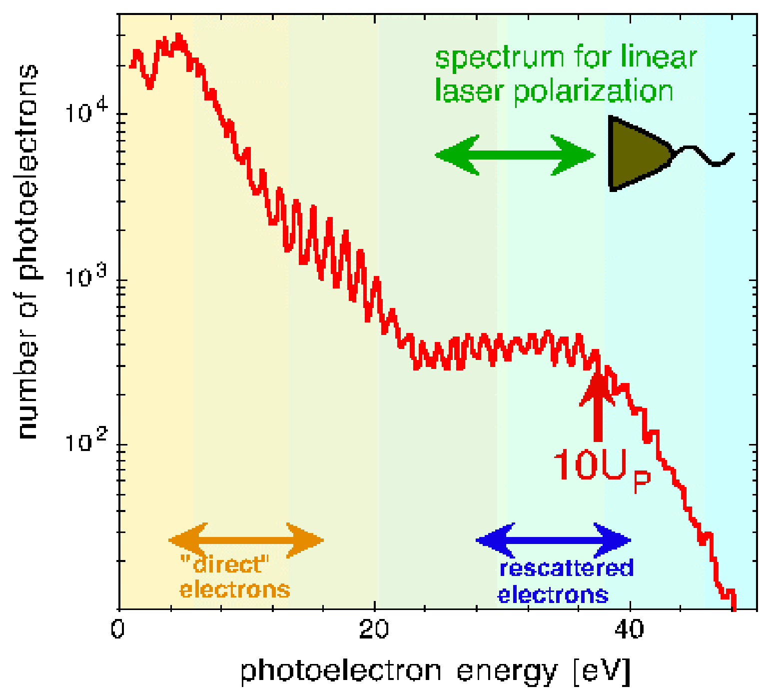

Strong Laser Field

High Harmonics

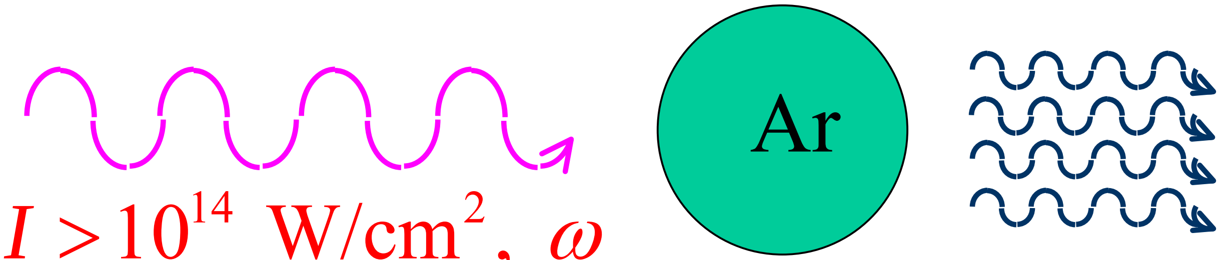

$I > 10^{14}$ W/cm^2, ω

$3\omega, 5\omega, 7\omega, \ldots$

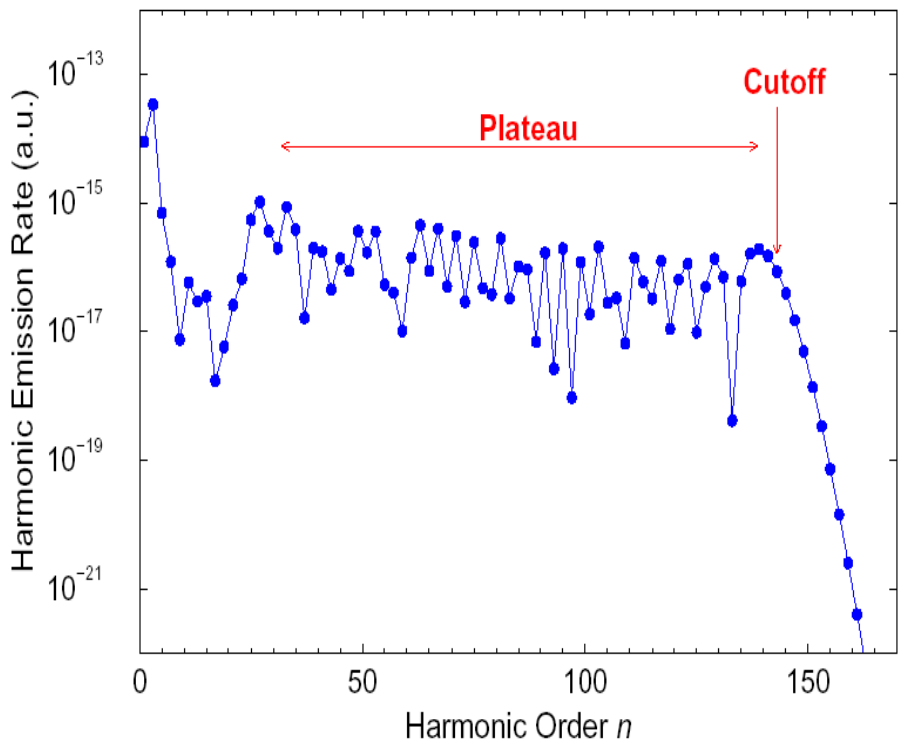

High-order harmonic generation (1987)

Three-step model

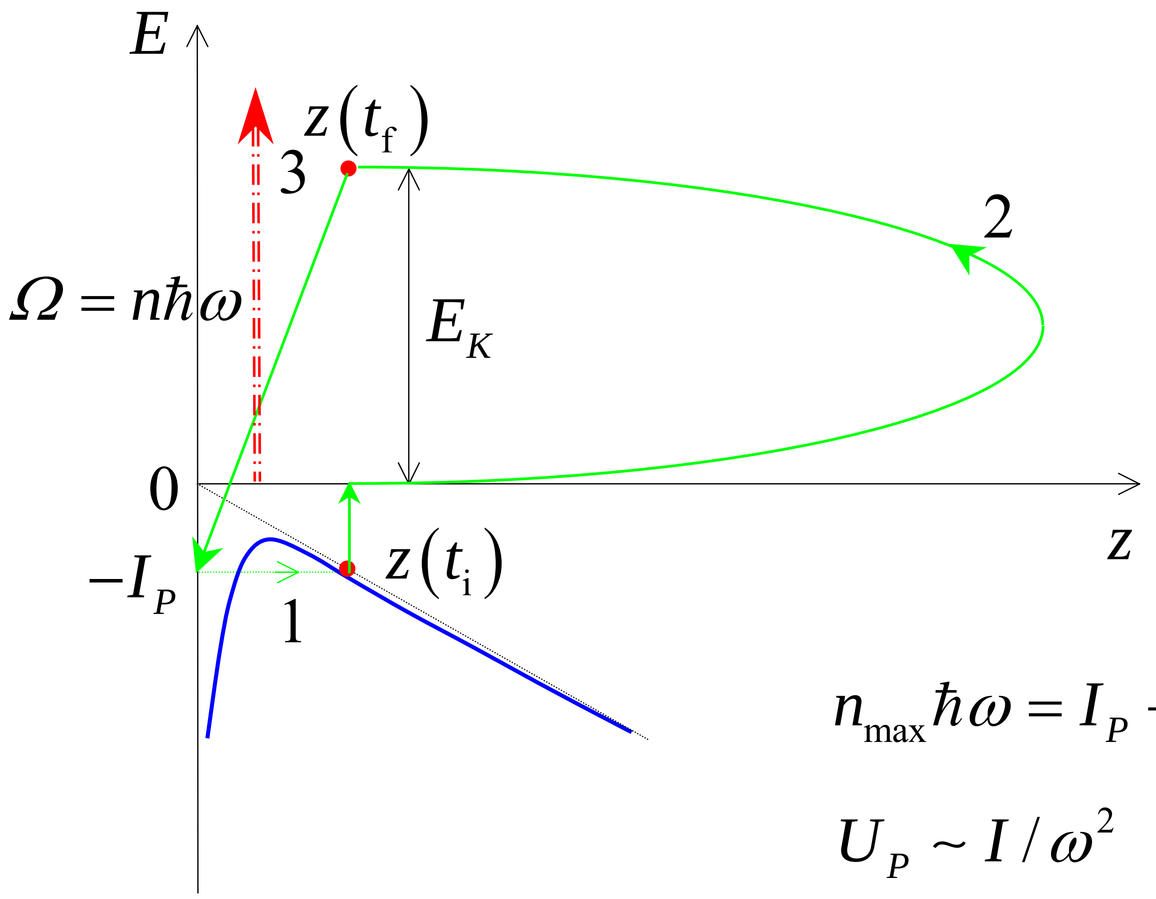

$$n_{max}\hbar\omega = I_P + 3.17U_P$$

$$U_P \sim I/\omega^2$$

X-ray – atom scattering

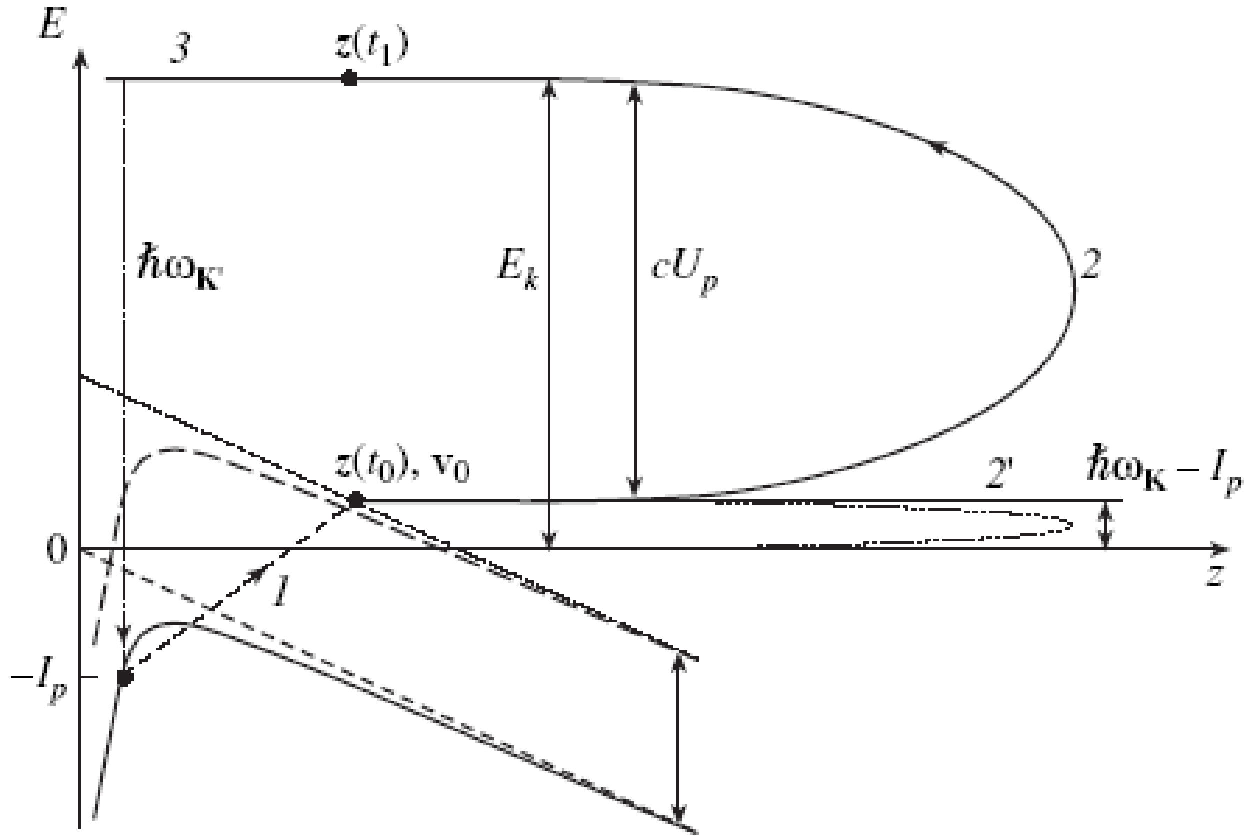

$$\hbar\omega_{\mathbf{K}'} = E_k + I_p = \hbar\omega_{\mathbf{K}} + n\hbar\omega$$

Fig. 2. Schematic of laser-assisted x-ray-atom scattering, presented similarly to Fig. 1. The combined atomic and electric field potential is shifted by the incident x-ray photon energy $\hbar\omega_{\mathbf{K}}$. The electron propagation step of the three-step model is denoted by *2* (*2'*) for the process in which a positive (negative) n plateau is formed.

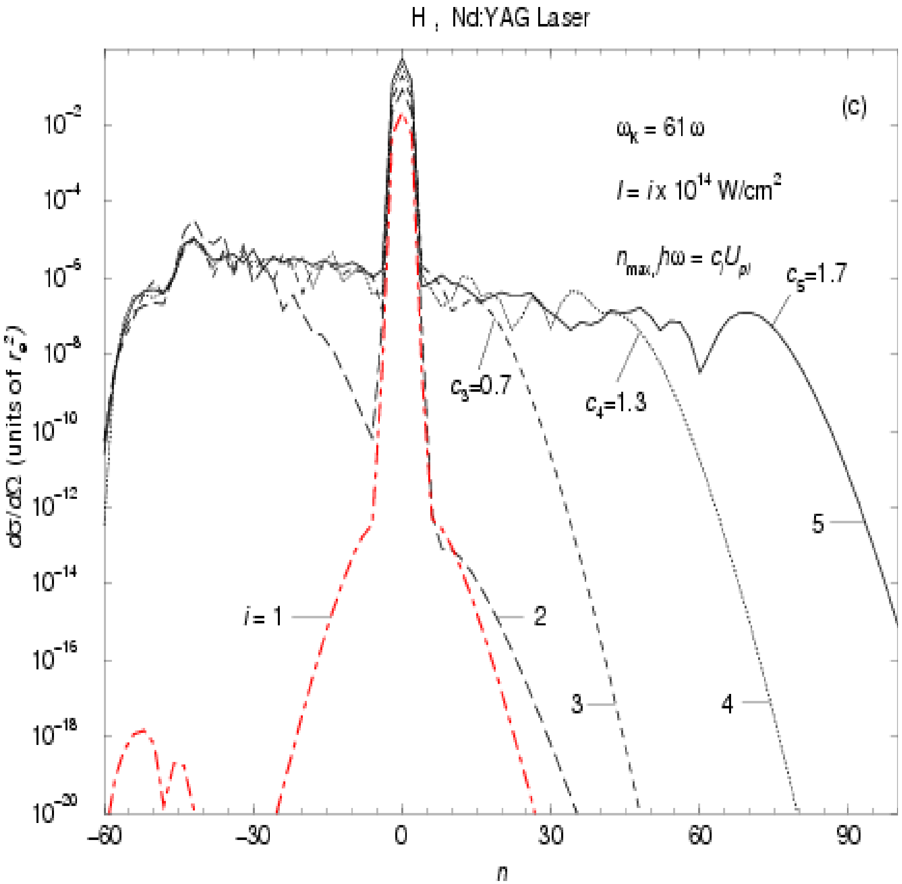

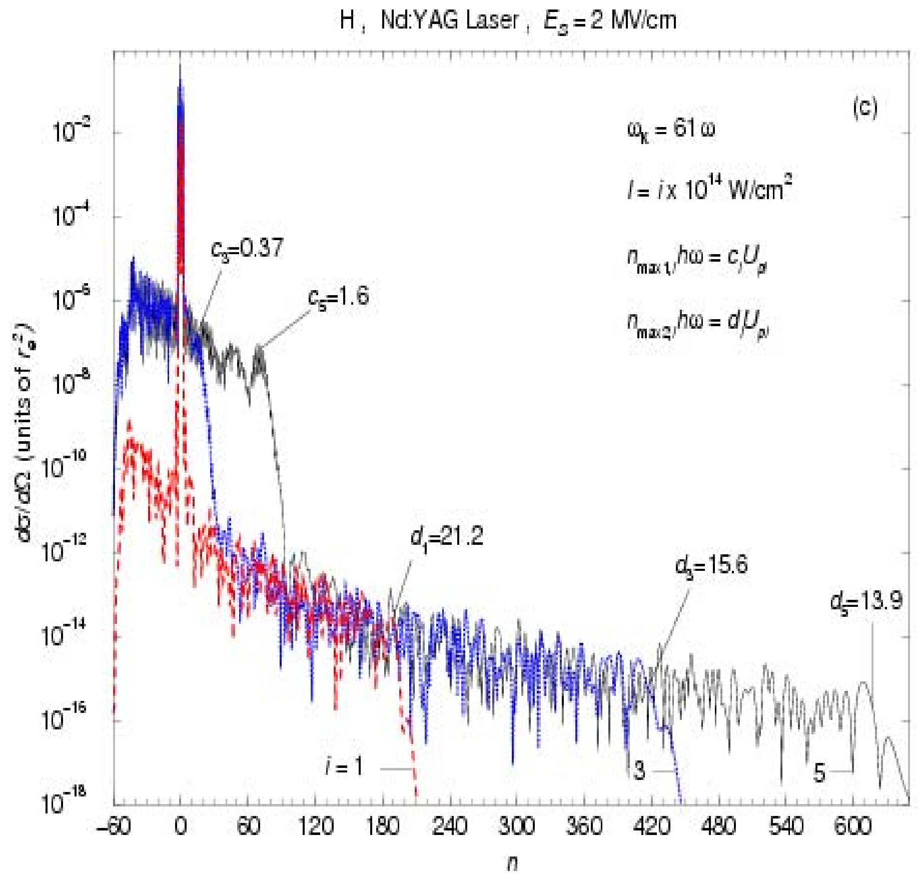

DBM, F. Ehlotzky, PRA 58, 2319 (1998); Adv. AMOP 49, 373 (2003)

DBM, A. Starace, PRL 81, 5097 (1998); PRA 60, 3943 (1999); Laser Phys. 10, 278 (2000)

Electron – atom scattering

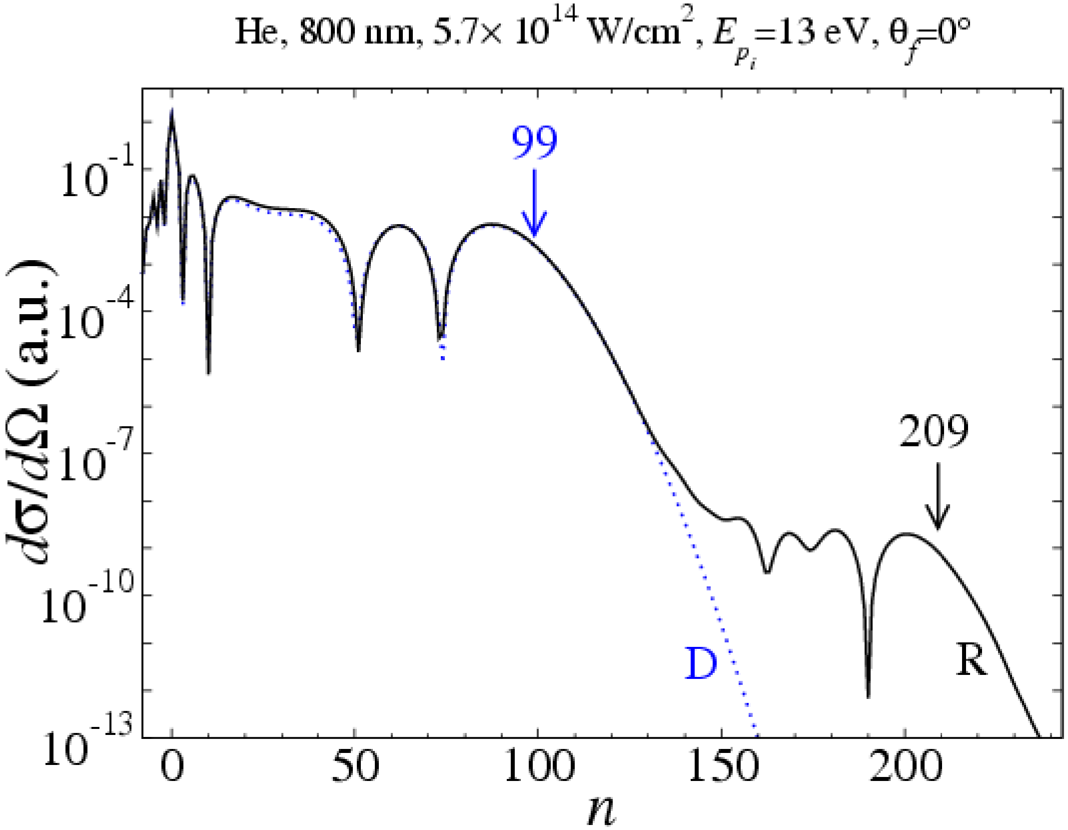

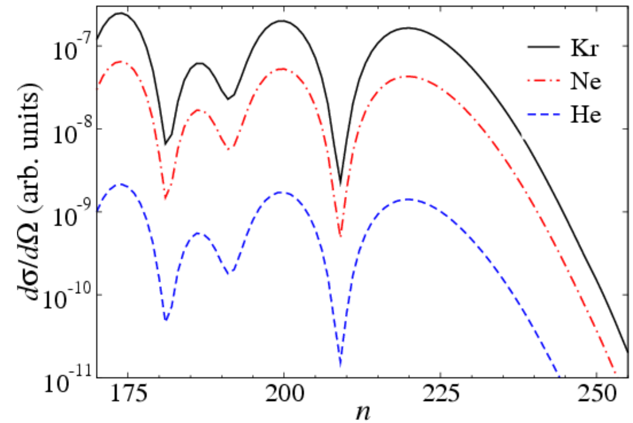

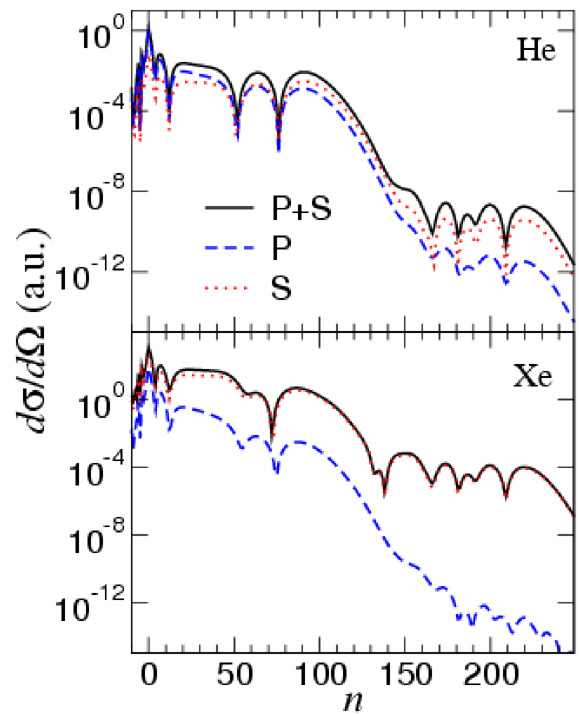

A. Čerkić, DBM, PRA 65, 053402 (2004)

Laser Phys. 15, 268 (2005)

Electron – ion recombination

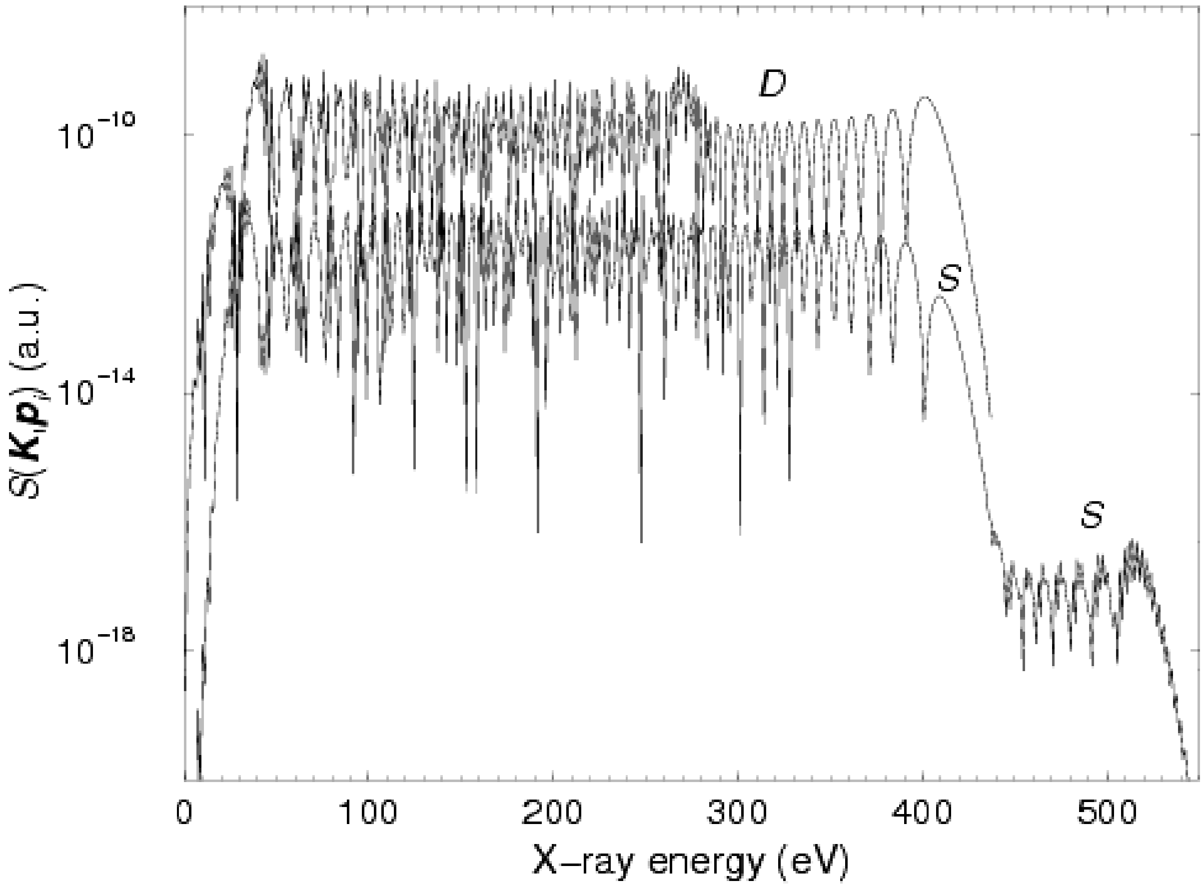

DBM and F. Ehlotzky, PRA 65, 042504 (2002)

JMO 50, 657 (2003); Adv. AMOP 49, 373 (2003)

The black box of S-matrix theory

$$M_{fi} = \lim_{t \to \infty,\, t' \to -\infty} \left\langle \psi_f(t) \middle| \hat{U}(t,t') \middle| \psi_i(t') \right\rangle$$

FEYNMAN's PATH INTEGRAL

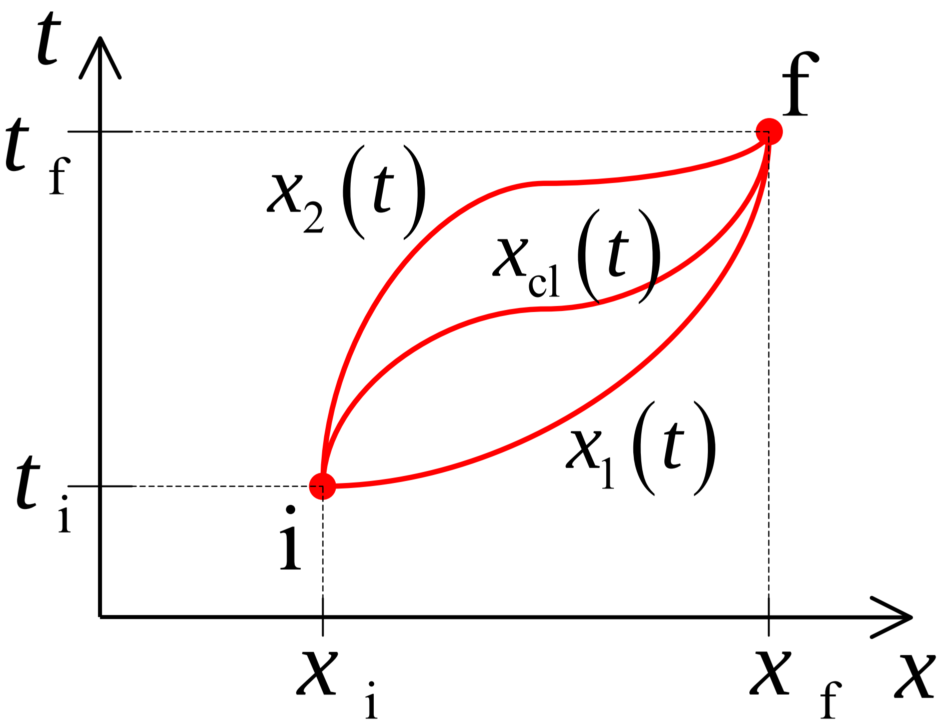

$$M_{fi} \propto \sum_{\substack{\text{all paths}\\ \text{from i to f}}} e^{iS[x(t)]/\hbar}$$

$$S = \int_{t_i}^{t_f} dt\, L\big(x(t), \dot{x}(t), t\big)$$

Classical limit: $S >> \hbar$, Hamilton principle: $\delta S = 0$

SFA (Strong Field Approximation) $\Rightarrow$

$$M_{\mathrm{fi}} \propto \int_{-\infty}^{\infty} dt_{\mathrm{f}} \int d^3\vec{p} \int_{-\infty}^{t_{\mathrm{f}}} dt_{\mathrm{i}} \langle \psi_{\mathrm{f}} | H_{\mathrm{f}} U_{\mathrm{fi}}^{(\mathrm{L})} H_{\mathrm{i}} | \psi_{\mathrm{i}} \rangle \mathrm{e}^{iS(t_{\mathrm{i}}, t_{\mathrm{f}}; \vec{p})/\hbar}$$

SPM (Saddle Point Method) $\Rightarrow$

$$\frac{\partial S}{\partial t_{\mathrm{i}}} = \frac{\partial S}{\partial \vec{p}} = \frac{\partial S}{\partial t_{\mathrm{f}}} = 0 \quad \Rightarrow \quad t_{\mathrm{i}}, t_{\mathrm{f}}, \vec{p} \in \mathbb{C}$$

$$M_{\mathrm{fi}} \propto \sum_{\substack{\text{relevant} \\ \text{paths:} \\ \text{quantum} \\ \text{orbits } s}} A_{\mathrm{fis}} \exp\left(i\Phi_{\mathrm{fis}}\right)$$

$$\left.\begin{array}{l} -I_P:\ \text{HHG, }\underline{\text{HATI}}\text{, HATD, NSDI} \\ \omega_{\vec{K}} - I_P:\ \text{XSCA} \\ \tfrac{1}{2}\left[\vec{p}_{\mathrm{i}} + \vec{A}(t_{\mathrm{i}})\right]^2:\ \text{LAR, LAS} \end{array}\right\} = \tfrac{1}{2}\left[\vec{p} + \vec{A}(t_{\mathrm{i}})\right]^2 \qquad (I)$$

$$(t_{\mathrm{f}} - t_{\mathrm{i}})\,\vec{p} = \int_{t_{\mathrm{i}}}^{t_{\mathrm{f}}} \vec{A}(\tau)\,d\tau \iff \vec{r}(t_{\mathrm{f}}) = \vec{r}(t_{\mathrm{i}}) \qquad (II)$$

$$\tfrac{1}{2}\left[\vec{p} + \vec{A}(t_{\mathrm{f}})\right]^2 = \left\{\begin{array}{l} X - I_P:\ \text{HHG}(n\omega),\ \text{LAR}(\omega_{\vec{K}}),\ \text{XSCA}(\omega_{\vec{K}'}) \\ \tfrac{1}{2}\left[\vec{p}_{\mathrm{f}} + \vec{A}(t_{\mathrm{f}})\right]^2:\ \underline{\text{HATI}}\text{, LAS} \\ \tfrac{1}{2}\sum_{j=1,2}\left[\vec{p}_{\mathrm{f}j} + \vec{A}(t_{\mathrm{f}})\right]^2 + I_{P2}:\ \text{NSDI} \end{array}\right. \qquad (III)$$

S-th QUANTUM ORBIT:

$$\vec{r}_{ns}(t_{\mathrm{R}}) = (t_{\mathrm{R}} - t_{\mathrm{is}})\,\vec{p}_s + \int_{t_{\mathrm{is}}}^{t_{\mathrm{R}}} d\tau \vec{A}(\tau) \quad (\mathrm{Re}\,t_{\mathrm{is}} \le t_{\mathrm{R}} \le \mathrm{Re}\,t_{\mathrm{fs}})$$

$$\vec{r}_s(t_{\mathrm{R}}) = (t_{\mathrm{R}} - t_{\mathrm{fs}})\,\vec{p}_{\mathrm{f}} + \int_{t_{\mathrm{fs}}}^{t_{\mathrm{R}}} d\tau \vec{A}(\tau) \quad (t_{\mathrm{R}} \ge \mathrm{Re}\,t_{\mathrm{fs}})\ (\mathrm{HATI})$$

t_R – real time $\Rightarrow$ Quantum orbits depart from the “exit of the tunnel”

$\vec{r}(t_{\mathrm{i}}) = \vec{r}(t_{\mathrm{f}}) = \vec{0}$ and $t_{\mathrm{f}} \approx$ real $\Rightarrow$ Orbits return almost exactly to the origin

$\mathrm{Re}\,\vec{r}_{ns}(t_{\mathrm{R}})$

DBM *etal*, J. Mod. Opt. 53, 125 (2006)

Quantum orbits for elliptical polarization: Experiment vs. theory

$\xi = 0.36$

xenon at $0.77 \times 10^{14} W cm^{-2}$

The plateau becomes a staircase

The shortest orbits are not always the dominant orbits

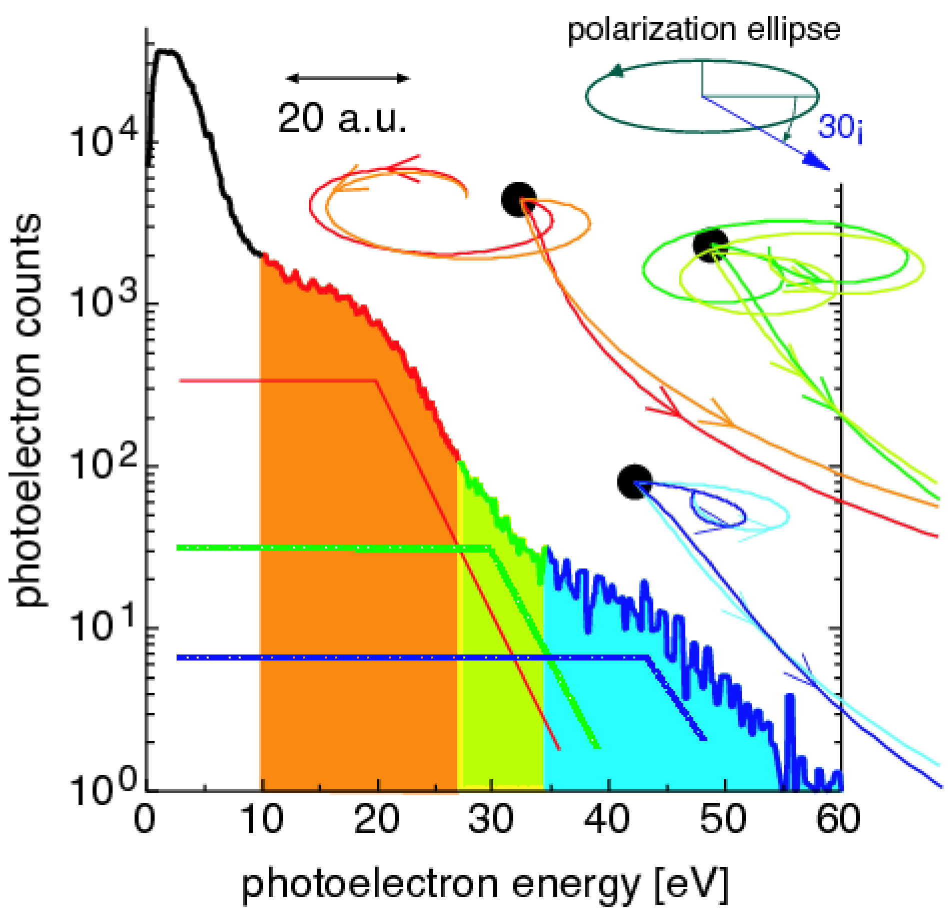

Salieres, Carre, Le Deroff, Grasbon, Paulus, Walther, Kopold, Becker, Milosevic, Sanpera, Lewenstein, Science 292, 902 (2001)

- High-order atomic processes in strong fields can be explained using SFA and QO theory
- Quantum orbits are superposed in the fashion of Feynman's path integral
- QO can be complex to account for the tunneling nature of the initial step of the process
- Fast calculations
  - Usually, only very few orbits need to be considered
  - If solutions are found for one set of parameters then the solutions for arbitrary parameters can be obtained by analytical continuation
- Future: application of quantum orbits to more complex strong-field processes, inclusion of the Coulomb effects, …
- Examples →

Bicircular field

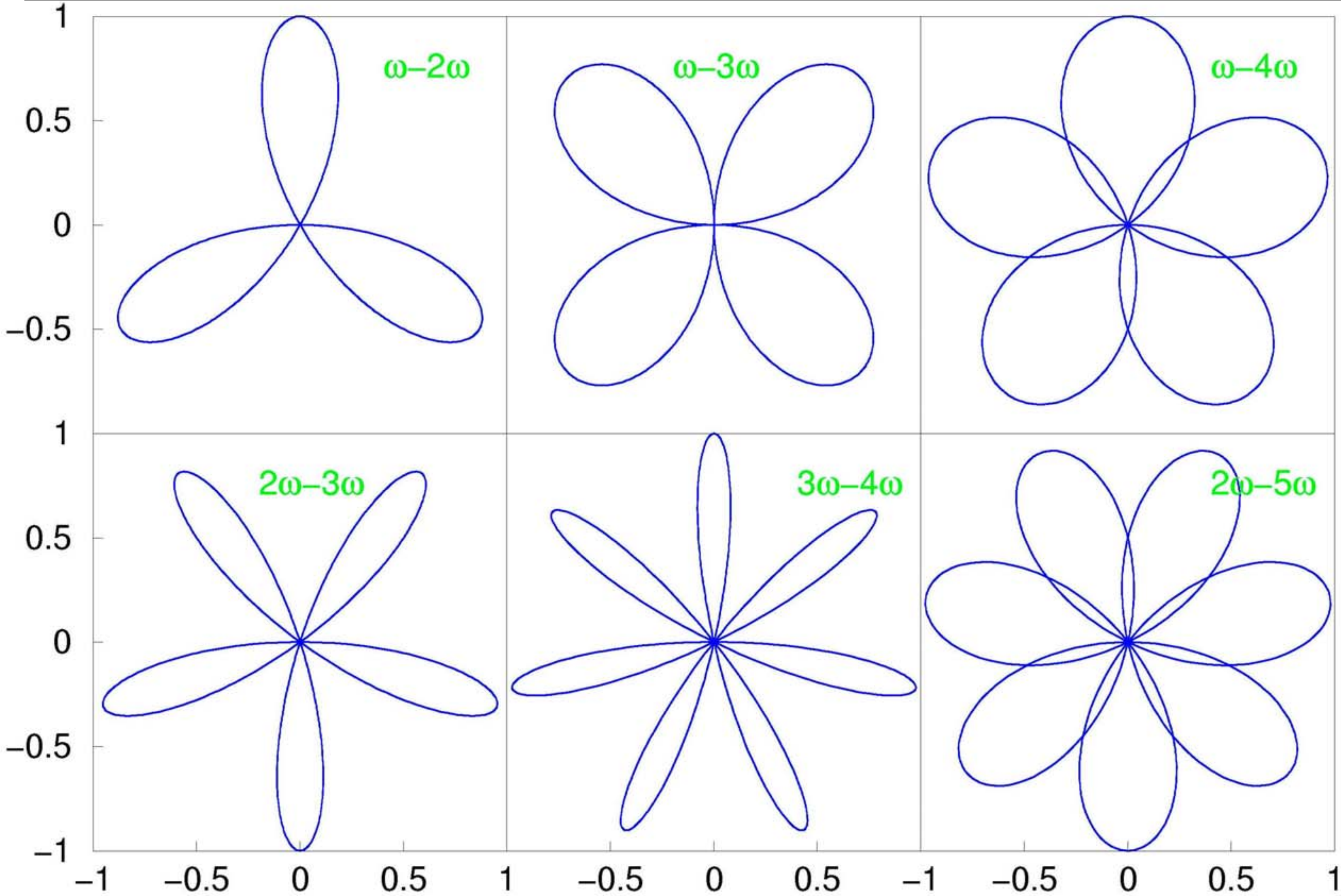

$$\vec{E}(t)=\frac{i}{2}\left(E_1\vec{e}_+e^{-ir\omega t}+E_2\vec{e}_-e^{-is\omega t}\right)+\text{c.c.},\ \vec{e}_\pm=\left(\hat{\vec{x}}\pm i\hat{\vec{y}}\right)/\sqrt{2}$$

Bicircular field

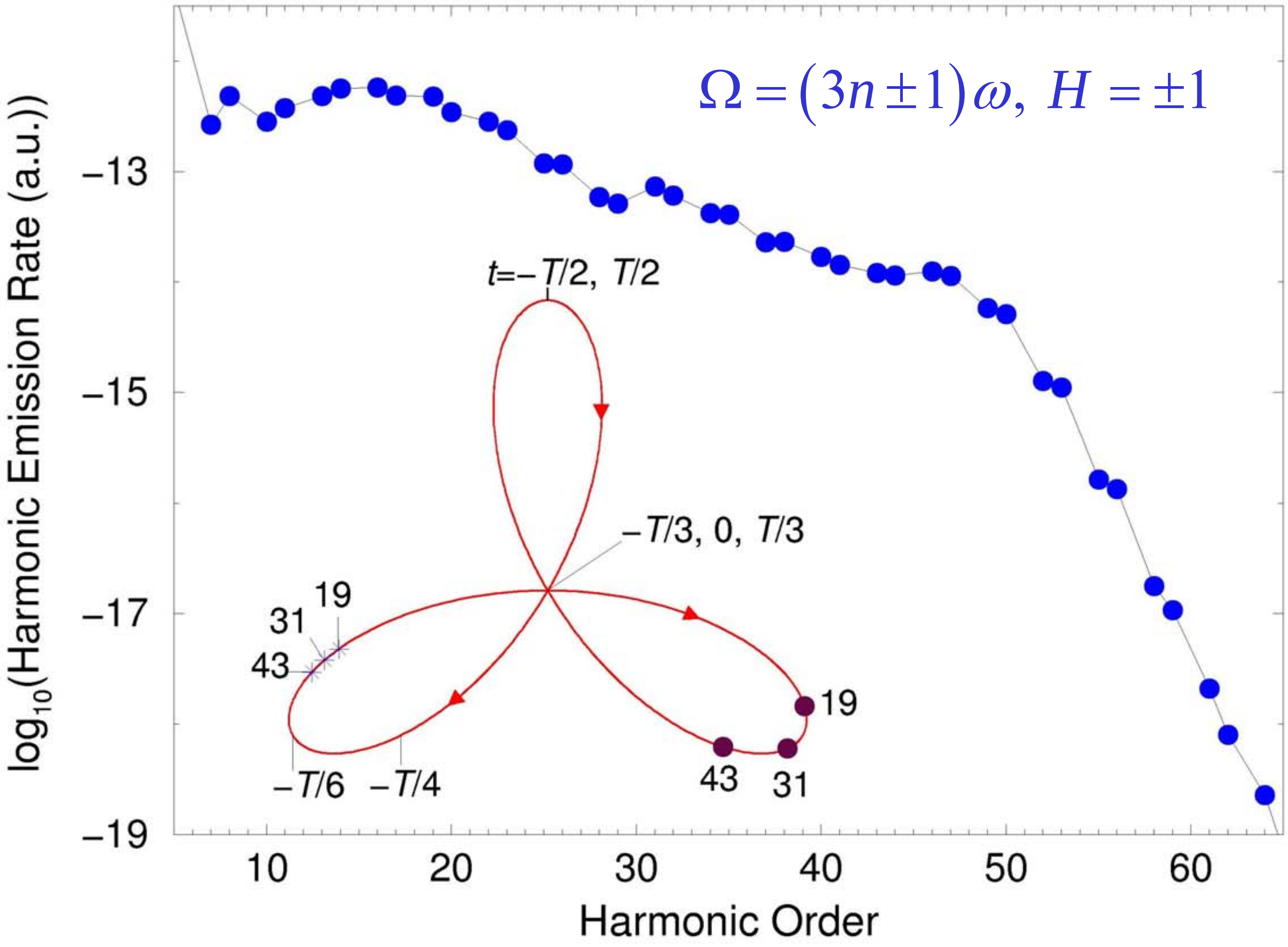

$$\vec{E}(t) = \frac{i}{2}\left(E_1 \vec{e}_+ e^{-i\omega t} + E_2 \vec{e}_- e^{-i2\omega t}\right) + \text{c.c.},\ \vec{e}_\pm = \left(\hat{\vec{x}} \pm i\hat{\vec{y}}\right)/\sqrt{2}$$

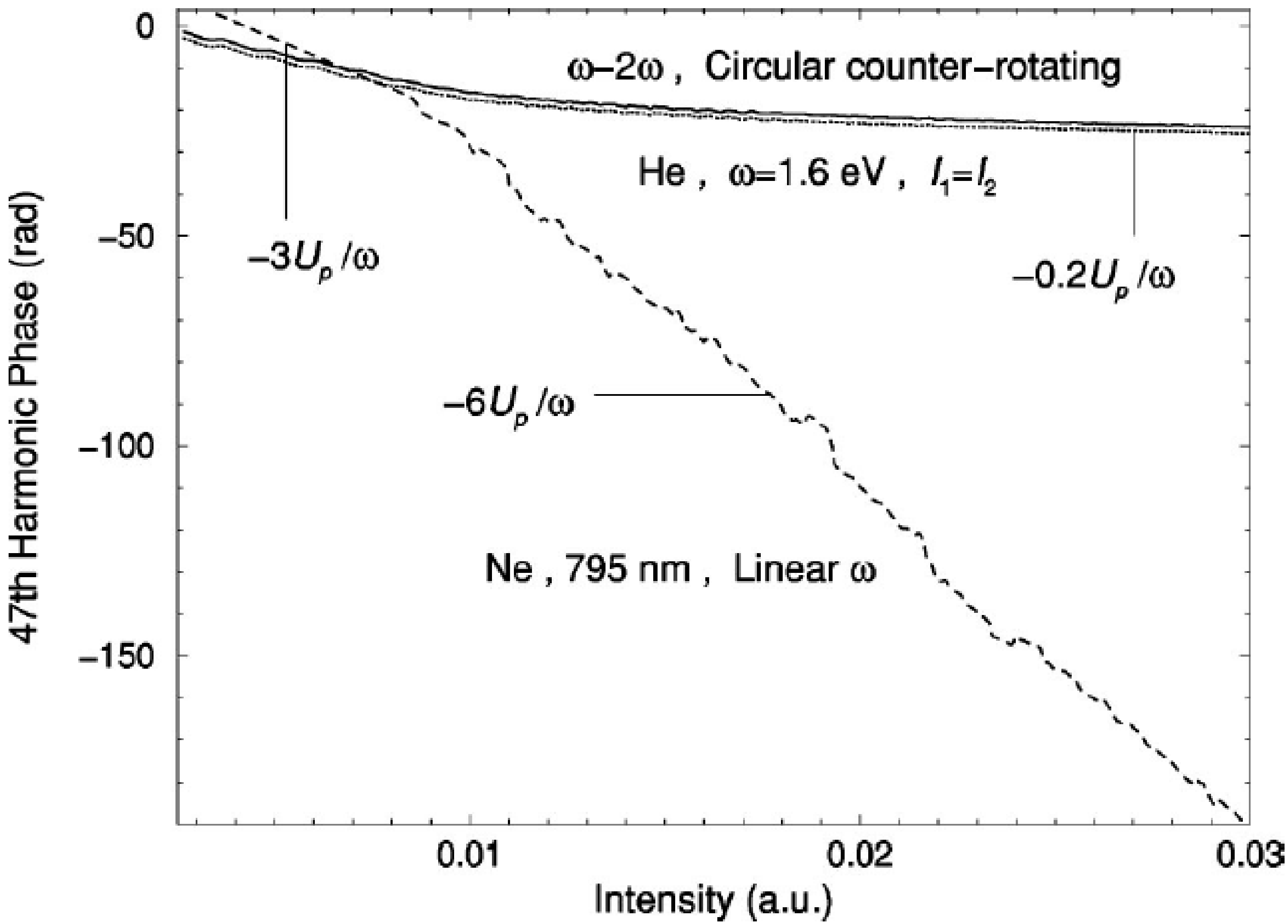

ω−2ω , Circular counter−rotating
He , ω=1.6 eV , I_1=I_2
−3U_p/ω
−0.2U_p/ω
−6U_p/ω
Ne , 795 nm , Linear ω
47th Harmonic Phase (rad)
Intensity (a.u.)
0
−50
−100
−150
0.01
0.02
0.03

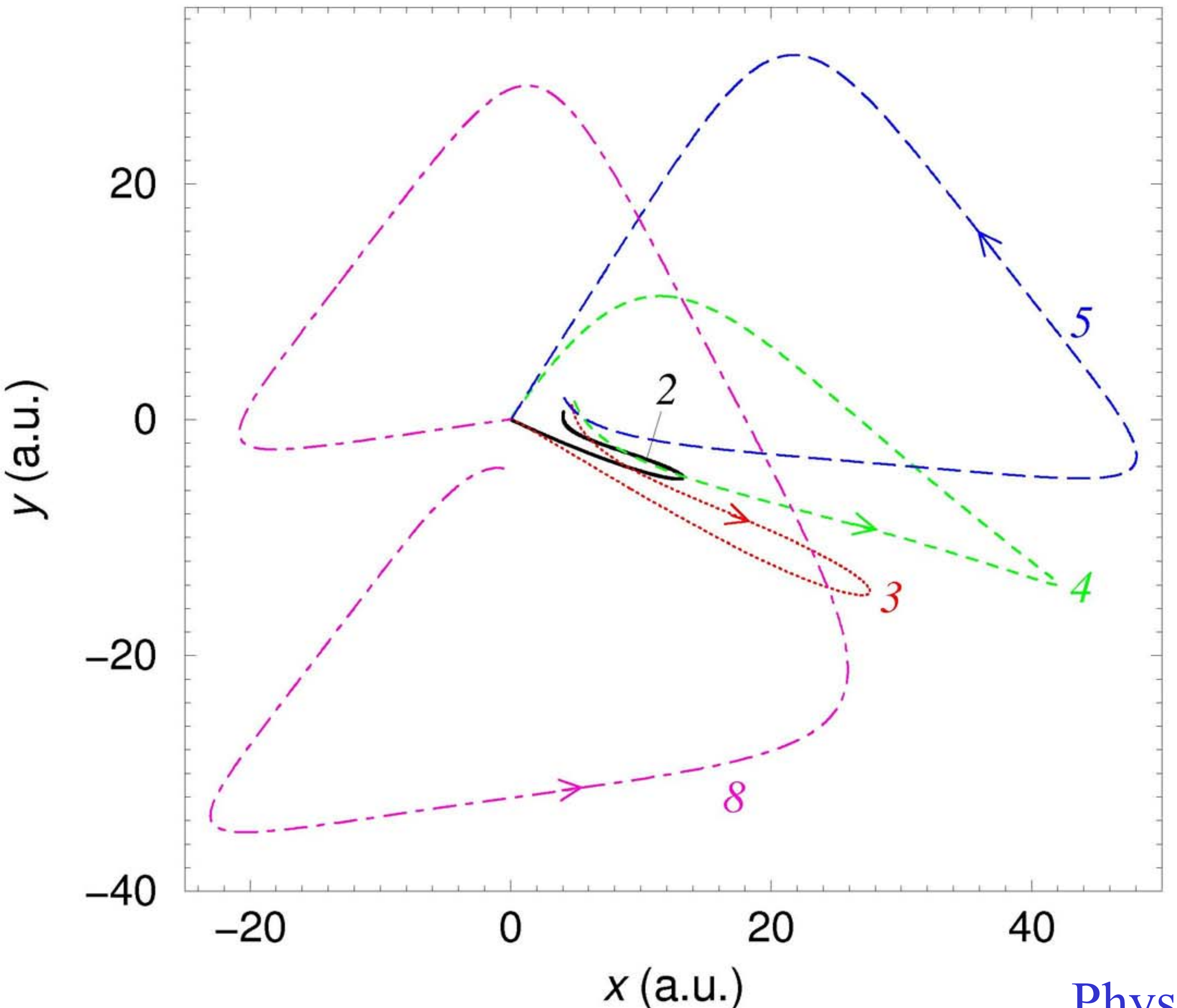

Phys. Rev. A **61**, 063403 (2000)

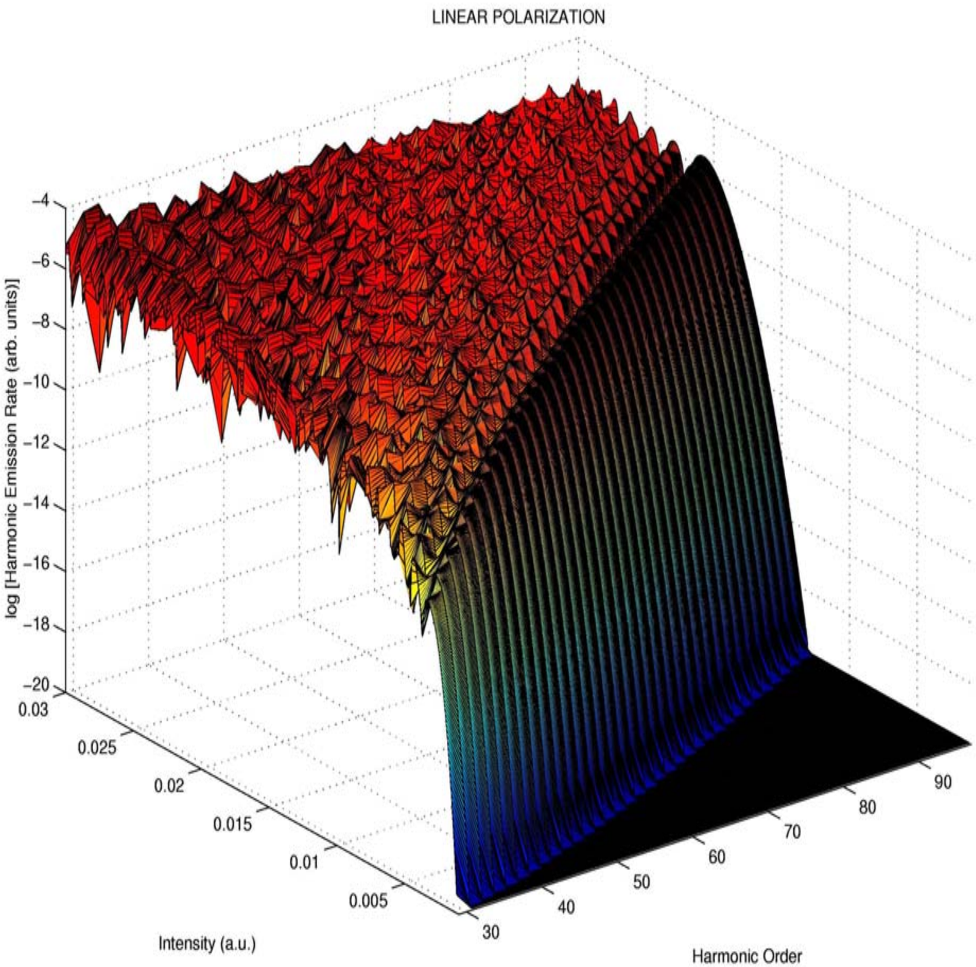
LINEAR POLARIZATION
log [Harmonic Emission Rate (arb. units)]
-4
-6
-8
-10
-12
-14
-16
-18
-20
0.03
0.025
0.02
0.015
0.01
0.005
Intensity (a.u.)
30
40
50
60
70
80
90
Harmonic Order

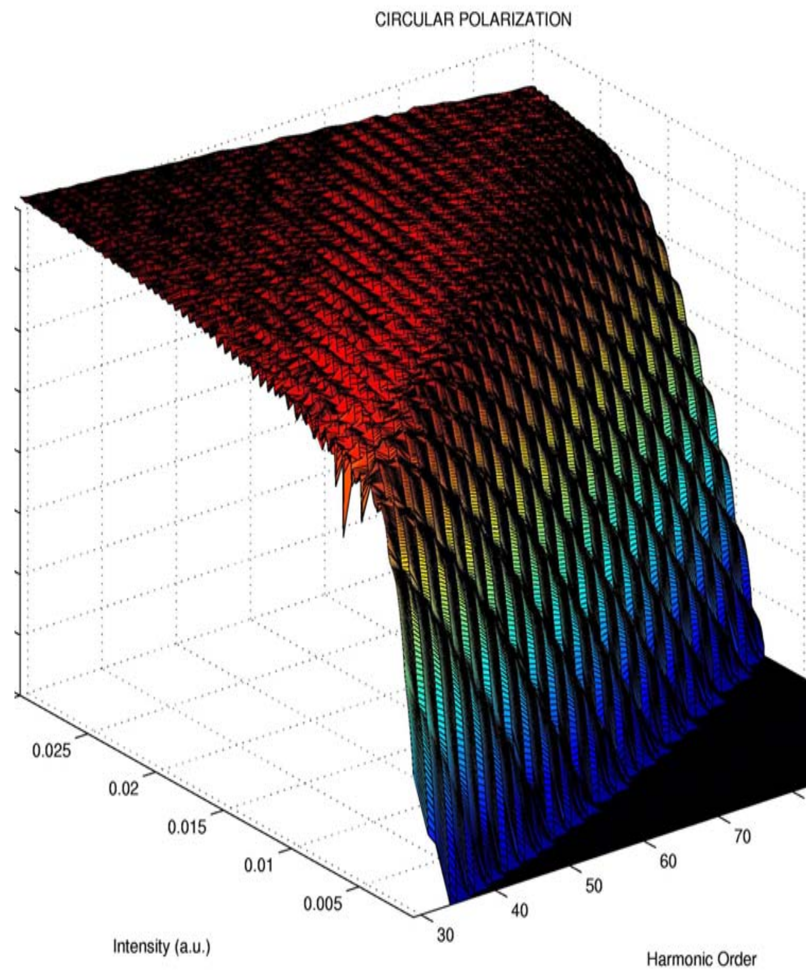
CIRCULAR POLARIZATION
0.025
0.02
0.015
0.01
0.005
Intensity (a.u.)
30
40
50
60
70
Harmonic Order

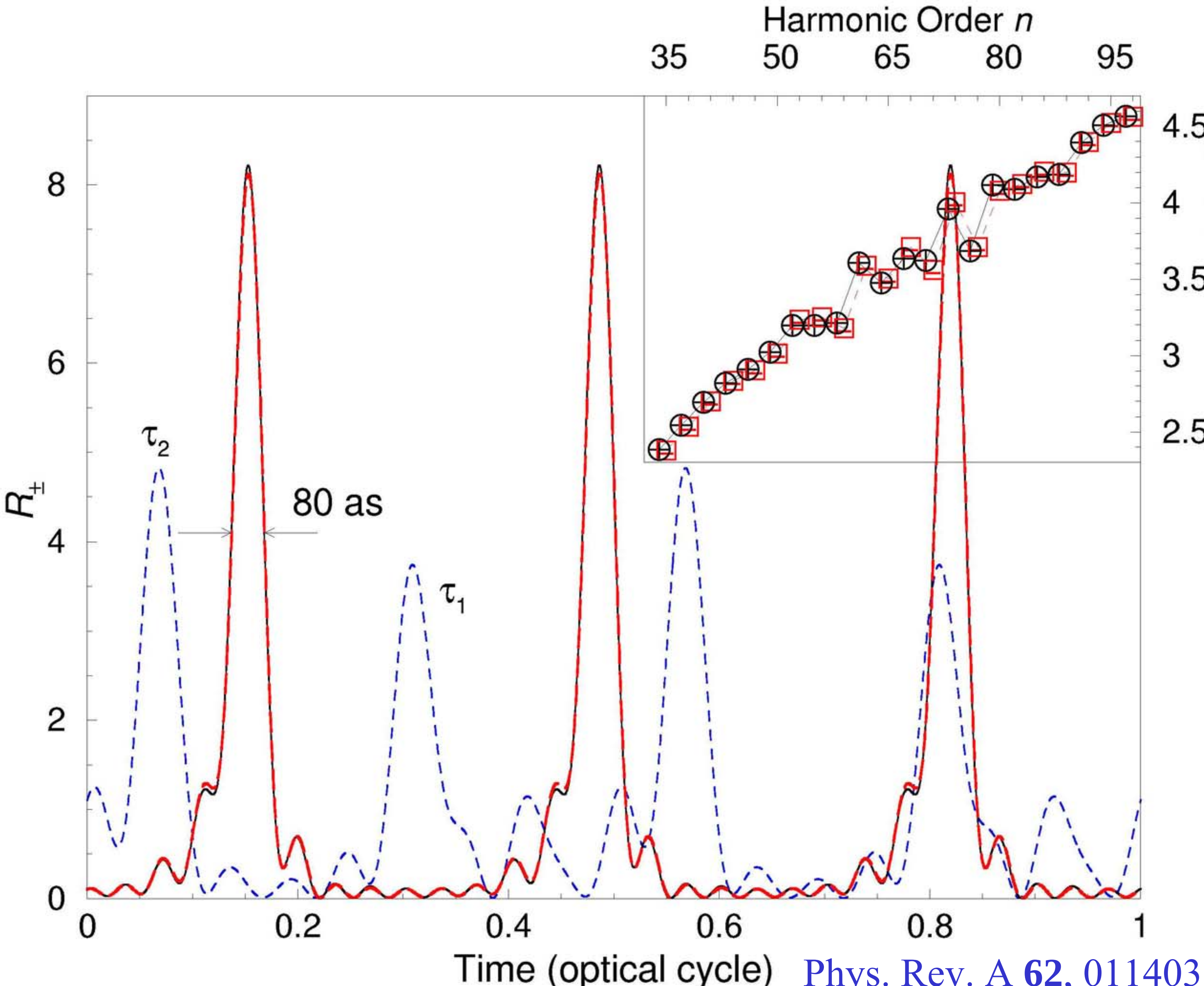

Phys. Rev. A **62**, 011403(R) (2000)

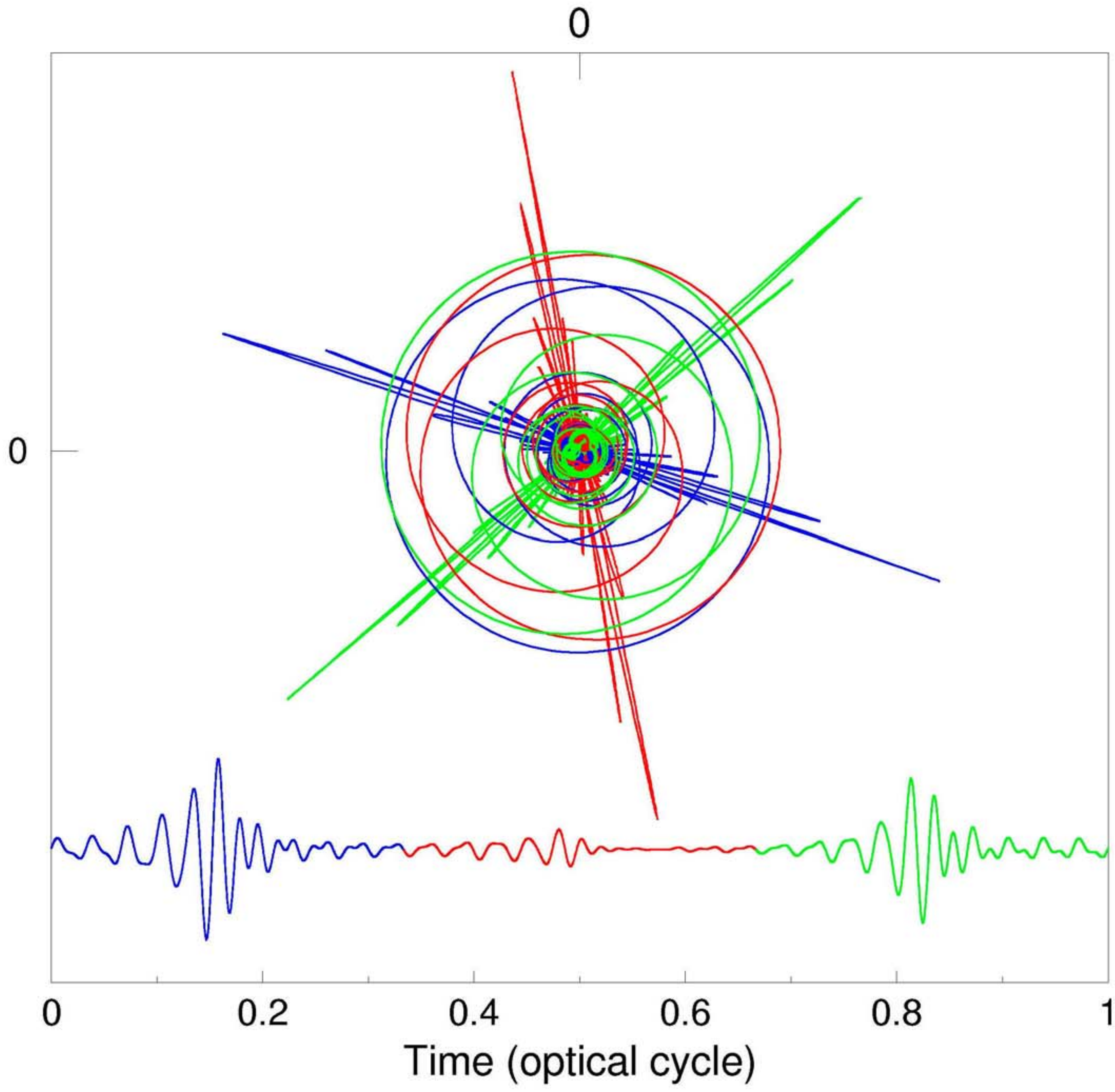

0
0
0
0.2
0.4
0.6
0.8
1
Time (optical cycle)

Stereo-ATI experiment

$\varphi = 0^\circ$

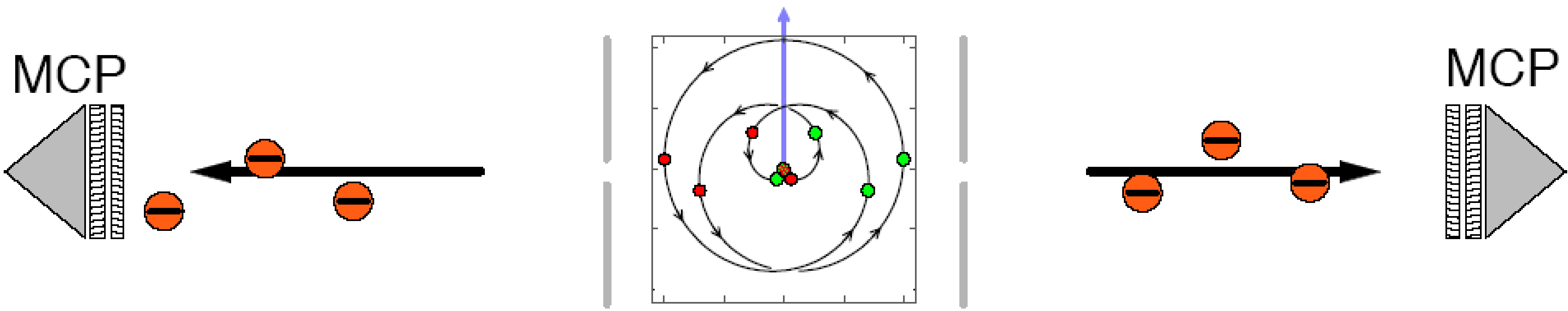

$\varphi = 90^\circ$

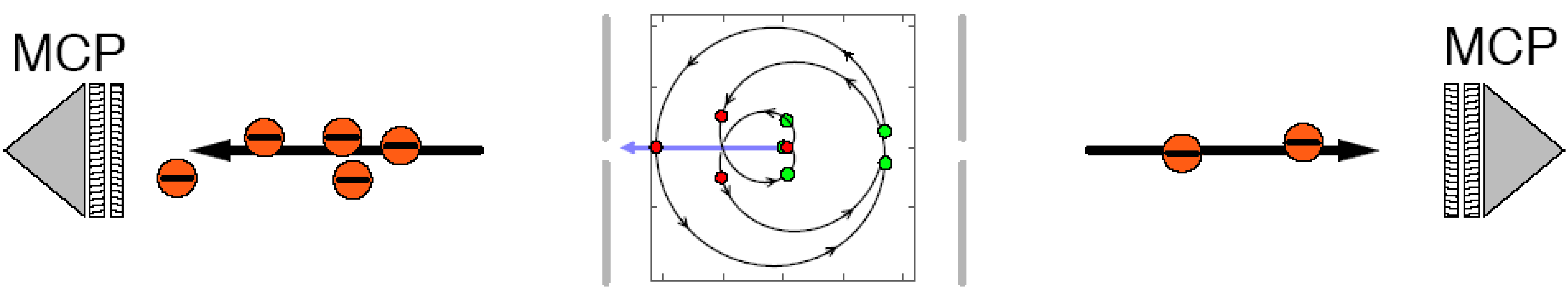

Stereo-ATI experiment: Correlation technique

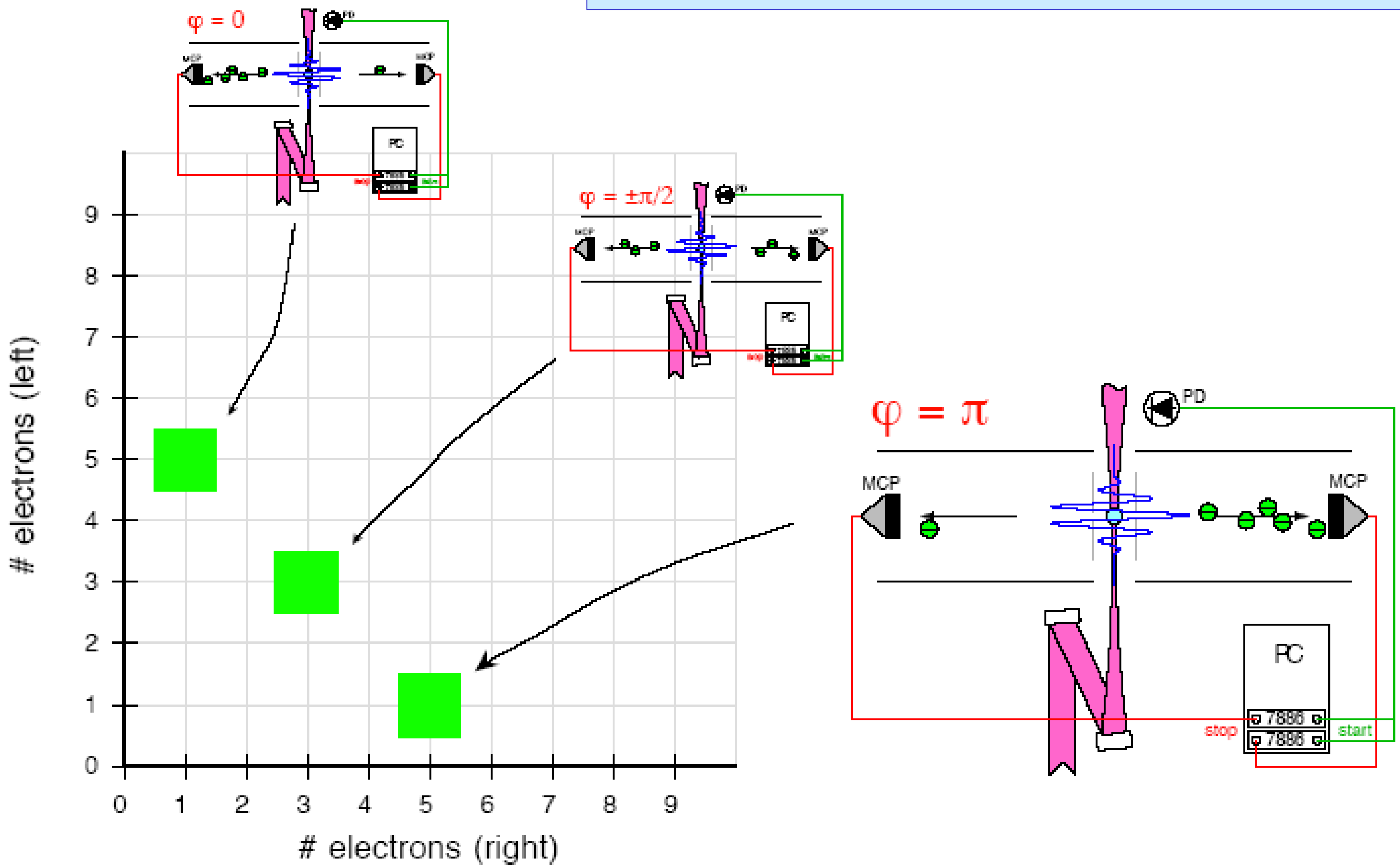

Stereo-ATI experiment: Experiment vs. theory

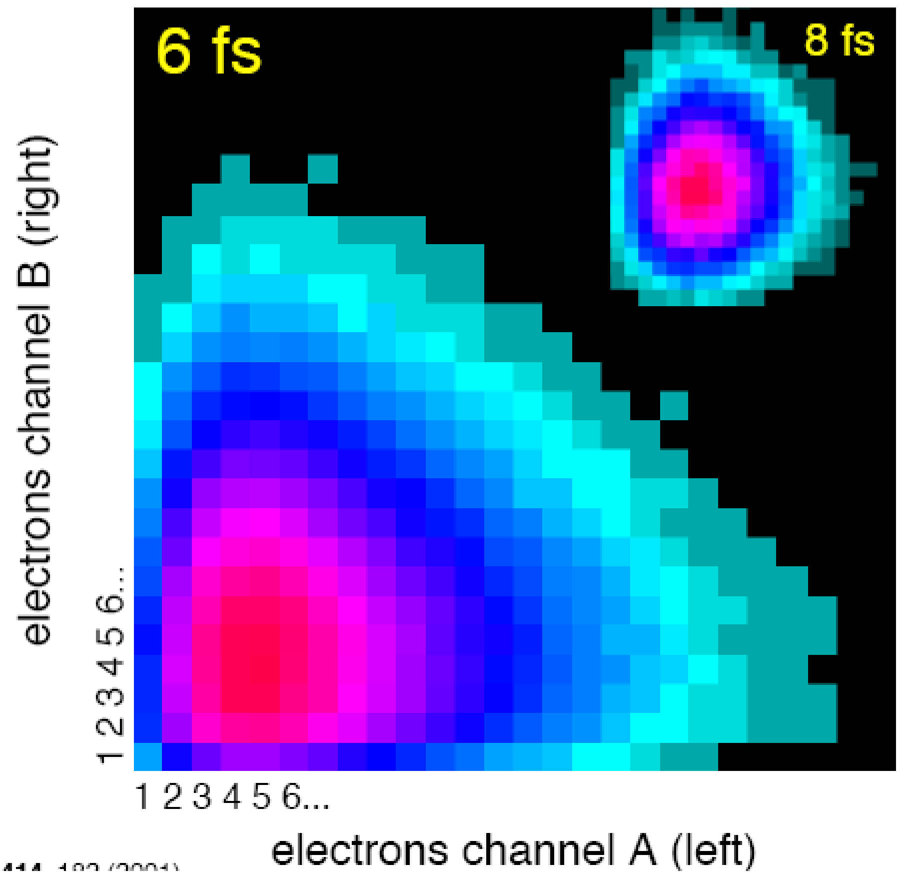

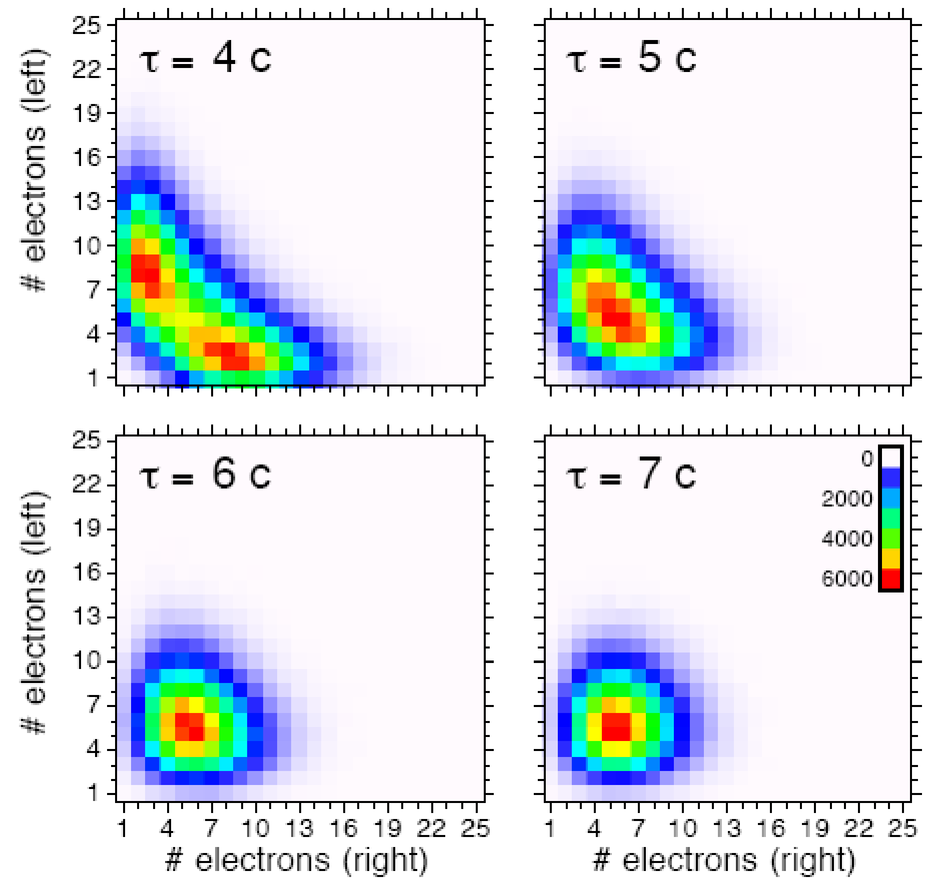

Paulus et al., Nature 2001

Milošević et al., PRL 2002

Stereo-HATI experiment: stable CE phase

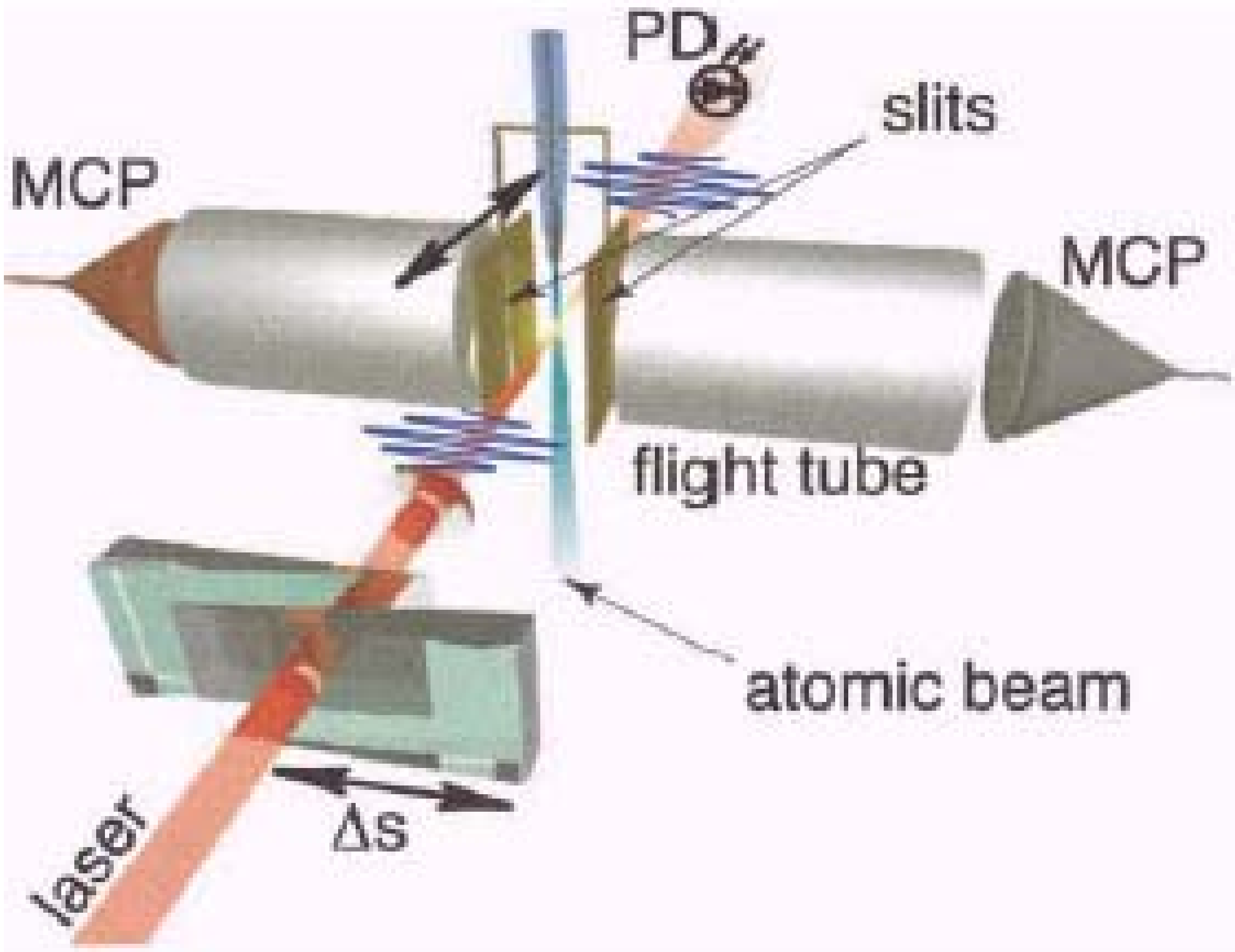

Paulus et al., Phys. Rev. Lett. 91, 253004 (2003)

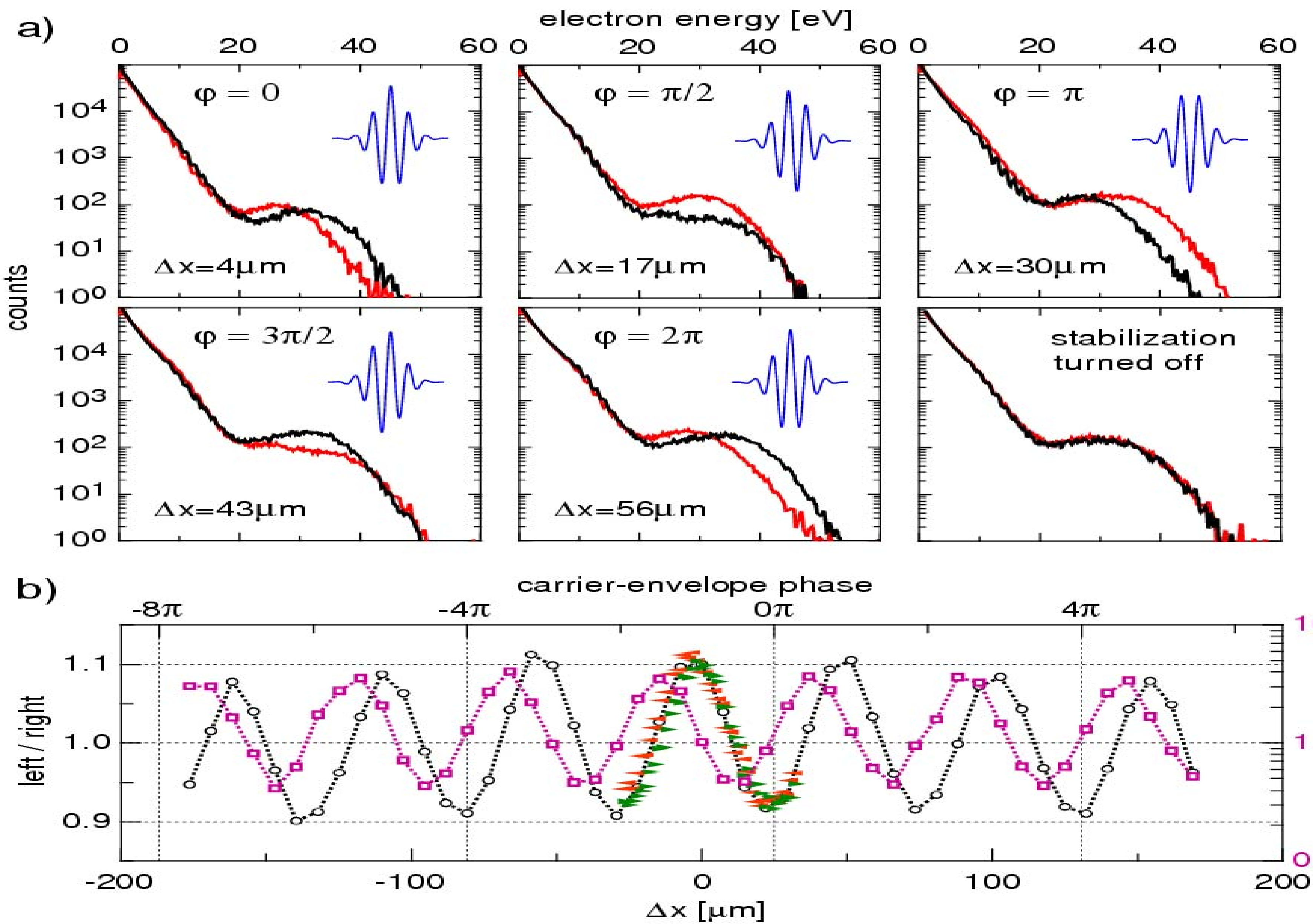

a)
electron energy [eV]
0 20 40 60
counts
10^0 10^1 10^2 10^3 10^4
φ = 0
Δx=4μm
φ = π/2
Δx=17μm
φ = π
Δx=30μm
φ = 3π/2
Δx=43μm
φ = 2π
Δx=56μm
stabilization turned off
b)
carrier-envelope phase
-8π -4π 0π 4π
left / right
0.9 1.0 1.1
0.1 1.0 10
-200 -100 0 100 200
Δx [μm]

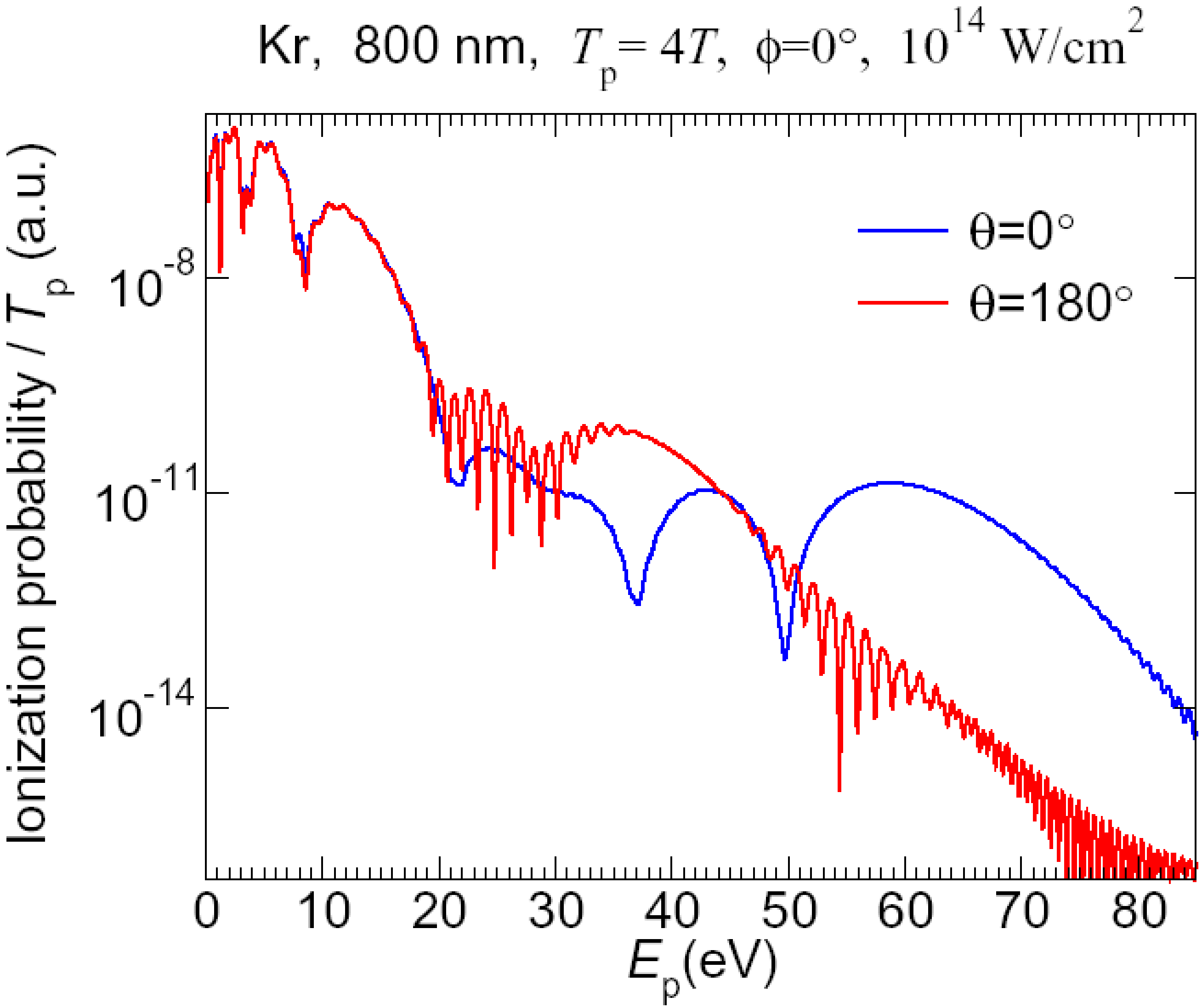

Milošević et al., Optics Express 11, 1418 (2003);
Laser Phys. Lett. 1, 93 (2004)

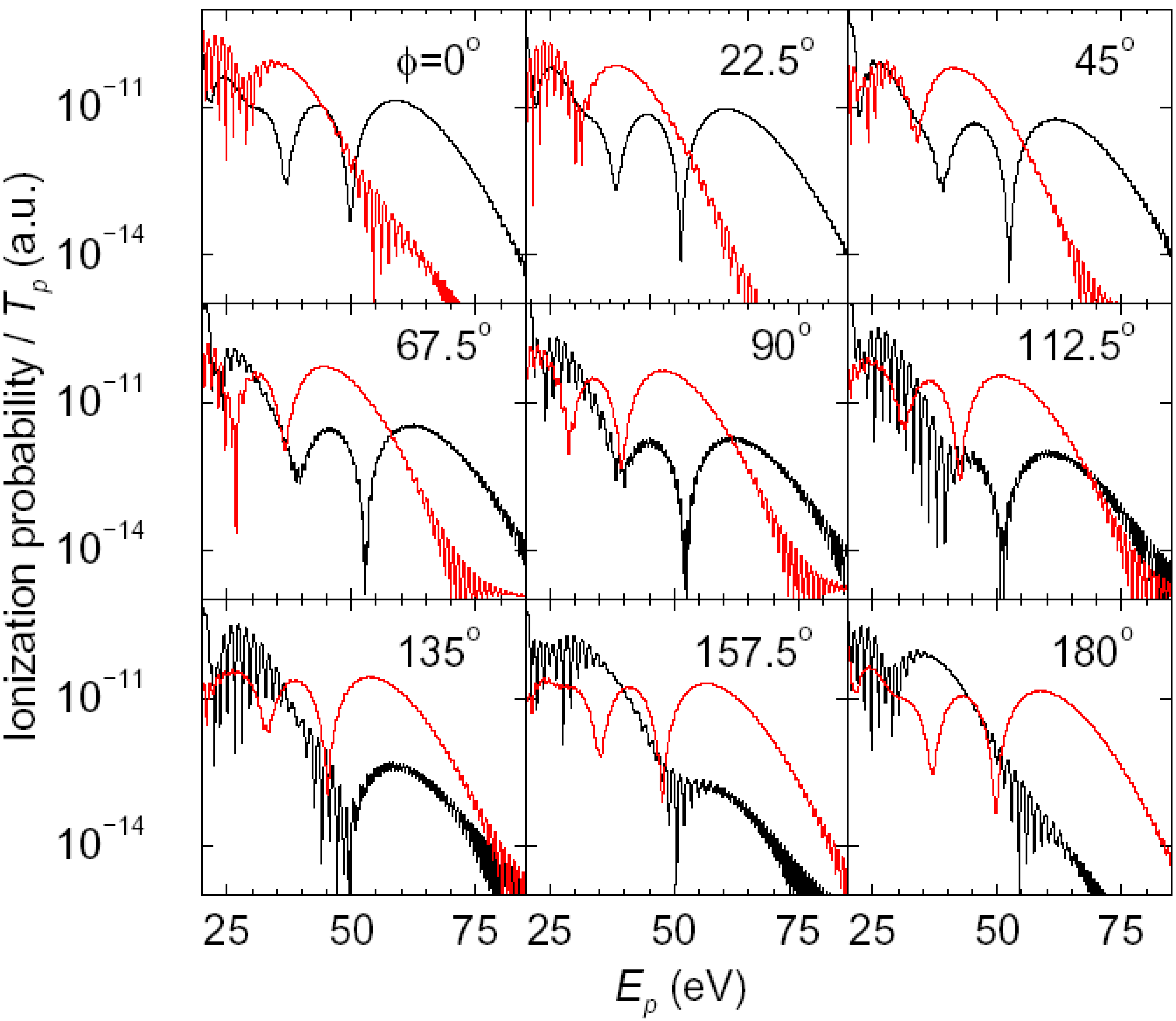

Ionization probability / T_p (a.u.)
10^{-11}
10^{-14}
ϕ=0°
22.5°
45°
67.5°
90°
112.5°
135°
157.5°
180°
25
50
75
E_p (eV)

HATI by bicircular ω-ω field:

Electron emission angle = CE phase / 2

$$\mathbf{E}_2(t) = \frac{E_2}{\sqrt{2}} \sin^2\left(\frac{\omega t}{2n_p}\right) \left[\hat{\mathbf{e}}_x \cos(\omega t + \phi) + \hat{\mathbf{e}}_y \sin(\omega t + \phi)\right]$$

$$\mathbf{E}(t) = \frac{E_1}{\sqrt{2}} \left(\hat{\mathbf{e}}_x \cos \omega t - \hat{\mathbf{e}}_y \sin \omega t\right) + \mathbf{E}_2(t)$$

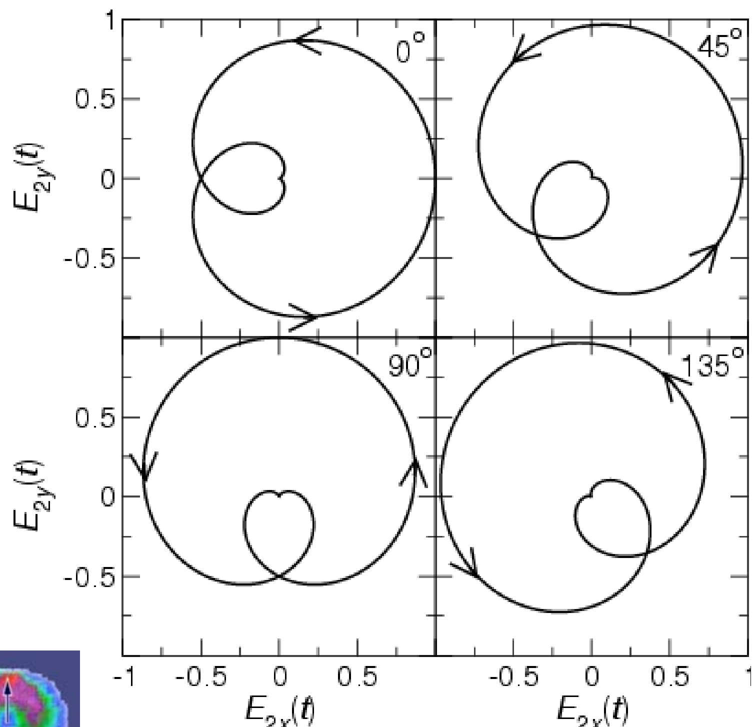

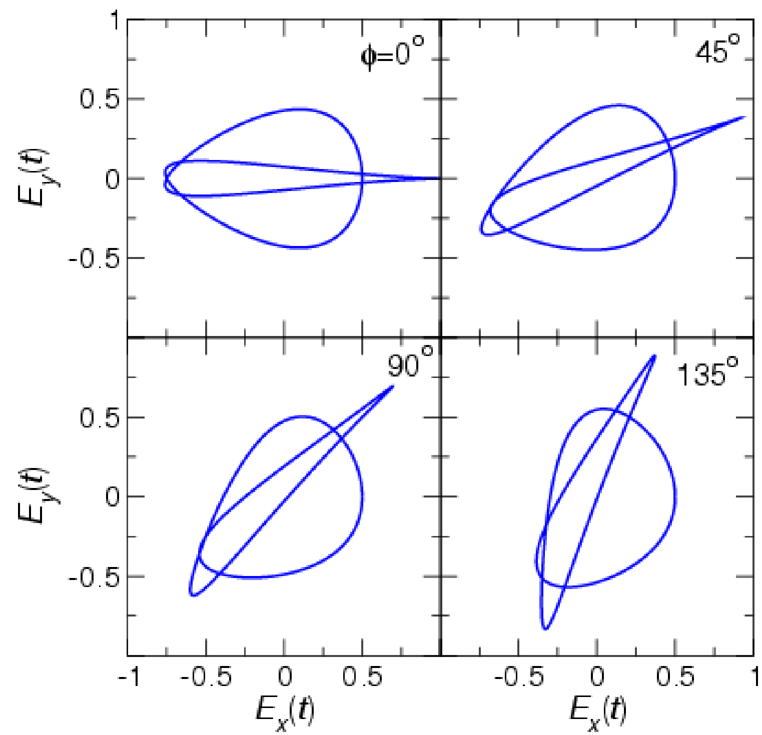

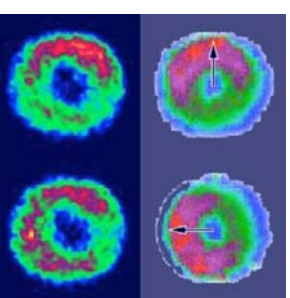

Biegert, Keller

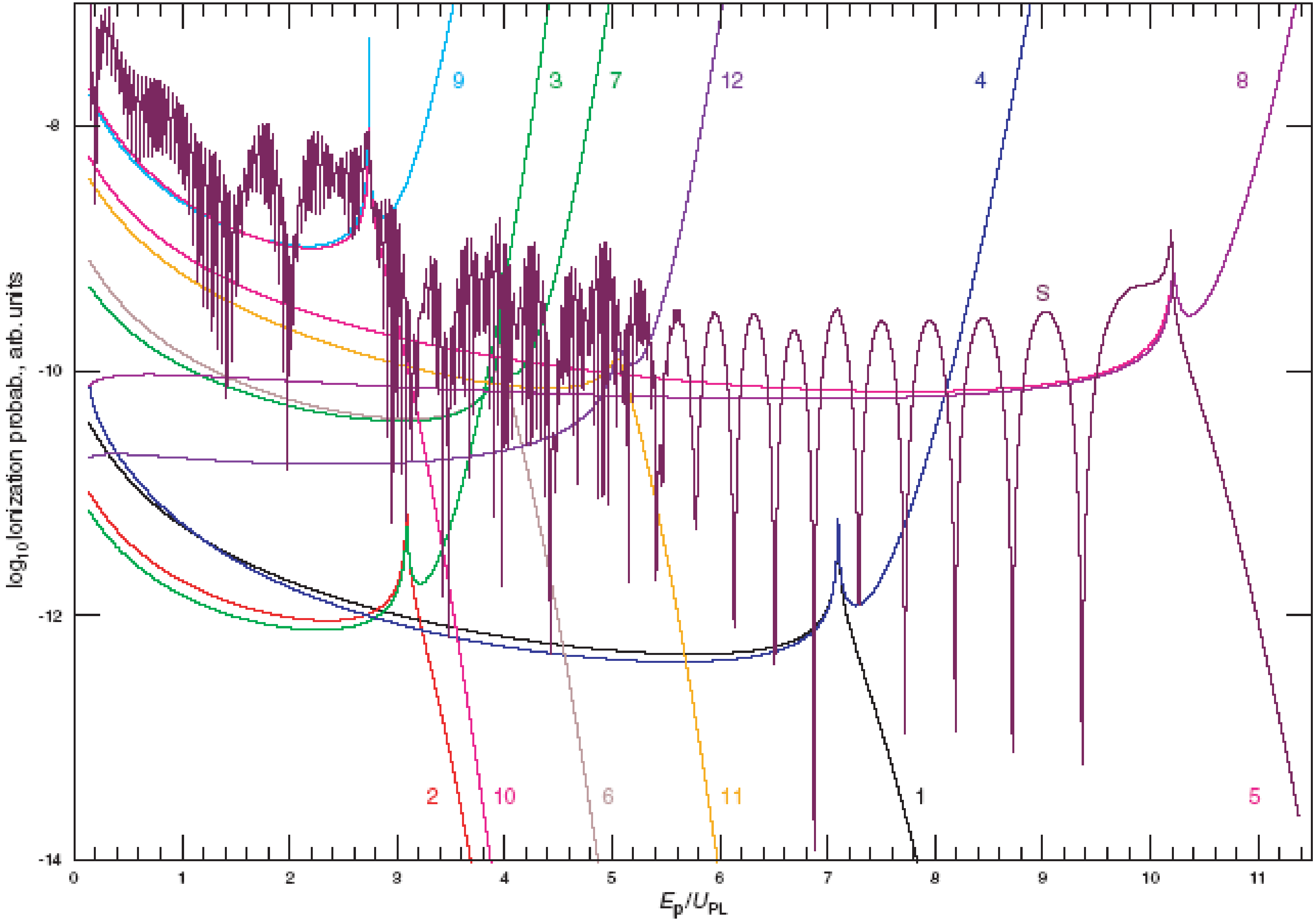

Figure 3 (online color at www.lphys.org) Logarithm of the differential ionization probability of argon as a function of the electron energy $E_{\mathbf{p}}$ in units of ponderomotive energy, for emission in the direction $\theta = 0°$, for the bicircular 4-cycle field (4) having the CE phase $\phi = 0$. The laser-field intensity is 3×10^{14} W/cm^2 and the wavelength 800 nm. The partial contributions of 12 different saddle points are presented separately

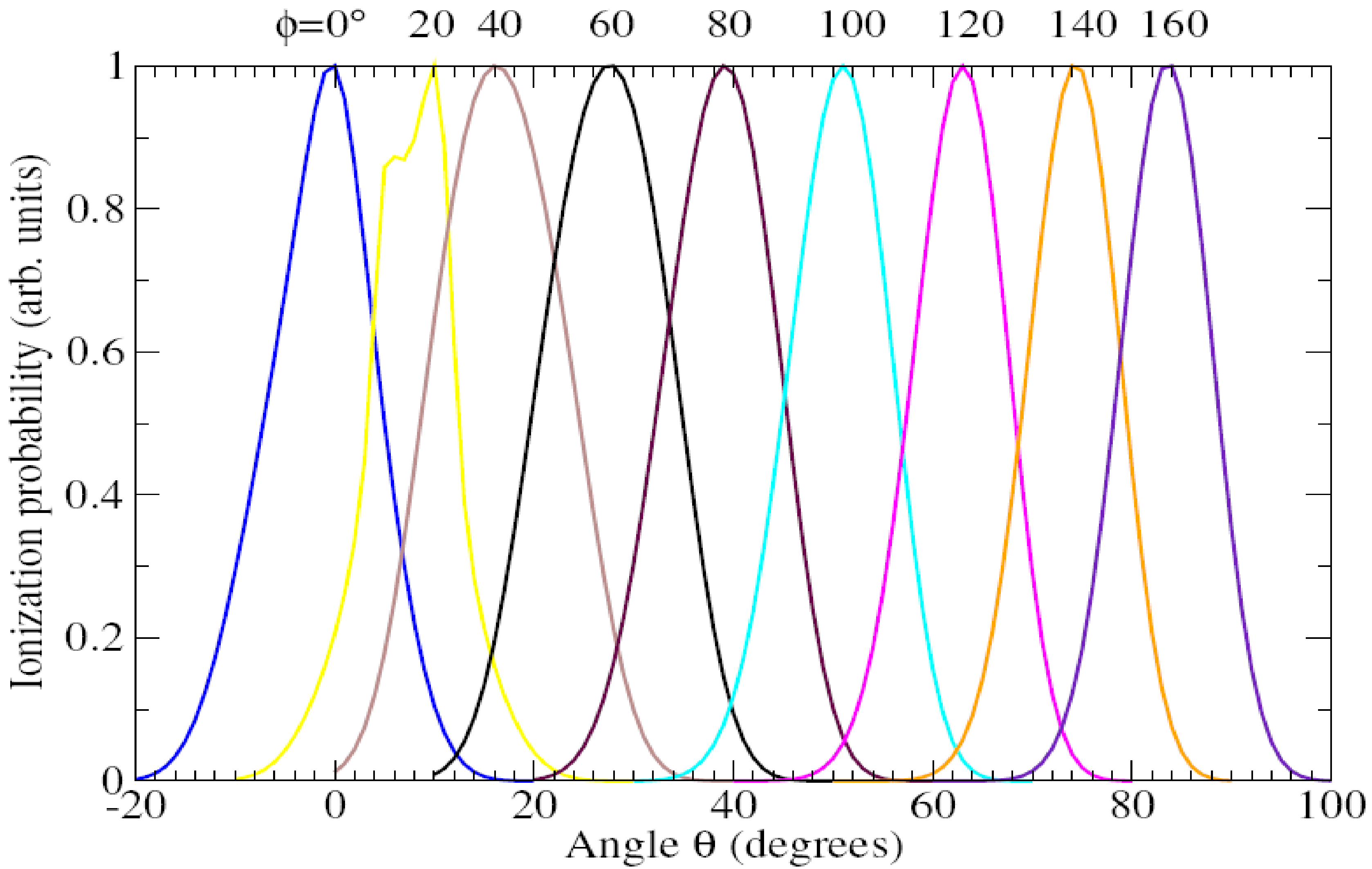

E. Hasović and DBM, Laser Phys. Lett. **3**, 200 (2006)

He, 800 nm, 10^{15} W/cm^2, CIR + Static (%)

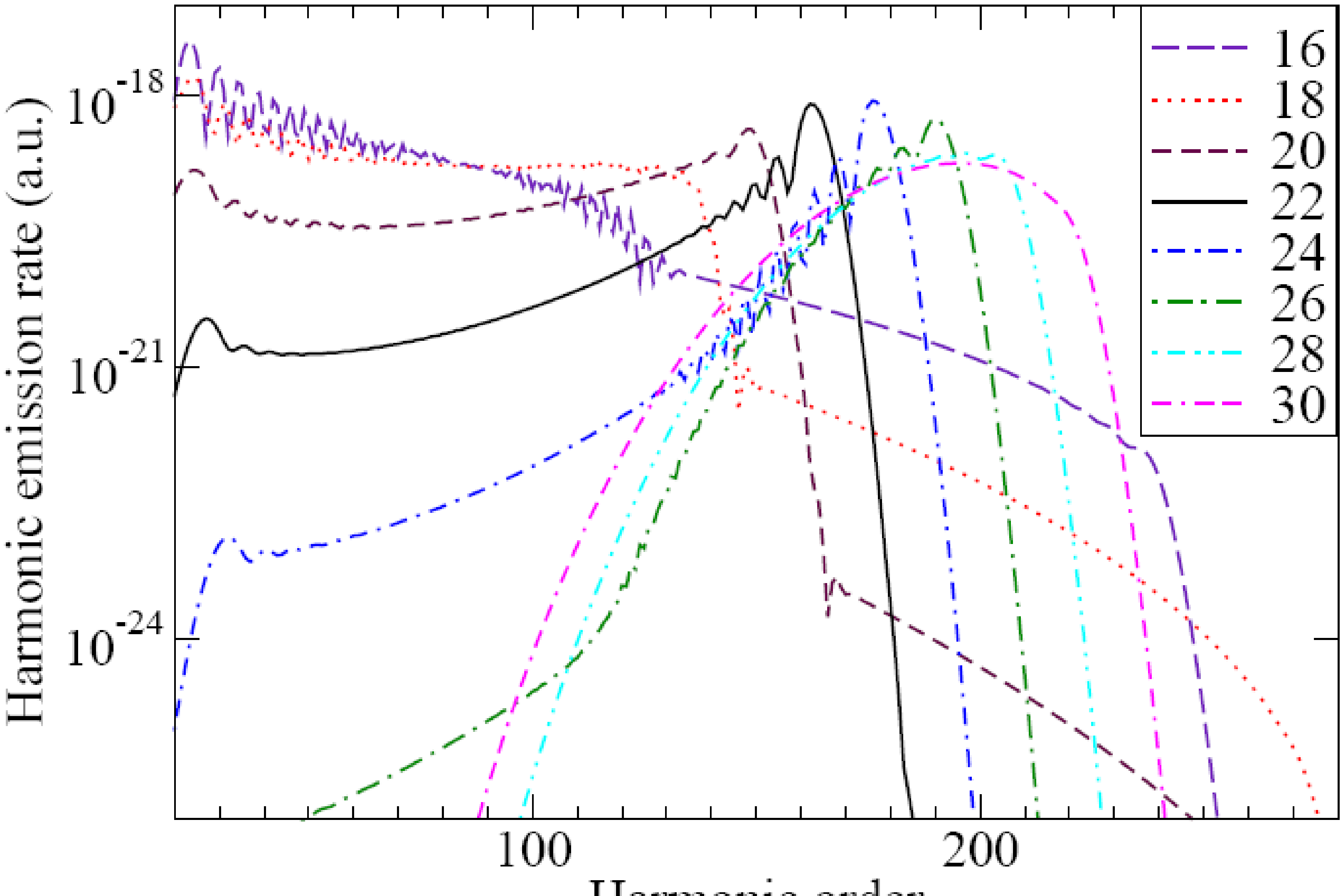

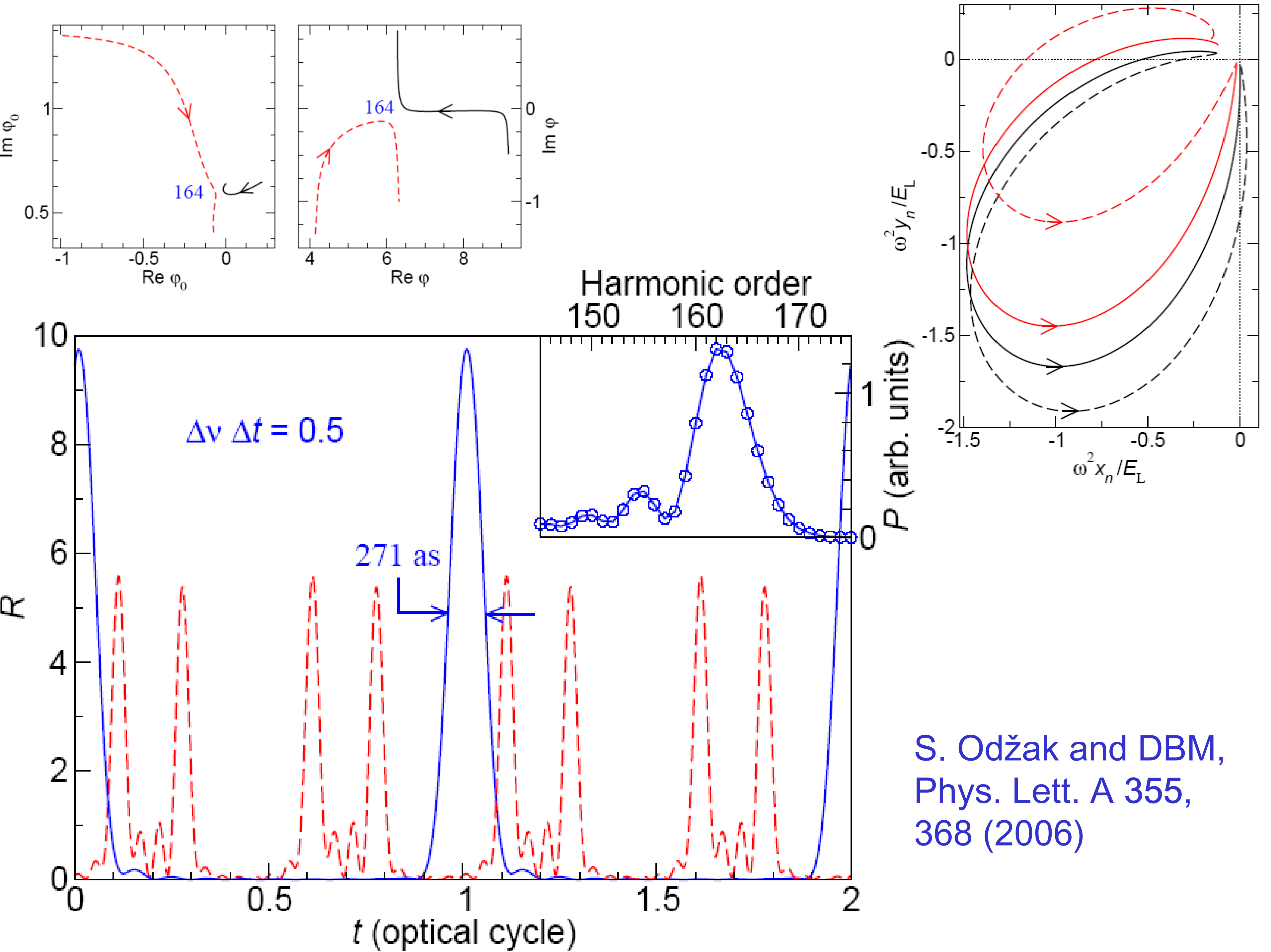

S. Odžak and DBM, Phys. Lett. A 355, 368 (2006)

Incoherent scattering

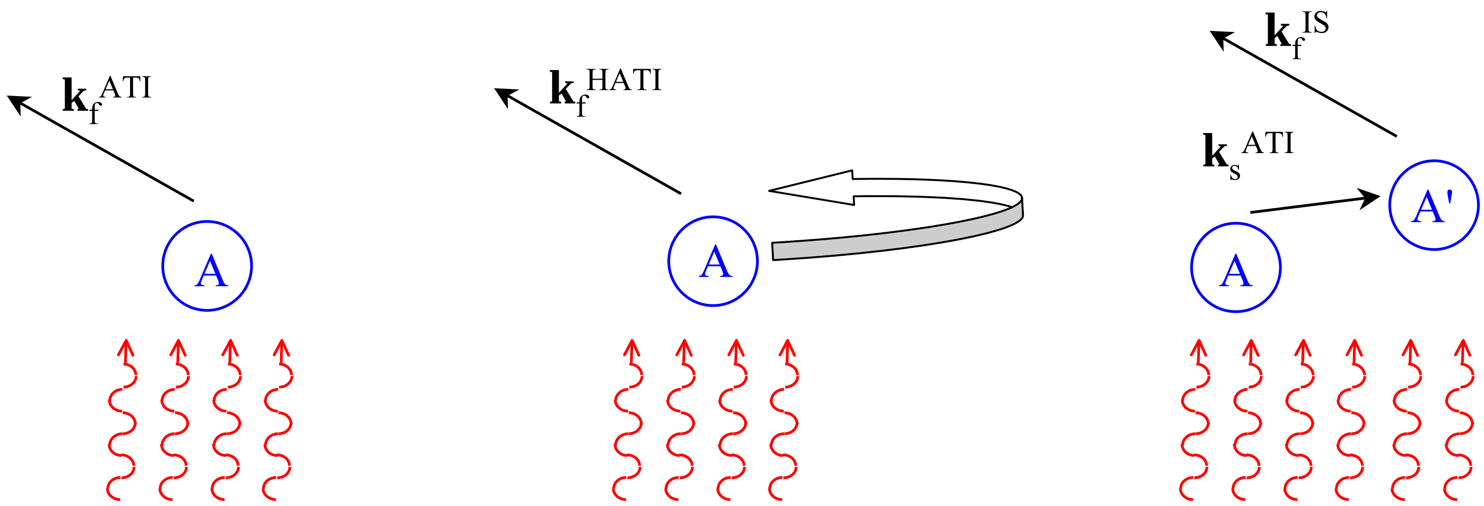

$$w_{\rm fi}^{\rm s}(M,\Omega_{\rm f}) = \rho \sum_N \int_0^{2\pi} {\rm d}\phi_{\rm s} \int_0^{\pi} {\rm d}\theta_{\rm s} \sin\theta_{\rm s} w_{\rm si}(N,\Omega_{\rm s}) {\rm d}\sigma_{\rm fs}(L,\Omega_{\rm f},\Omega_{\rm s})$$

A. Čerkić and DBM J. Phys. B submitted

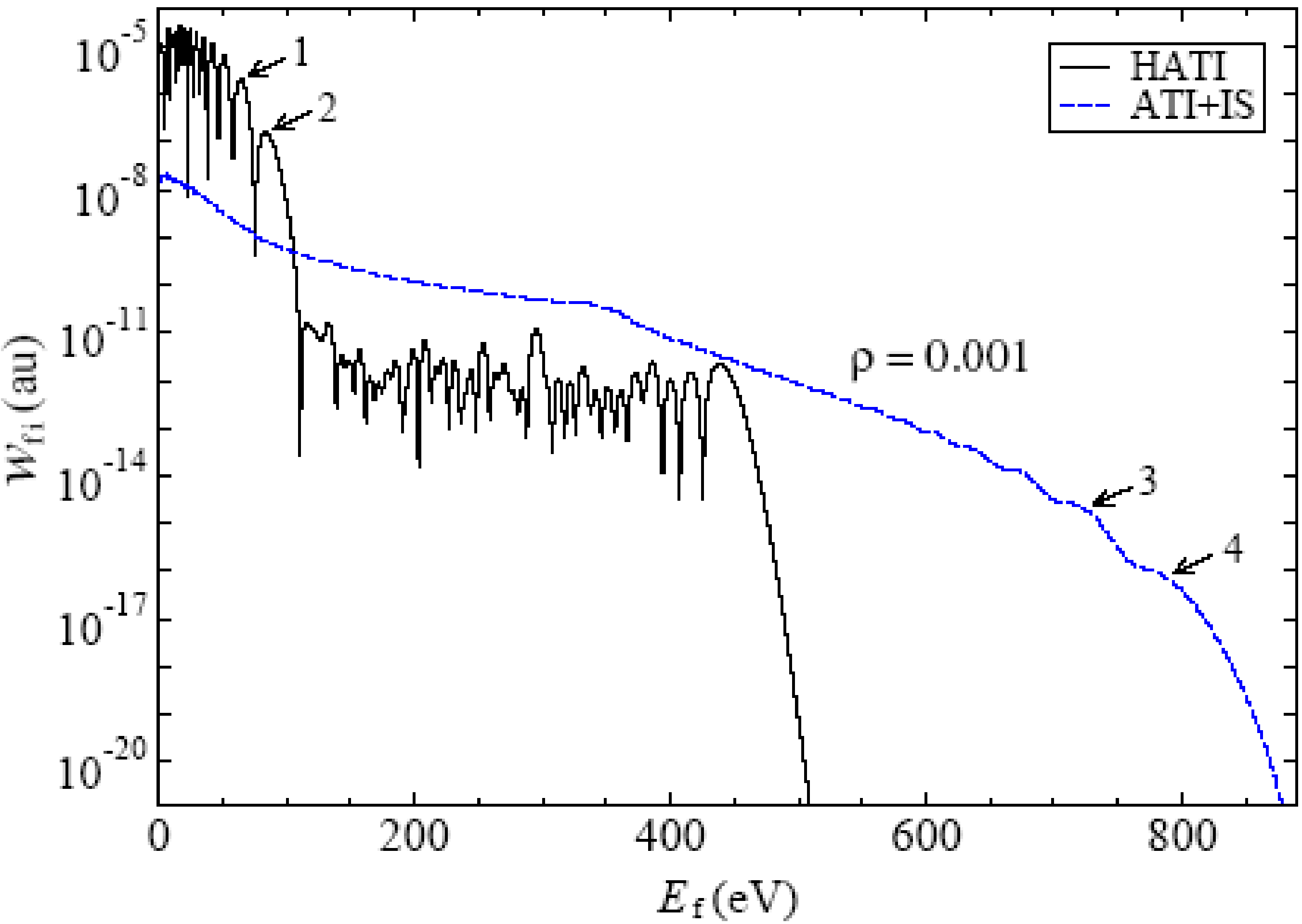

Figure 1. The differential ionization rates of the hydrogen atom in the presence of a monochromatic linearly polarized laser field, as functions of the final electron energy. The laser wavelength is 1300 nm and the intensity 2.8×10^{14} W cm^{-2}. The angle between the polarization vector of the laser field and the final momentum of the ionized electron is $\theta_f = 0°$. The results for HATI (solid line) and ATI+IS (dashed line) process are presented.

Few-cycle (H)ATI

See DBM *etal*, J. Phys. B 39, R203 (2006)

and talk by Wilhelm Becker at conference

KFR (direct) electron spectrum

$$M_{\mathbf{p}} \sim \int dt \langle \psi_{\mathbf{p}}^{\text{Volkov}}(t) | V(\mathbf{r}) | \psi_0(t) \rangle \sim \int_{-\infty}^{\infty} dt V_{\mathbf{p},0} e^{iS_{\mathbf{p},E_0}(t)}$$

V_{p0} = <p-eA(t)|V|0>

$$S_{\mathbf{p},E_0}(t) = |E_0|t + \frac{1}{2m} \int^t d\tau [\mathbf{p} - e\mathbf{A}(\tau)]^2$$

Long periodic pulse:

$$S_{\mathbf{p},E_0}(t+T) = \left(|E_0| + \tfrac{\mathbf{p}^2}{2m} + U_P \right) T + S_{\mathbf{p},E_0}(t)$$

Recall

$$\sum_{n=-\infty}^{\infty} e^{inx} = 2\pi \sum_{n=-\infty}^{\infty} \delta(x - 2n\pi)$$

$$M_{\mathbf{p}} \sim \sum_{n=-\infty}^{\infty} \delta \left(\frac{\mathbf{p}^2}{2m} + U_P + |E_0| - n\omega \right) \int_0^T dt V_{\mathbf{p},0} e^{iS_{\mathbf{p},E_0}(t)}$$

Interference from many cycles generates discrete spectrum

Saddle-point evaluation of the remaining integral over **one** cycle

$$\frac{d}{dt} S_{\mathrm{p},E_0}(t) = 2m|E_0| + [\mathrm{p} - e\mathbf{A}(t)]^2 \stackrel{!}{=} 0$$

(Notice $\mathrm{p} = e\mathbf{A}(t)$ in the tunneling limit)

solutions $t \equiv t_s(\mathrm{p}) \quad (s = 1, 2, \ldots)$

$$M_{\mathrm{p}} = \sum_n \delta\left(\frac{\mathrm{p}^2}{2m} + U_p + |E_0| - n\hbar\omega\right) \times \sum_{s,\text{one cycle}} [S''_{\mathrm{p},E_0}(t_s)]^{-1/2} e^{iS_{\mathrm{p},E_0}(t_s)}$$

- Interference from different cycles generates discrete peaks
- Interference from within one cycle generates structure of the spectral envelope

For a few-cycle pulse: no discrete peaks! Just a few contributions interfere

One cycle vs many cycles

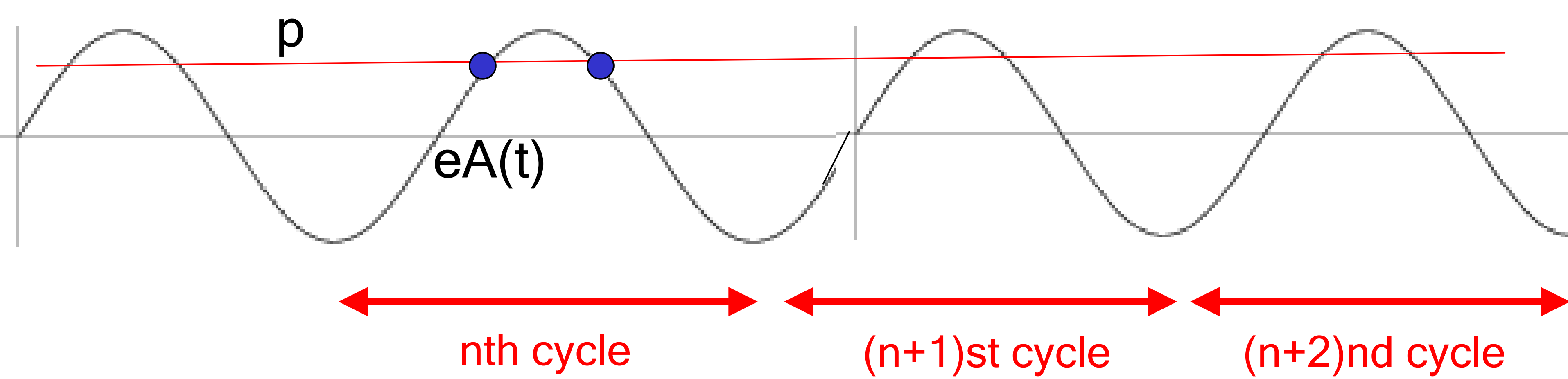

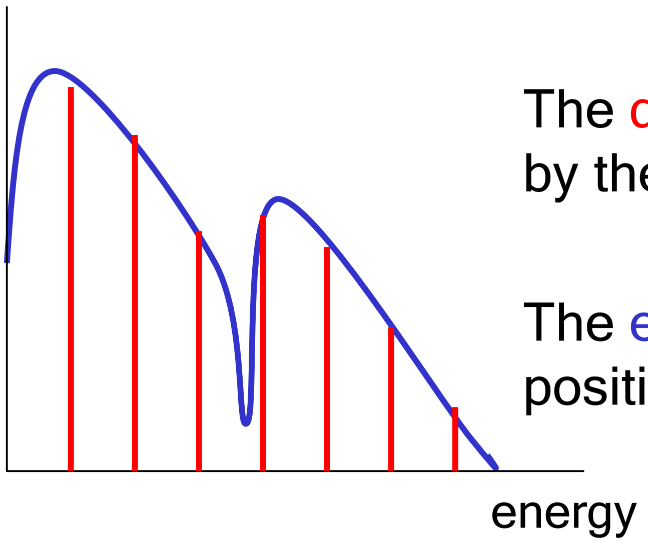

The discreteness of the spectrum is generated by the superposition of all cycles

The envelope is generated by the superposition of the two solutions within one cycle

Examples of direct quantum orbits

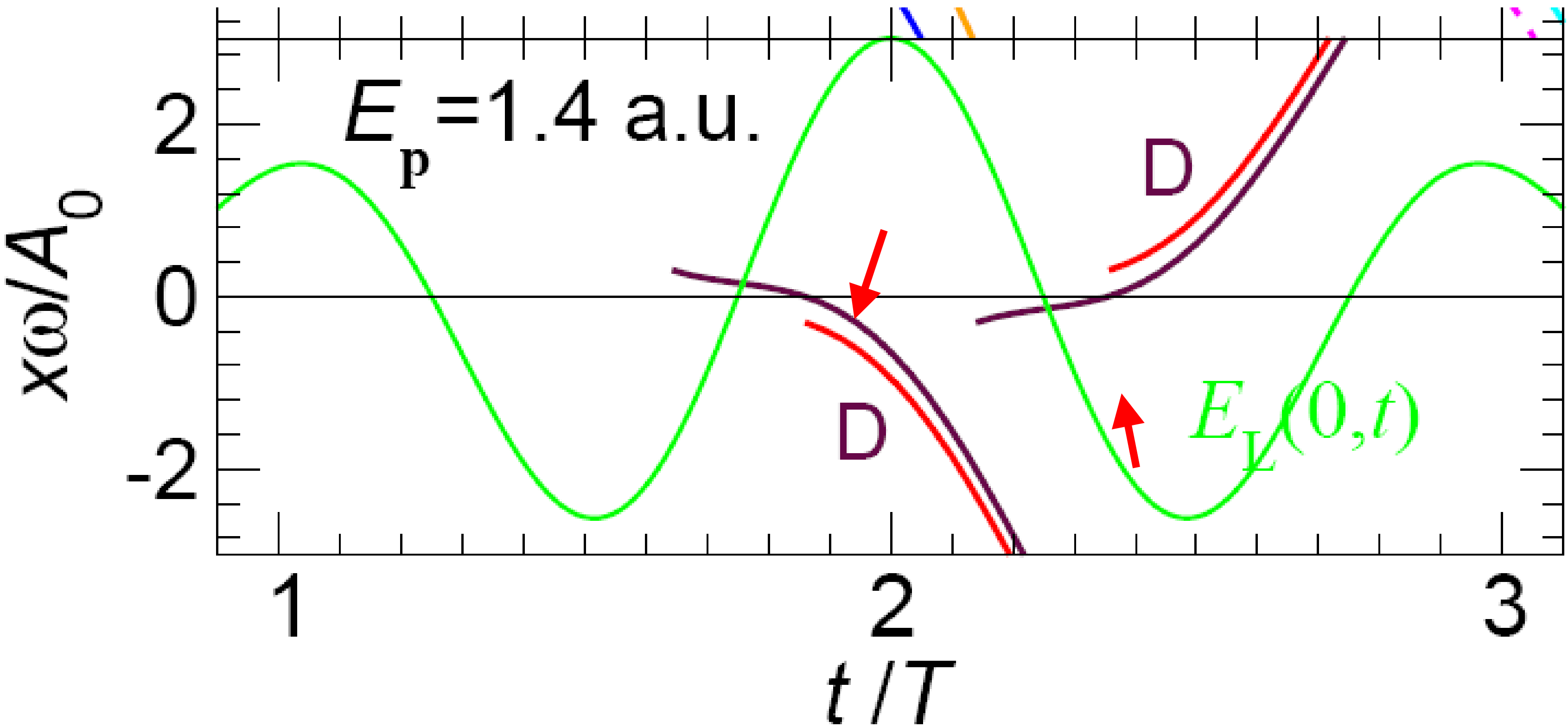

One member of a pair of orbits experiences the Coulomb potential more than the other

Interference of the two solutions from within one cycle

(includes focal averaging)

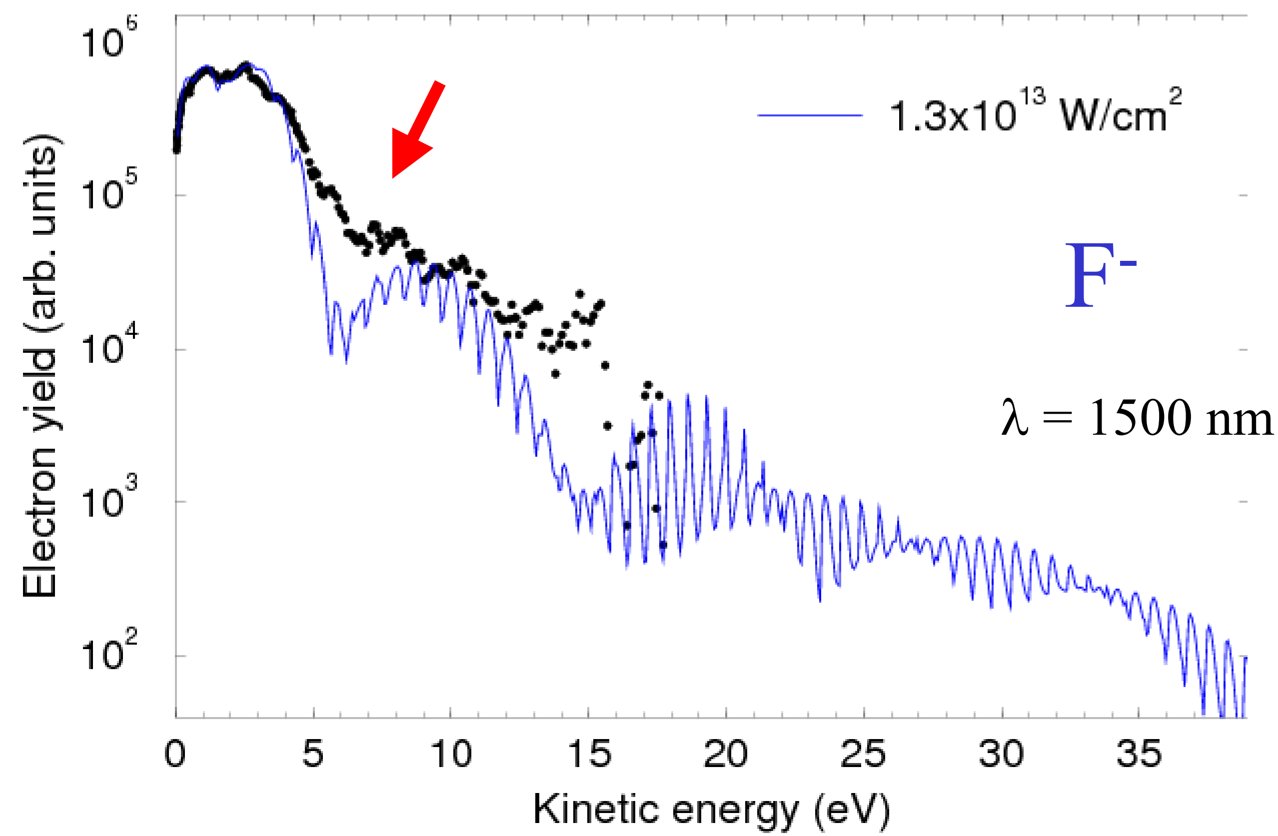

Data: I. Yu Kiyan, H. Helm, PRL 90, 183001 (2003)
(1.1×10^{13} Wcm^{-2})
Theory: D.B. Milosevic et al., PRA 68, 070502(R) (2003)
(1.3×10^{13} Wcm^{-2})

cf. M.V. Frolov, N.M. Manakov, E.A. Pronin, A.F. Starace, JPB 36, L419 (2003)

Rescattered quantum orbits in space and time

ionization time = t′ t = recollision time

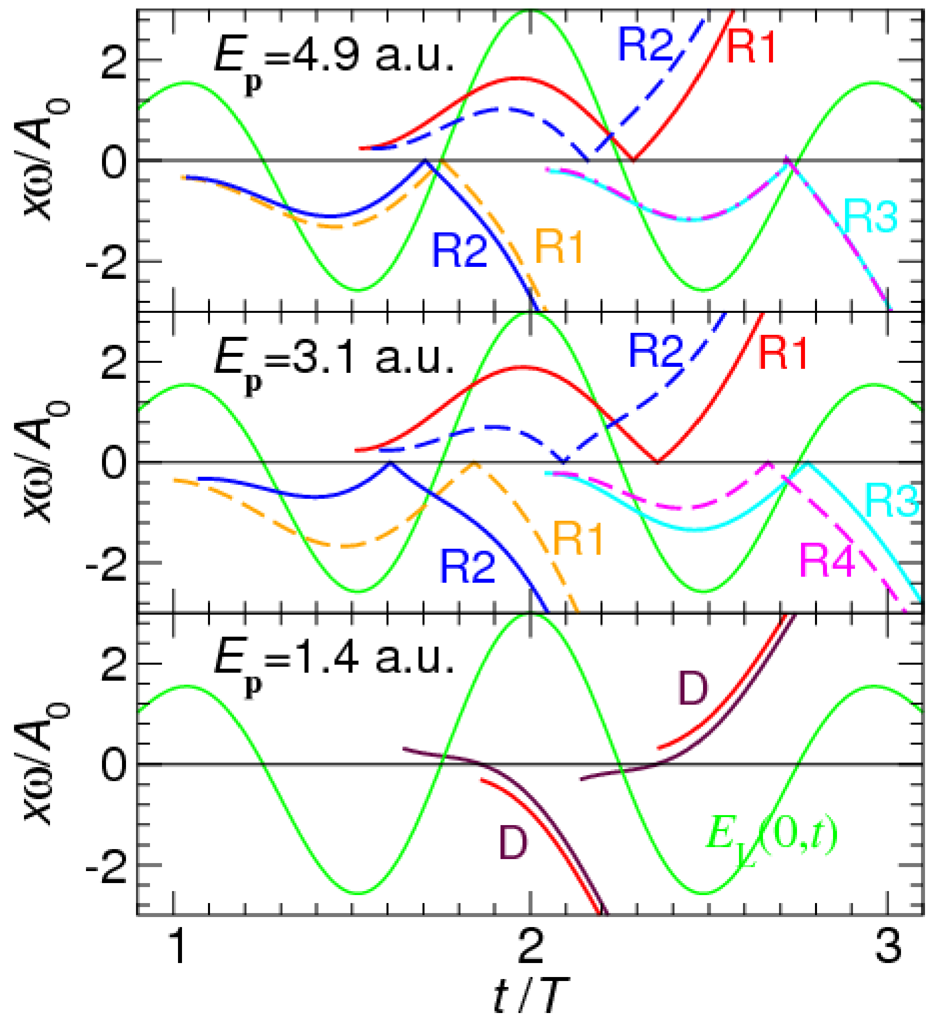

Few-cycle-pulse ATI spectrum: violation of backward-forward symmetry

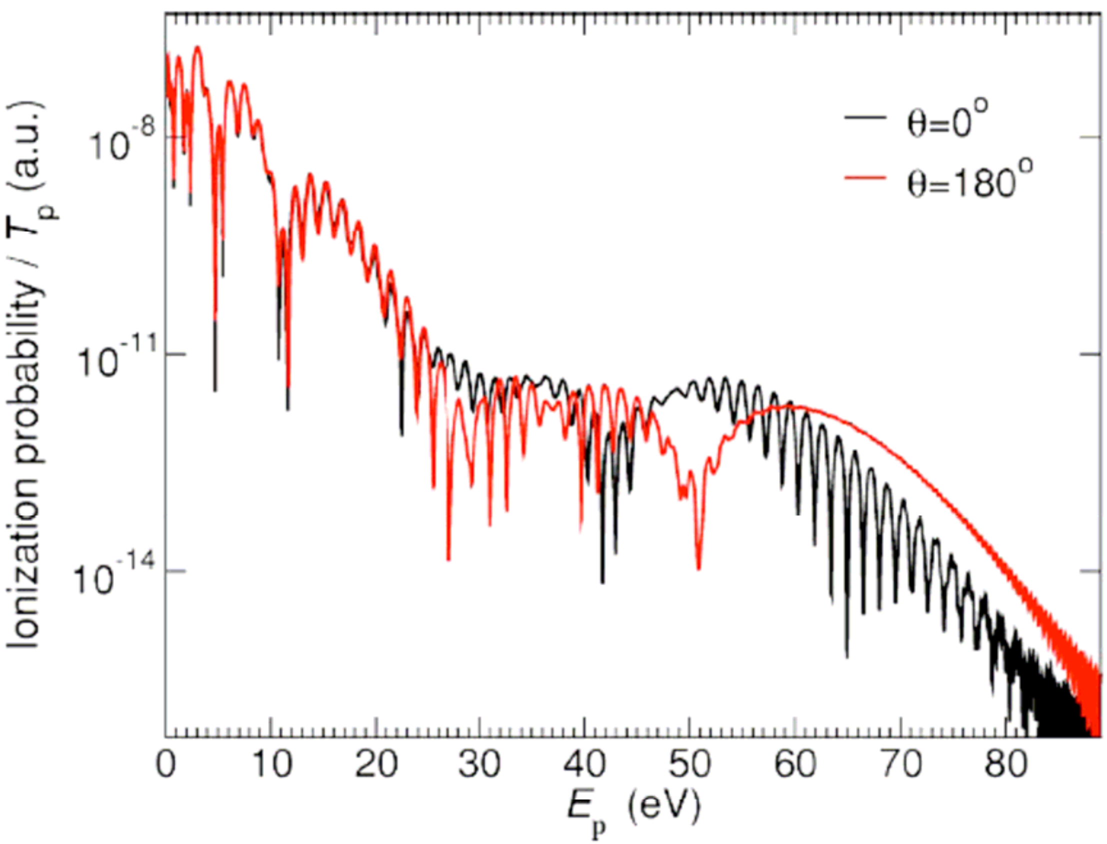

argon, 800 nm
7-cycle duration
sine square envelope
cosine pulse, CEP = 0
10^{14} Wcm^{-2}

Different cutoffs

Peaks vs no peaks

D. B. Milosevic, G. G. Paulus, WB, PRA 71, 061404 (2005)

Building up the spectrum from quantum orbits

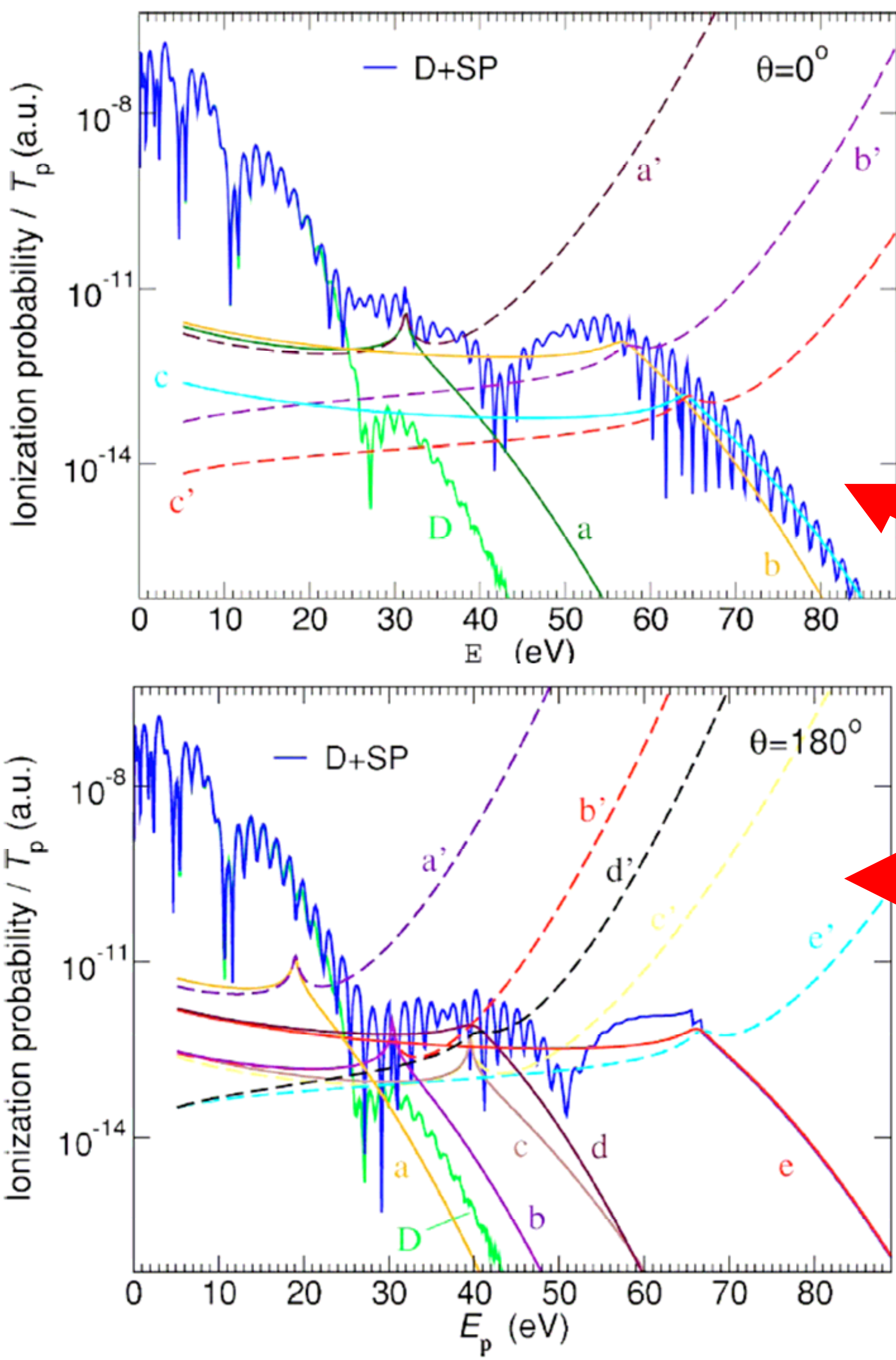

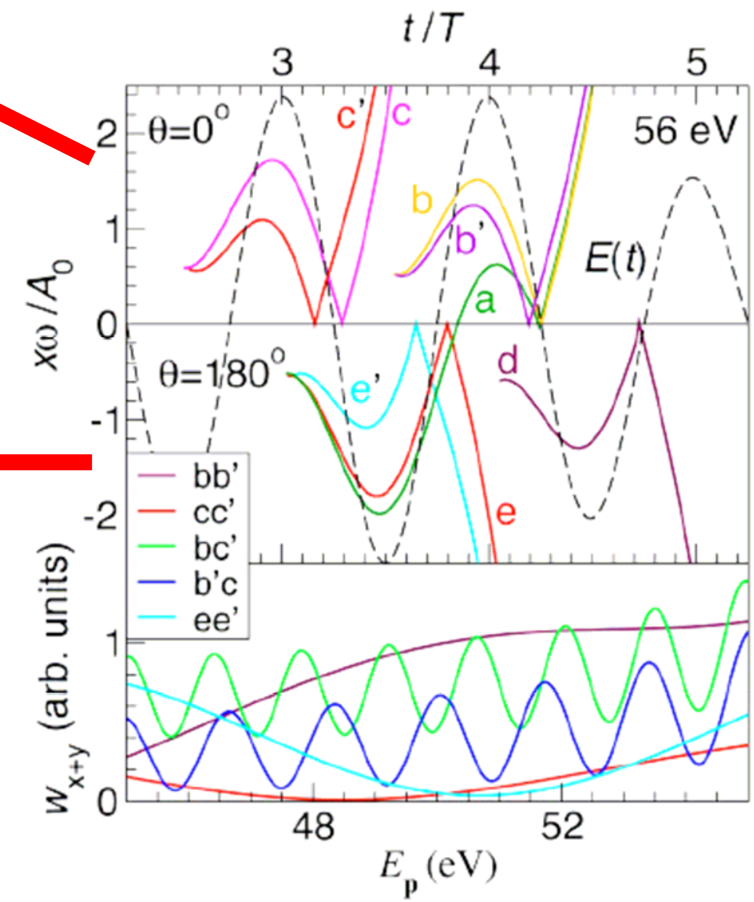

The black box of S-matrix theory ...

|out> = S|in>

... has been made transparent

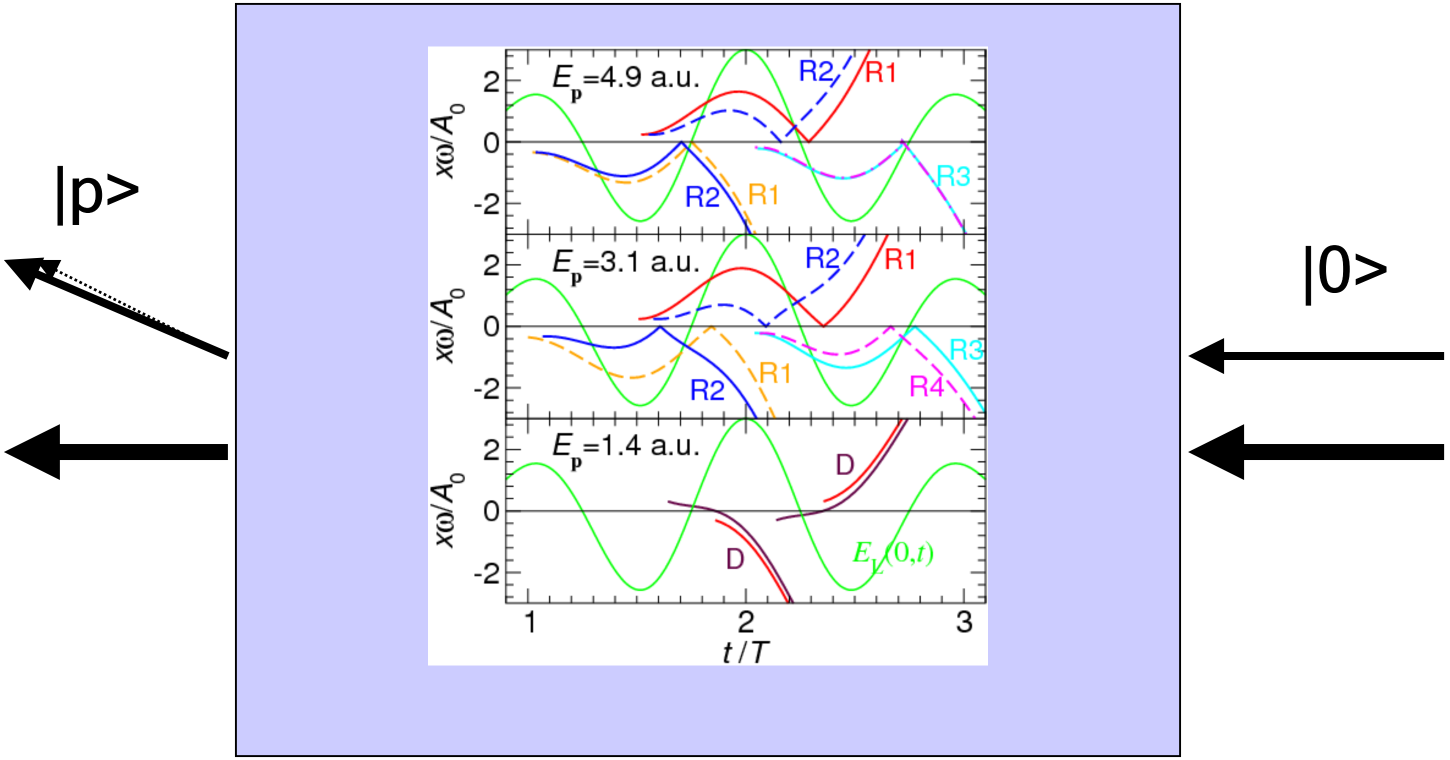

ATI simulation

- S-matrix theory
- SFA (1BA) with rescattering (2BA)
- Physical interpretation via Quantum Orbits
- Focal averaging + saturation effects
- Gauge aspects are important (see WB)
- Choice of the ground-state wave function
- Coulomb effects for ATI (not included yet)

QM transition amplitude

Exact: $$M_{\vec{p}i} = -i \lim_{t\to\infty} \int_0^t dt' \langle \psi_{\vec{p}}(t) | U(t,t') \vec{r}\cdot\vec{E}(t') | \psi_i(t') \rangle$$

SFA: $$M_{\vec{p}i} = M_{\vec{p}i}^{(0)} + M_{\vec{p}i}^{(1)} + \cdots$$

$$M_{\vec{p}i}^{(0)} = -i \int_0^{T_p} dt_0 \langle \vec{p} + \vec{A}(t_0) | \vec{r}\cdot\vec{E}(t_0) | \psi_i \rangle \exp\left[iS_{\vec{p}}^{(0)}(t_0) \right]$$

$$M_{\vec{p}i}^{(1)} = -\int_0^{T_p} dt_0 \int_{t_0}^{\infty} dt_1 \int d^3\vec{k} \langle \vec{p} + \vec{A}(t_1) | V | \vec{k} + \vec{A}(t_1) \rangle$$

$$\times \langle \vec{k} + \vec{A}(t_0) | \vec{r}\cdot\vec{E}(t_0) | \psi_i \rangle \exp\left[iS_{\vec{p}}^{(1)}(t_0, t_1, \vec{k}) \right]$$

Hartree-Fock ground-state wave functions, expanded on basis set of atomic Slater orbitals:

$$\psi_i\left(\vec{r}\right) = \sum_j C_j N_j r^{n_j - 1} e^{\varsigma_j r} Y_{l0}\left(\hat{\vec{r}}\right)$$

Independent-particle-model optimized potential, represented by the double Yukawa potential:

$$V\left(\vec{r}\right) = -\frac{Z}{H}\frac{e^{-r/D}}{r}\left[1+\left(H-1\right)e^{-Hr/D}\right],\ H = DZ^{0.4}$$

He (1s, Z=2), Ne, Ar, Kr, Xe (5p, Z=54)

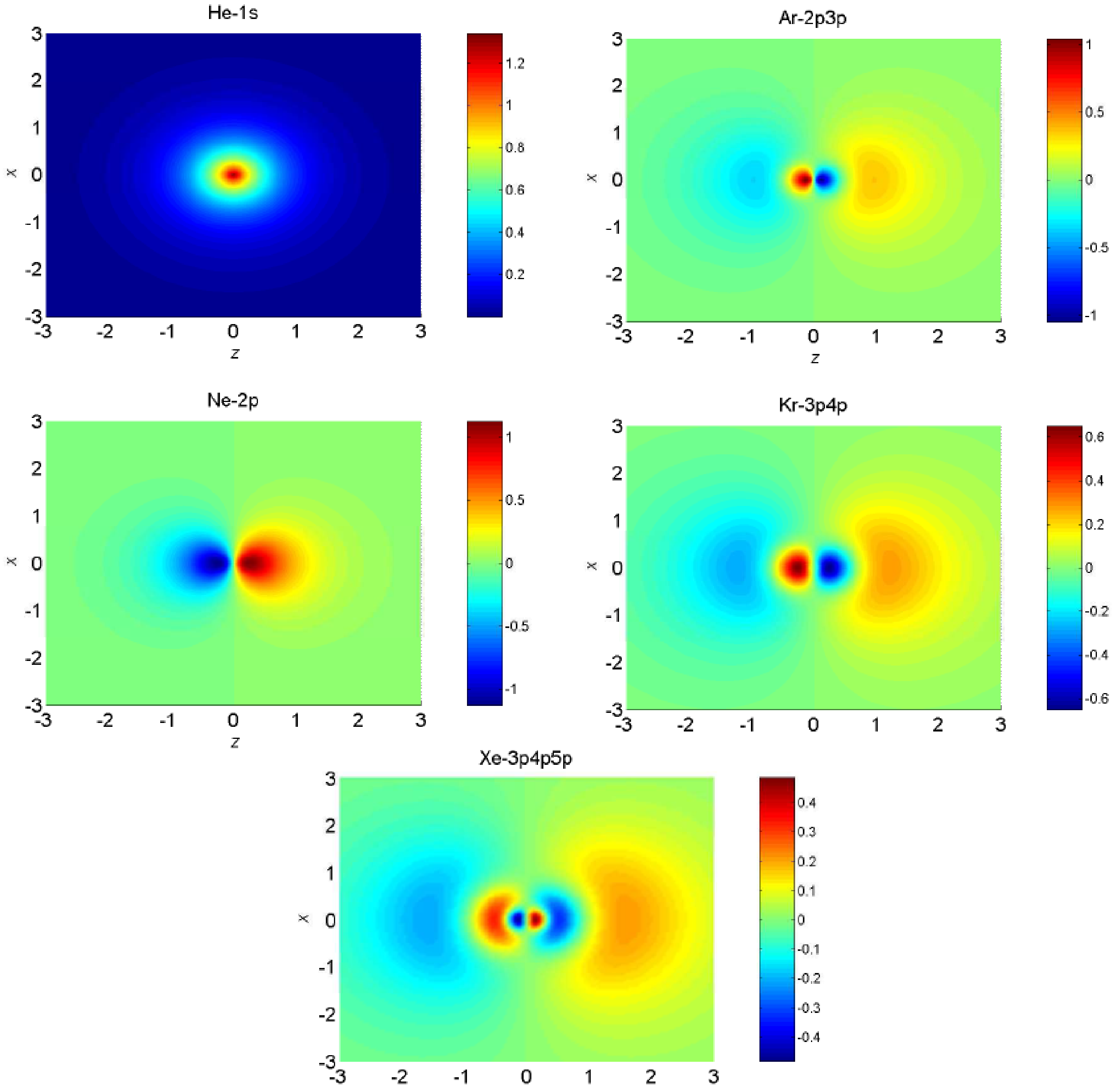

He-1s
Ar-2p3p
Ne-2p
Kr-3p4p
Xe-3p4p5p
x
z

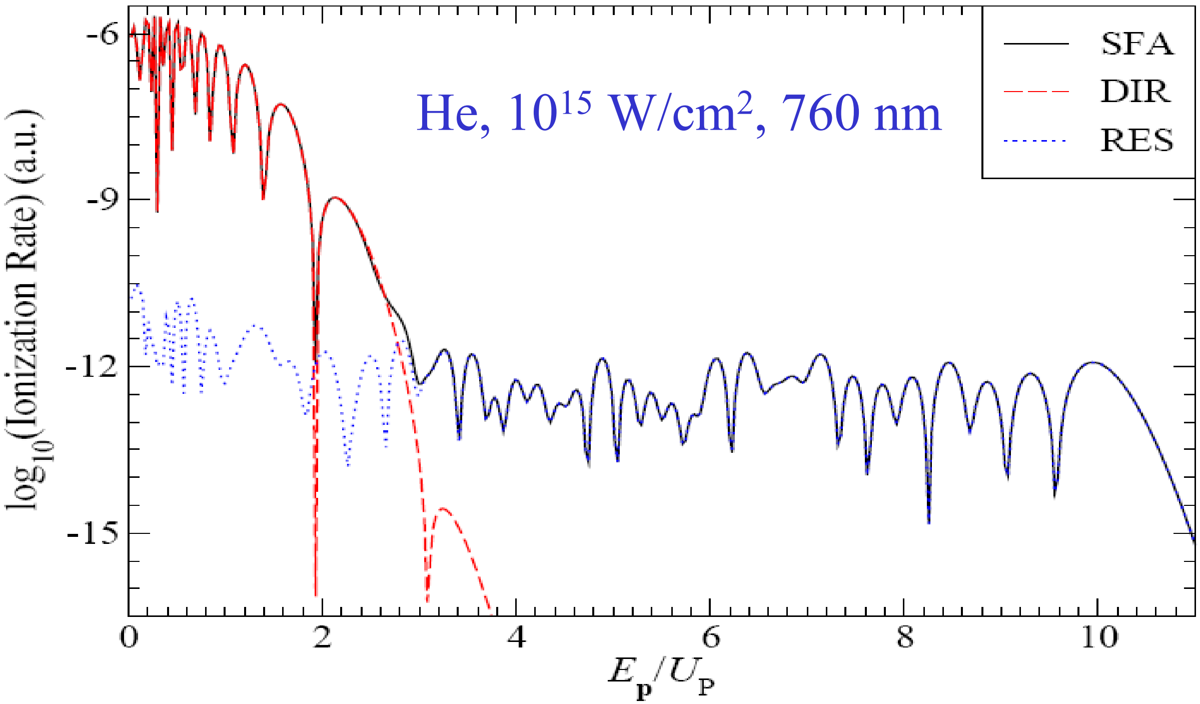

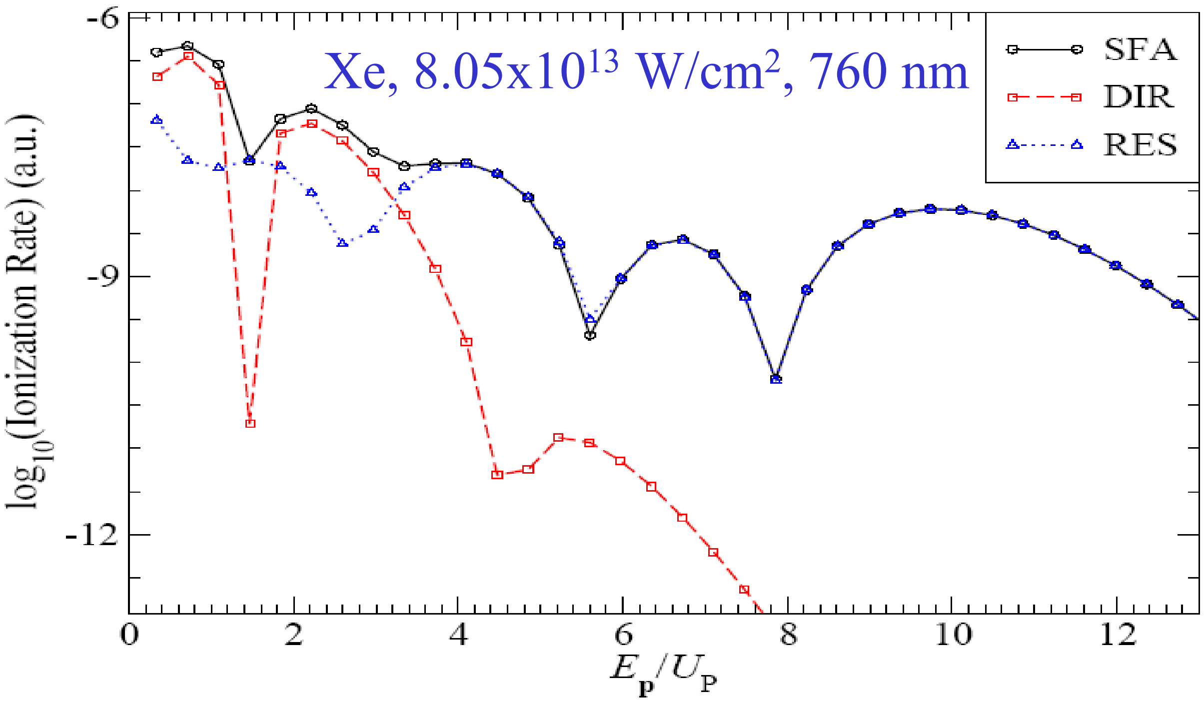

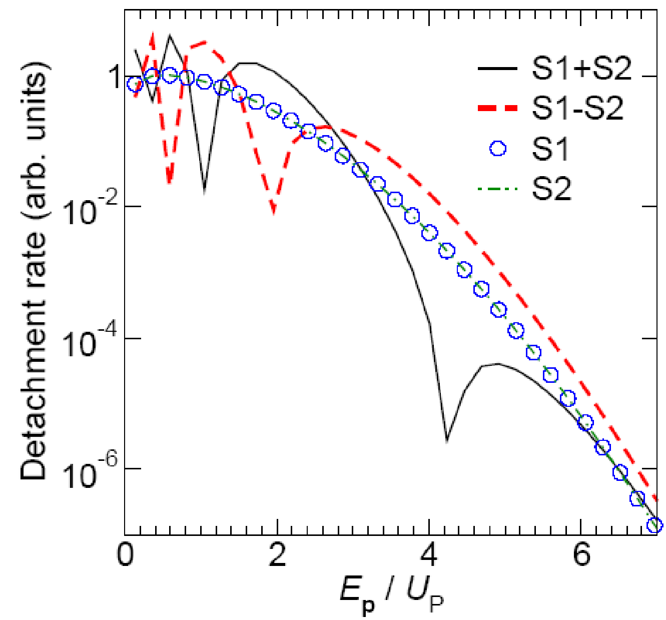

$$T_{\vec{p}i} \propto M_1 + (-1)^l M_2$$

SPM for HATI and QO theory

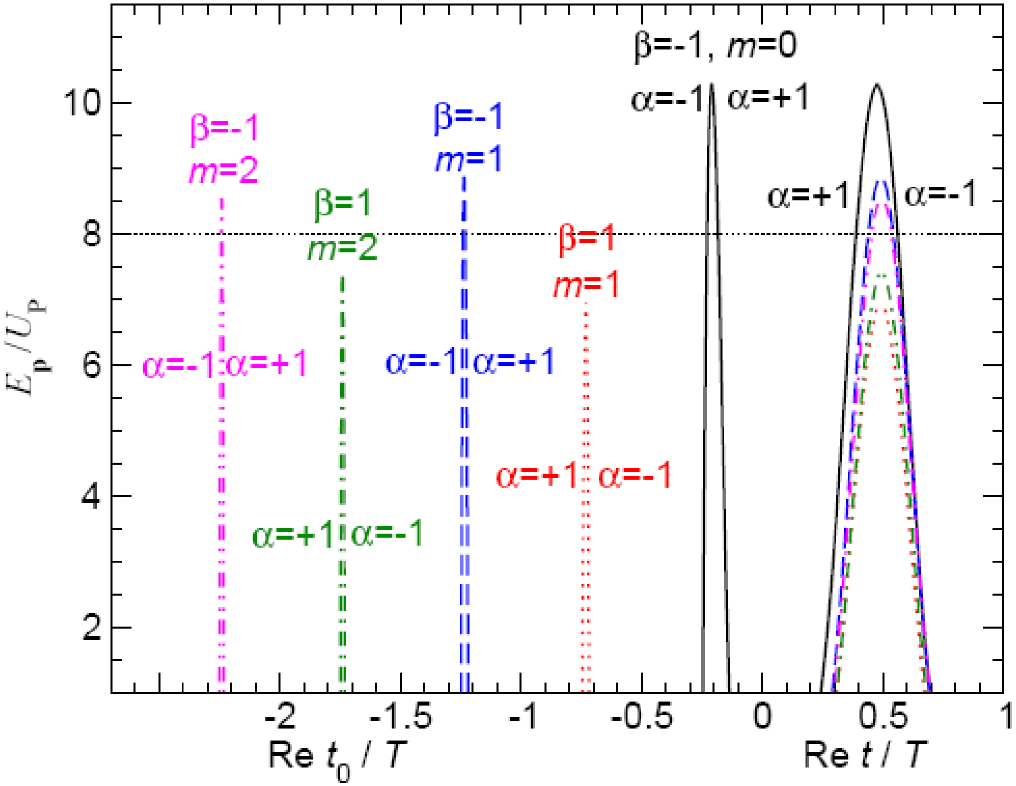

Classification of saddle-point solutions: $\alpha\beta m$

The uniform approximation

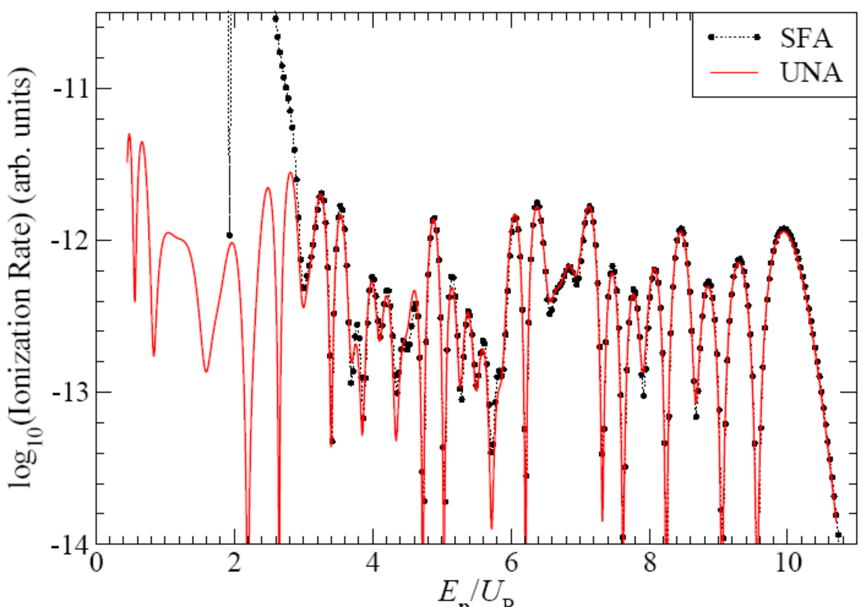

Semiclassical analysis. Cutoff law

Busuladzic et al,

Laser Phys. **16**, 289 (2006)

$$E_{\vec{p}\max} = 10.007U_p + 0.538I_p$$

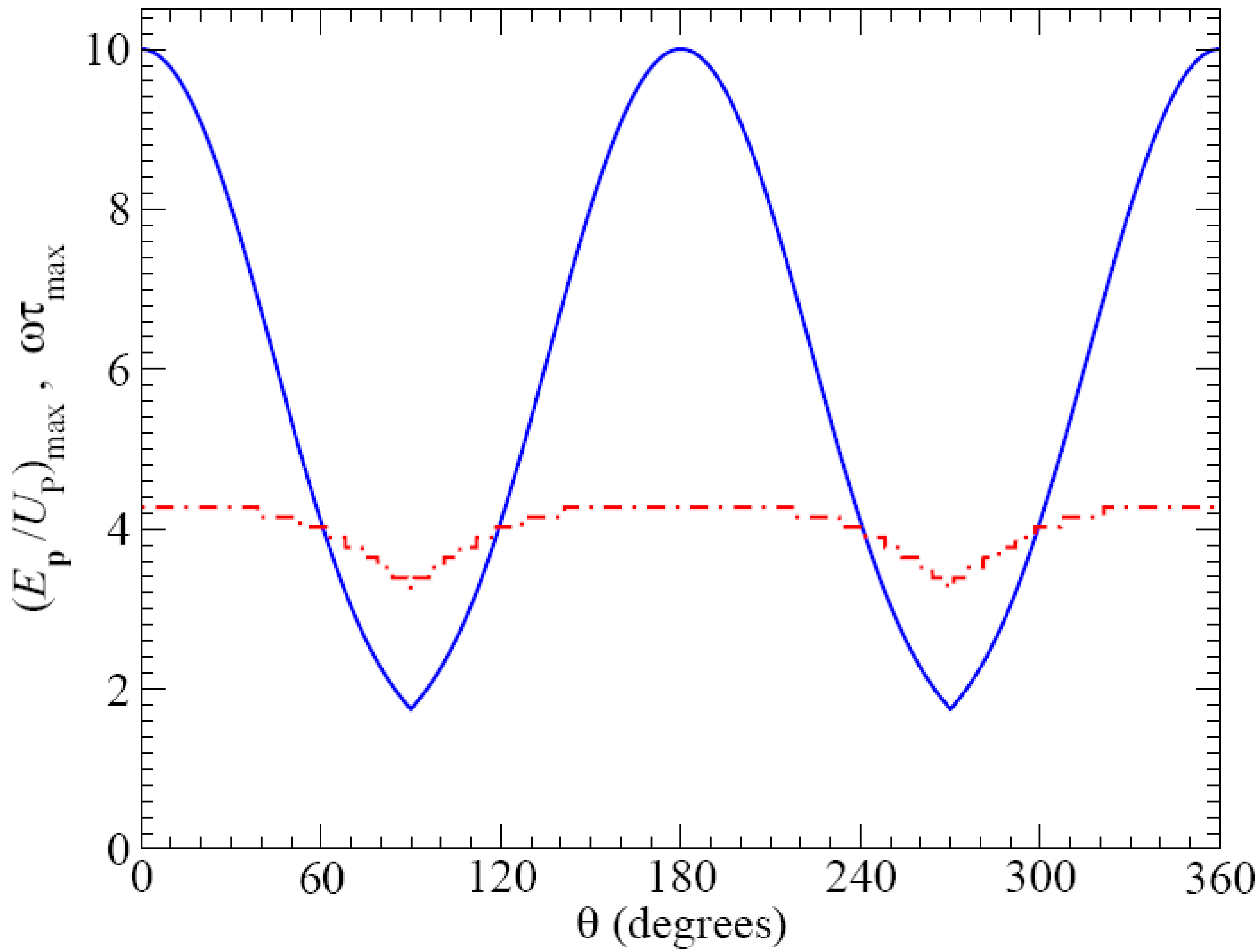

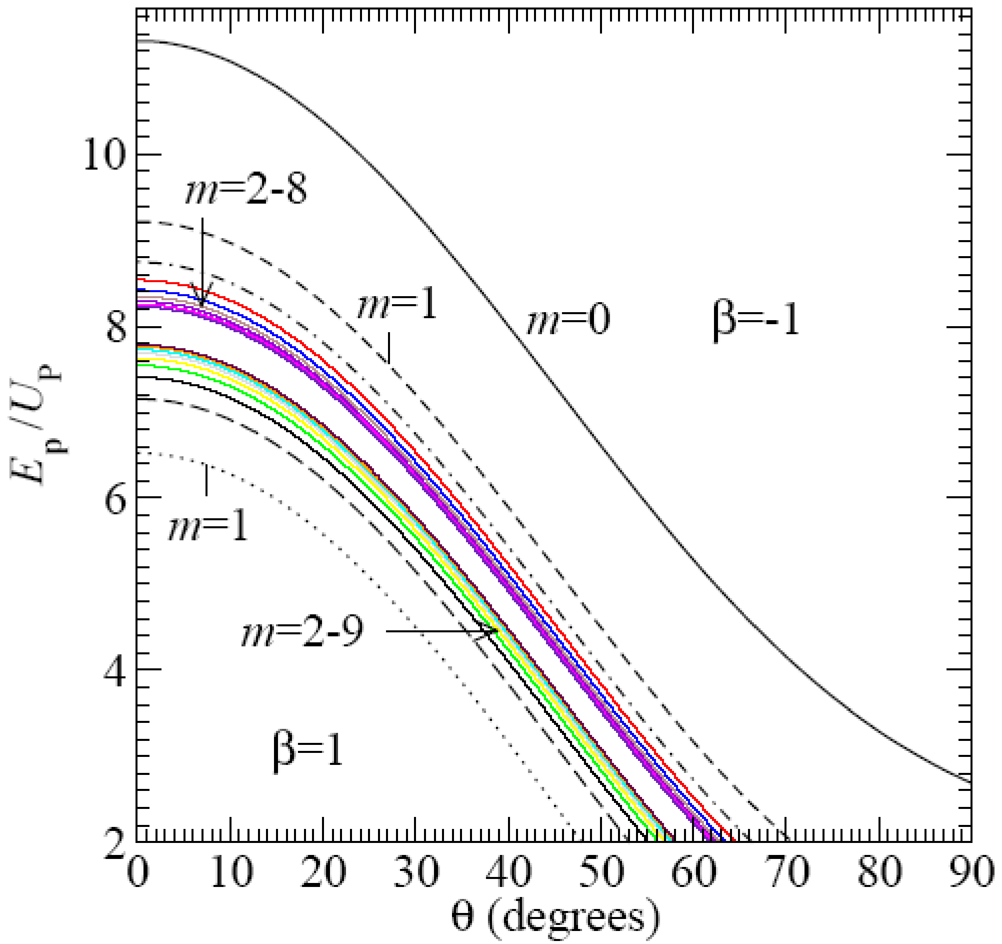

• Enhancement of HATI at channel closings

Gaussian focal averaging

Kopold et al, J. Phys. B 35, 217 (2002)

$$\left\langle w_{\vec{p}i} \right\rangle \propto \int_0^{I_{\max}} \frac{dI}{I} \left(\ln \frac{I_{\max}}{I} \right)^{1/2} \sum_n w_{\vec{p}i}(n) \delta\left(E_{\vec{p}} + I_p + U_p - n\omega \right)$$

Improved algorithm which includes saturation effects – important for new Br^- ATD experiments

$$\left\langle w_{\vec{p}lm} \right\rangle \propto \sum_n \int_0^{\infty} d\rho\rho \int_{-\infty}^{\infty} dt \delta\left(E_{\vec{p}} + I_p + \frac{I(\rho,t)}{4\omega^2} - n\omega \right)$$

$$\times w_{\vec{p}lm}\left(n; I(\rho,t)\right) \exp\left(-\int_{-\infty}^{t} dt' w_{lm}\left(I(\rho,t')\right) \right)$$

No averaging

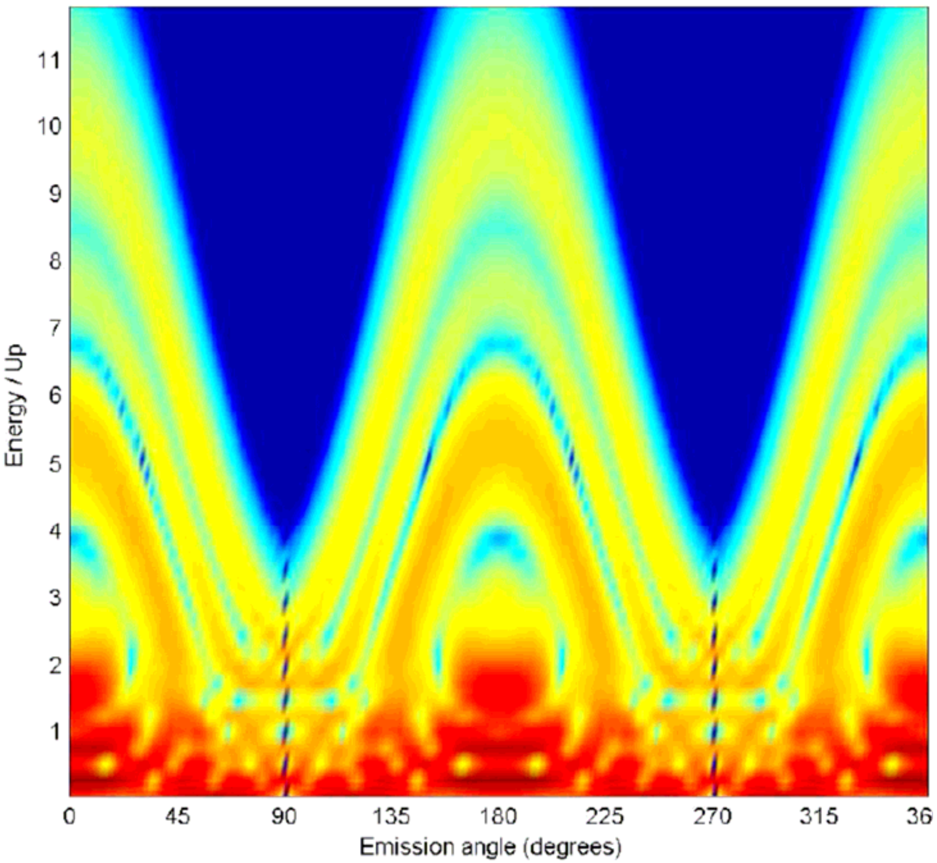

Focal averaging

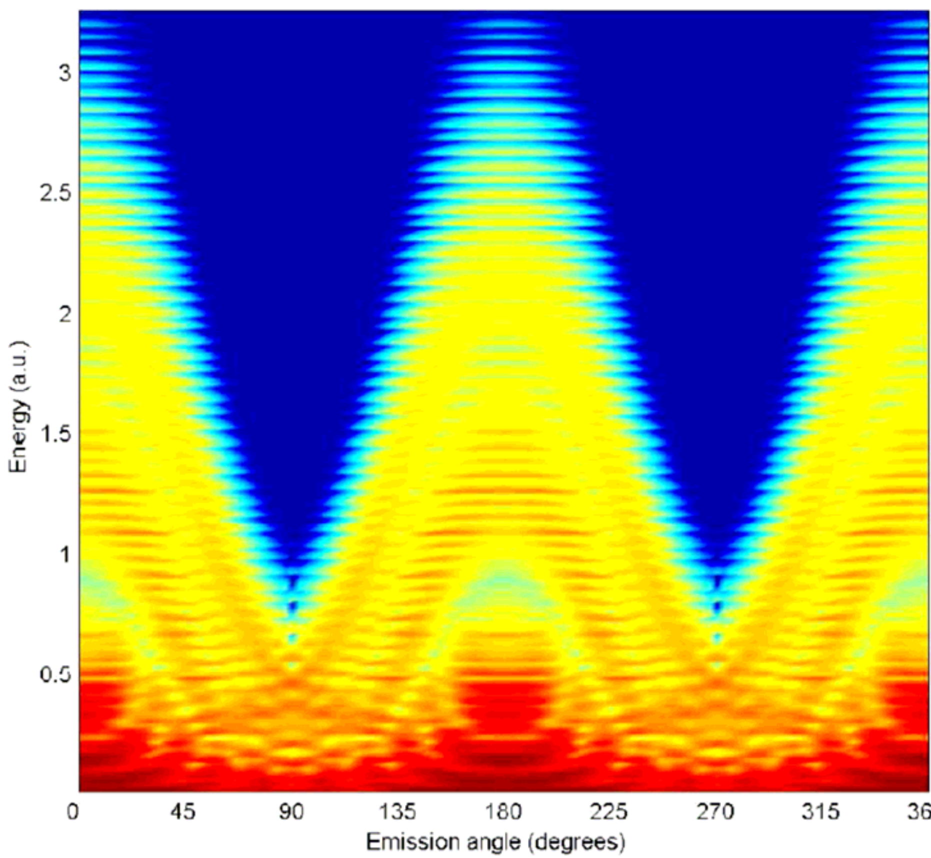

$$E_{\vec{p}} = n\omega - I_p - \frac{I}{4\omega^2}$$

$$n_c\omega = I_p + U_p \qquad E_{\vec{p}} = (n - n_c)\omega$$

n_c-photon channel is closed

- Resonant-like enhancement at particular I
- Channel-closing effect in HATI
- Near channel closing E_p is low
- Many QO interfere constructively
- All intensities from $I=0$ to $I=I_{\max}$ contribute to the focal-averaged electron yield
- Channel-closing intensities are:

$$I_c = (n_c\omega - I_p)4\omega^2$$

$$n_c = n_{c,\min}, n_{c,\min} + 1, \ldots, n_{c,\max}$$

$$n_{c,\min} = [I_p/\omega] + 1, \quad I_{c,\max} \le I_{\max}$$

$n_{c,\max} - n_{c,\min} + 1$ enhancement regions – a series of rounded tops in the envelope of the electron spectra

Intensity-dependent enhancements

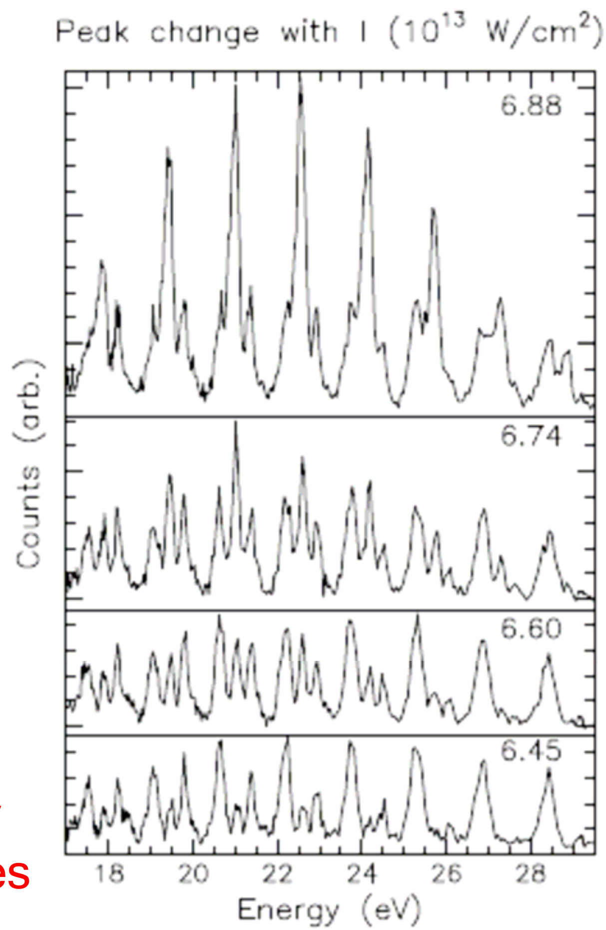

intensity increases by 6%

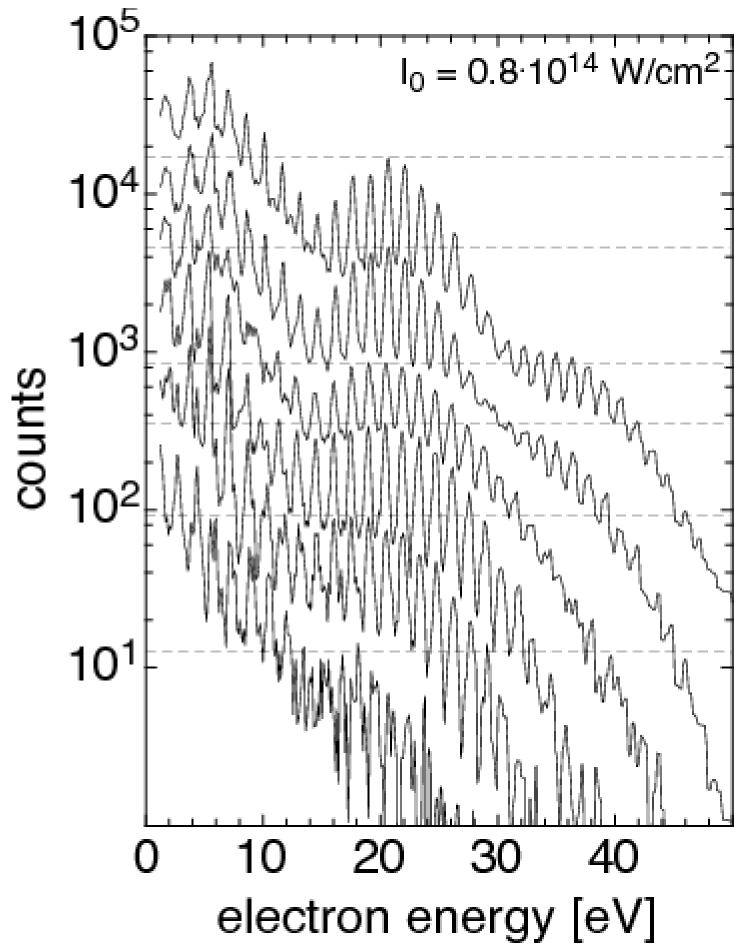

Hertlein, Bucksbaum, Muller, JPB 30, L197 (1997)

Paulus et al., PRA 64, 021401 (2001)

see, also, Hansch, Walker, van Woerkom, PRA 55, R2535 (1997)

Physical origin of the enhancements

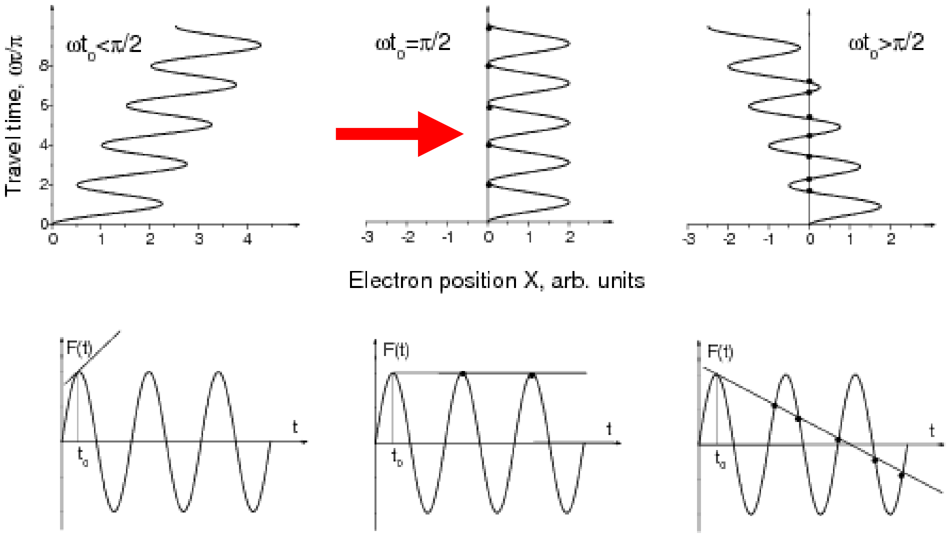

For zero drift momentum, p = 0, the electron revisits infinitely often

$$p^2/(2m) = N\omega - I_p - U_p = 0$$

$$I_p + U_p = N\omega$$

„Channel Closing“

Constructive interference of long quantum orbits

Quantum effect!!!

Analytical proof:

S.V. Popruzhenko, P.A. Korneev, S.P. Goreslavskii, WB, PRL 89, 023001 (2002)

D.B. Milosevic, WB, PRA 66, 063417 (2002)

Alternative explanations of the intensity-dependent enhancements

Threshold cusps a la Wigner/Baz:

B. Borca, M.V. Frolov, N.L. Manakov, A.F. Starace, PRL 88, 193001 (2002)

Multiphoton resonance with ponderomotively upshifted Rydberg state:

H.G. Muller, F.C. Kooiman, PRL 81, 1207 (1998)
H.G. Muller, PRL 83, 3158 (1999)
J. Wassaf, V. Veniard, R. Taieb, A. Maquet, PRL 90, 013003 (2003)

Enhancements disappear for short pulses

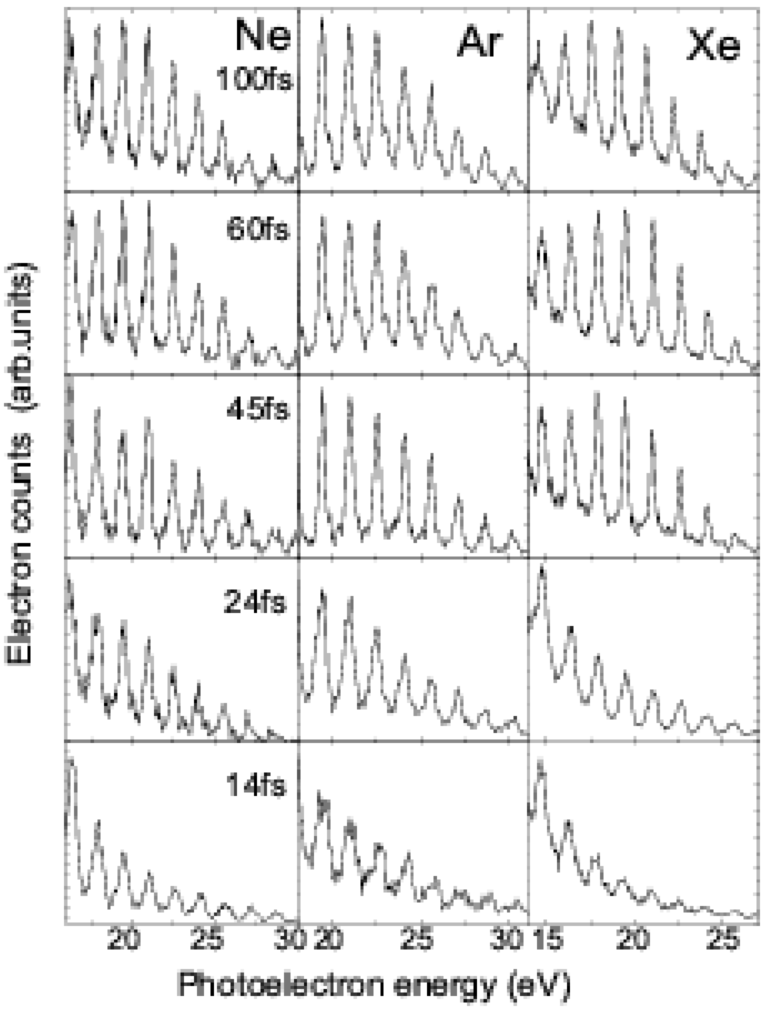

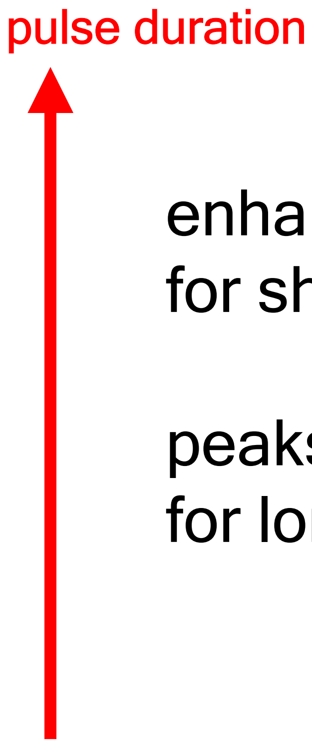

enhancements disappear for short pulses

peaks become narrower for long pulses

Focal-averaged angular-resolved ATI energy spectrum

xenon, 760 nm, 8 x 10^{13} Wcm^{-2}

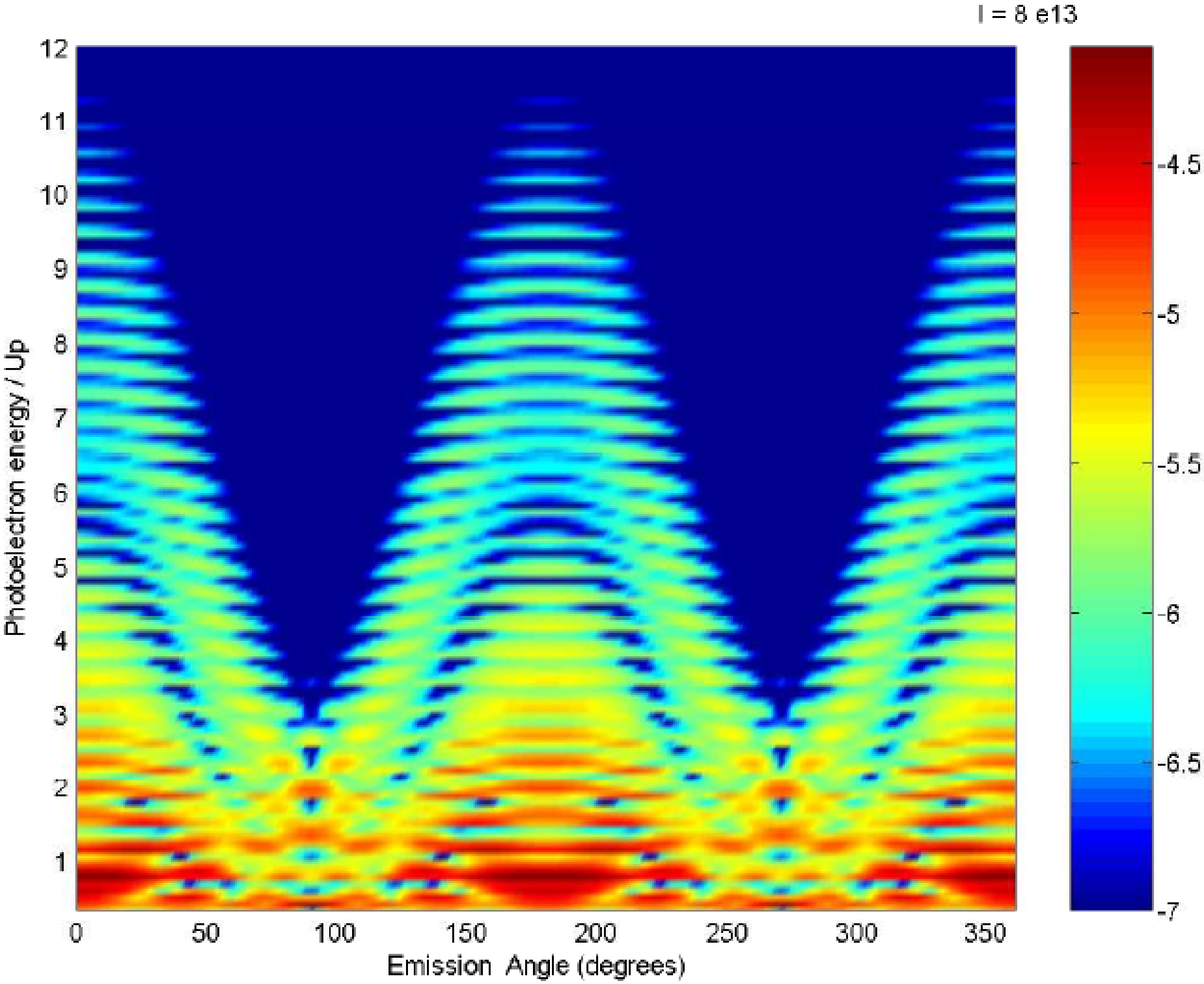

contains the effects of

channel closings (several)

cutoff (rainbow) enhancements

con-/destructive interferences of pairs of quantum orbits and/or the two members of each pair

Even (odd) CC vs. s (p) ground states

Manakov and Frolov, JETP Lett. **83**, 536 (2006)

Krajewska, Fabrikant, and Starace, Phys. Rev. A (submitted)

DBM *etal* (in preparation)

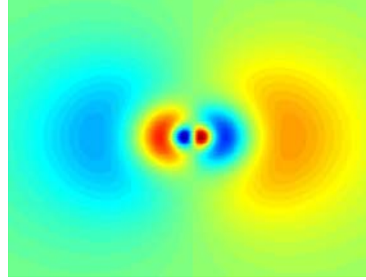

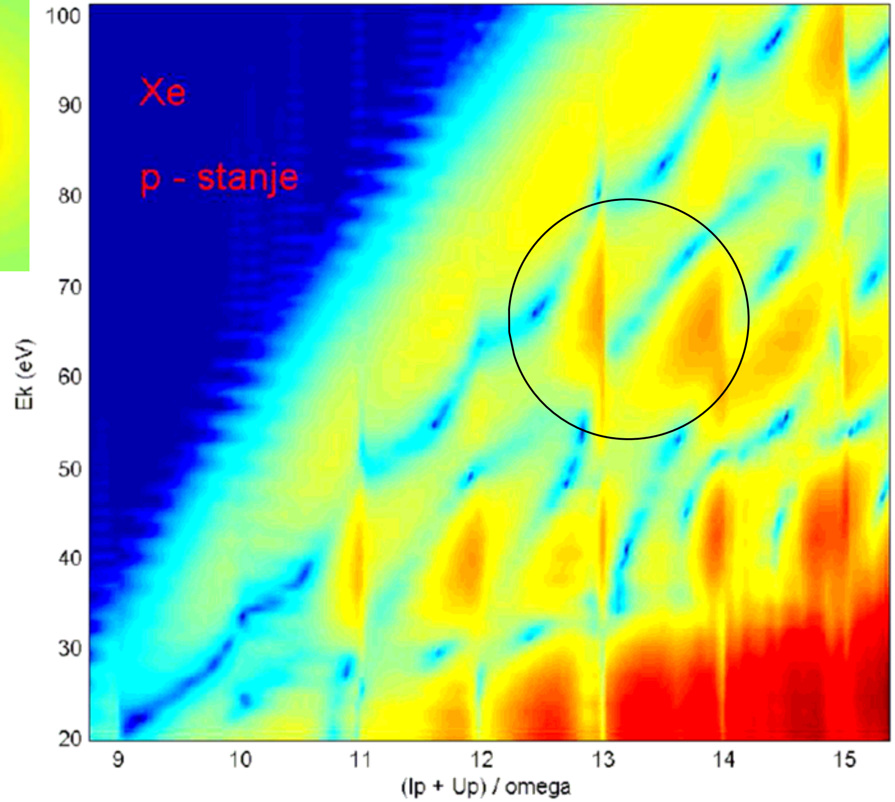
Xe
p - stanje
Ek (eV)
100
90
80
70
60
50
40
30
20
9
10
11
12
13
14
15
(Ip + Up) / omega

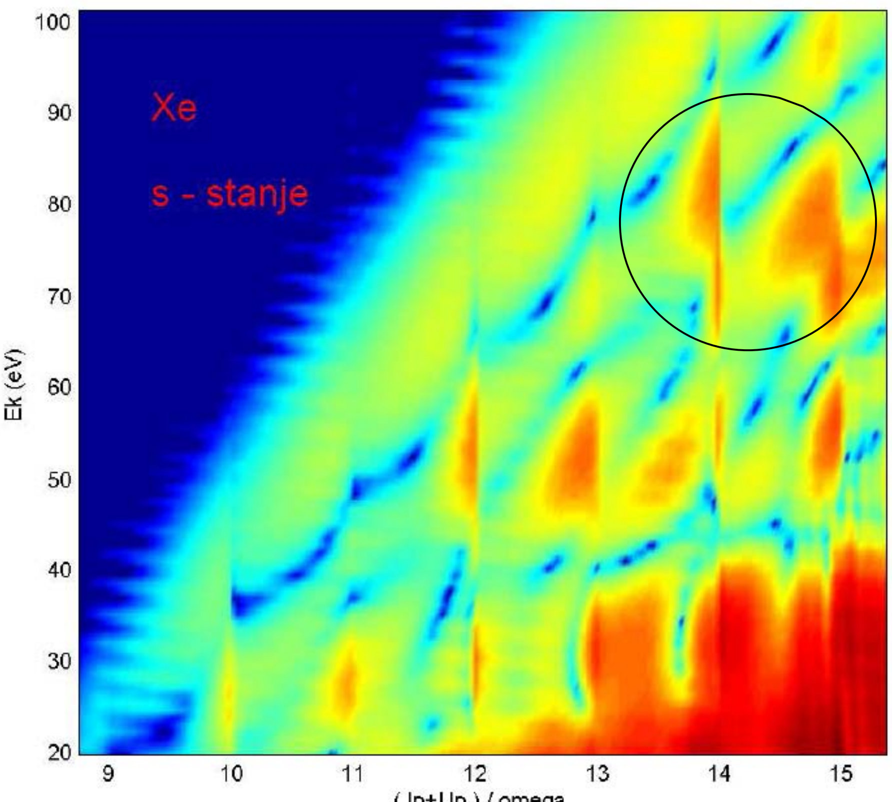
Xe
s - stanje
Ek (eV)
100
90
80
70
60
50
40
30
20
9
10
11
12
13
14
15
(Ip+Up) / omega

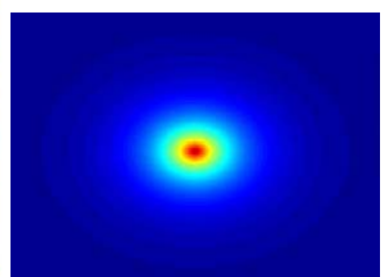

Conclusions

- Realistic choices of the initial wave function and the rescattering potential (improved SFA)
- Plateau height: direct vs. rescattering
  He (6 orders), Xe, Kr (1-2 orders)
- Plateau length:
  Direct: s-state (2-3 U_p), p-state (4 U_p => interf.)
  Rescattering: $E_{\vec{p}\max} = 10.007U_p + 0.538I_p$
- Quantum orbits $\alpha\beta m$, θ – dependent cutoff
- Focal averaging and saturation
- Qualitative change due to channel closing eff.
- CC – pronounced enhancement
- Agreement with experimental results

Ionization of a diatomic molecule by a strong laser field

$$H_{\text{tot}} = \frac{\vec{P}_A^2}{2M_A} + \frac{\vec{P}_B^2}{2M_B} + \frac{\vec{p}_e^2}{2m_e} - \left(e\vec{r}_e + e_A\vec{R}_A + e_B\vec{R}_B\right)\cdot\vec{E}(t) + V\left(\vec{r}_e, \vec{R}_A, \vec{R}_B\right)$$

$$\vec{r}_e, \vec{R}_A, \vec{R}_B \xrightarrow{\text{Jacobi}} \vec{r}, \vec{R}, \vec{R}_{CM} \quad \rightarrow \quad i\partial_t \Phi\left(\vec{r}, \vec{R}, t\right) = H\Phi\left(\vec{r}, \vec{R}, t\right)$$

$$H = \frac{\vec{P}^2}{2\mu} + \frac{\vec{p}^2}{2m} - \left(e_r\vec{r} + e_R\vec{R}\right)\cdot\vec{E}(t) + V\left(\vec{r}, \vec{R}\right)$$

$$V\left(\vec{r}, \vec{R}\right) = V_e^A\left(\vec{r}_A\right) + V_e^B\left(\vec{r}_B\right) + V_{AB}\left(\vec{R}\right)$$

$$S_{fi} = \delta\left(\vec{P}_f^{\text{CM}} - \vec{P}_i^{\text{CM}}\right)\lim_{t\to\infty}\lim_{t'\to-\infty} M_{fi}\left(t, t'\right)$$

$$M_{fi}(t,t') = i\int_{t'}^{t} d\tau \int d^3\vec{r} \int d^3\vec{R}\,\Phi_f^*\left(\vec{r},\vec{R},t\right) \int d^3\vec{r}' \int d^3\vec{R}' \left\langle \vec{r},\vec{R} \middle| U(t,\tau) \middle| \vec{r}',\vec{R}' \right\rangle$$

$$\times \left(e_r\vec{r}' + e_R\vec{R}'\right)\cdot\vec{E}(\tau)\,\Phi_i\left(\vec{r}',\vec{R}',\tau\right)$$

Neglect e-a int: $H \to H_F = h_e^F + H_{AB}^F$

$$h_e^F = \frac{\vec{p}^{\,2}}{2m} - e_r\vec{r}\cdot\vec{E}(t), \quad H_{AB}^F = \frac{\vec{P}^2}{2\mu} - e_R\vec{R}\cdot\vec{E}(t) + V_{AB}\left(\vec{R}\right)$$

SFA: $\Phi_f^* U \to \Phi_f^*\left(\vec{r},\vec{R},t\right) = \phi_{e\vec{p}_f}^*\left(\vec{r},t\right)\varphi_{AB\nu_f}^*\left(\vec{R}\right)e^{iE_{AB\nu_f}t}$

BOA: $\Phi_i\left(\vec{r},\vec{R},t\right) = \phi_{ei}\left(\vec{r};\vec{R}\right)\varphi_{AB\nu_i}\left(\vec{R}\right)e^{i\left(E_{ei}\left(\vec{R}\right)+E_{AB\nu_i}\right)t}$

MO-LCAO: $\phi_{ei}\left(\vec{r};\vec{R}\right) = \sum_{J=A,B}\sum_a c_{Ja}\psi_a^{(0)}\left(\vec{r}_J\right)$

HFR-STO: $\psi_a^{(0)}\left(\vec{r}_J\right) = \dfrac{\left(2\varsigma_a\right)^{n_a+1/2}}{\sqrt{\left(2n_a\right)!}}\, r^{n_a-1}e^{-\varsigma_a r}Y_{l_a m_a}(\theta,\varphi)$

$$S_{fi} = -2\pi i\delta\left(\vec{P}_f^{\mathrm{CM}} - \vec{P}_i^{\mathrm{CM}}\right) S_{v_f v_i} \sum_n \delta\left(\vec{p}_f^{\,2}/2 + E_{ABv_f} - E_{ABv_f} - E_{ei}\left(\vec{R}_0\right) + U_p - n\omega\right) T_{fi}(n)$$

(i) for the length-gauge standard molecular SFA:

$$\mathcal{F}_{\mathrm{fi}}^{\mathrm{SL}}(t) = \sum_{sa} c_{sa} e^{is[\mathbf{p}_\mathrm{f}+\mathbf{A}(t)]\cdot\mathbf{R}_0/2} \times\Big[\langle \mathbf{p}_\mathrm{f} + \mathbf{A}(t)|\mathbf{E}(t)\cdot\mathbf{r}|\psi_a^{(0)}\rangle - \frac{s}{2}\mathbf{E}(t)\cdot\mathbf{R}_0\psi_a^{(0)}(\mathbf{p}_\mathrm{f}+\mathbf{A}(t))\Big],$$

(ii) for the dressed modified molecular SFA:

$$\mathcal{F}_{\mathrm{fi}}^{\mathrm{dML}}(t) = \sum_{sa} c_{sa} e^{is\mathbf{p}_\mathrm{f}\cdot\mathbf{R}_0/2} \times\langle \mathbf{p}_\mathrm{f} + \mathbf{A}(t)|\mathbf{E}(t)\cdot\mathbf{r}|\psi_a^{(0)}\rangle,$$

(iii) for the undressed modified molecular SFA:

$$\mathcal{F}_{\mathrm{fi}}^{\mathrm{uML}}(t) = \sum_{sa} c_{sa} e^{is[\mathbf{p}_\mathrm{f}+\mathbf{A}(t)]\cdot\mathbf{R}_0/2} \times\langle \mathbf{p}_\mathrm{f} + \mathbf{A}(t)|\mathbf{E}(t)\cdot\mathbf{r}|\psi_a^{(0)}\rangle,$$

(iv) for the velocity-gauge standard molecular SFA:

$$\mathcal{F}_{\mathrm{fi}}^{\mathrm{SV}}(t) = [\mathbf{p}_\mathrm{f} + \mathbf{A}(t)/2]\cdot\mathbf{A}(t) \times\sum_{sa} c_{sa} e^{is\mathbf{p}_\mathrm{f}\cdot\mathbf{R}_0/2}\psi_a^{(0)}(\mathbf{p}_\mathrm{f}).$$

$3\sigma_g$ HOMO of N_2

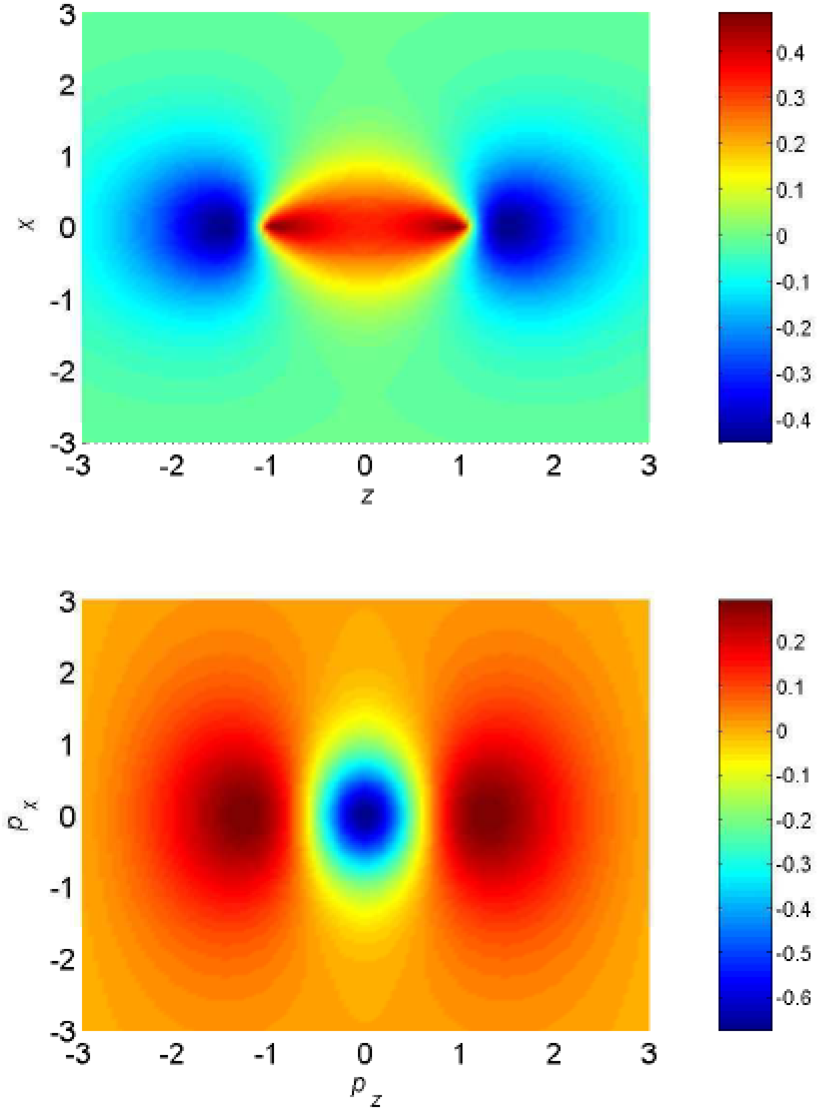

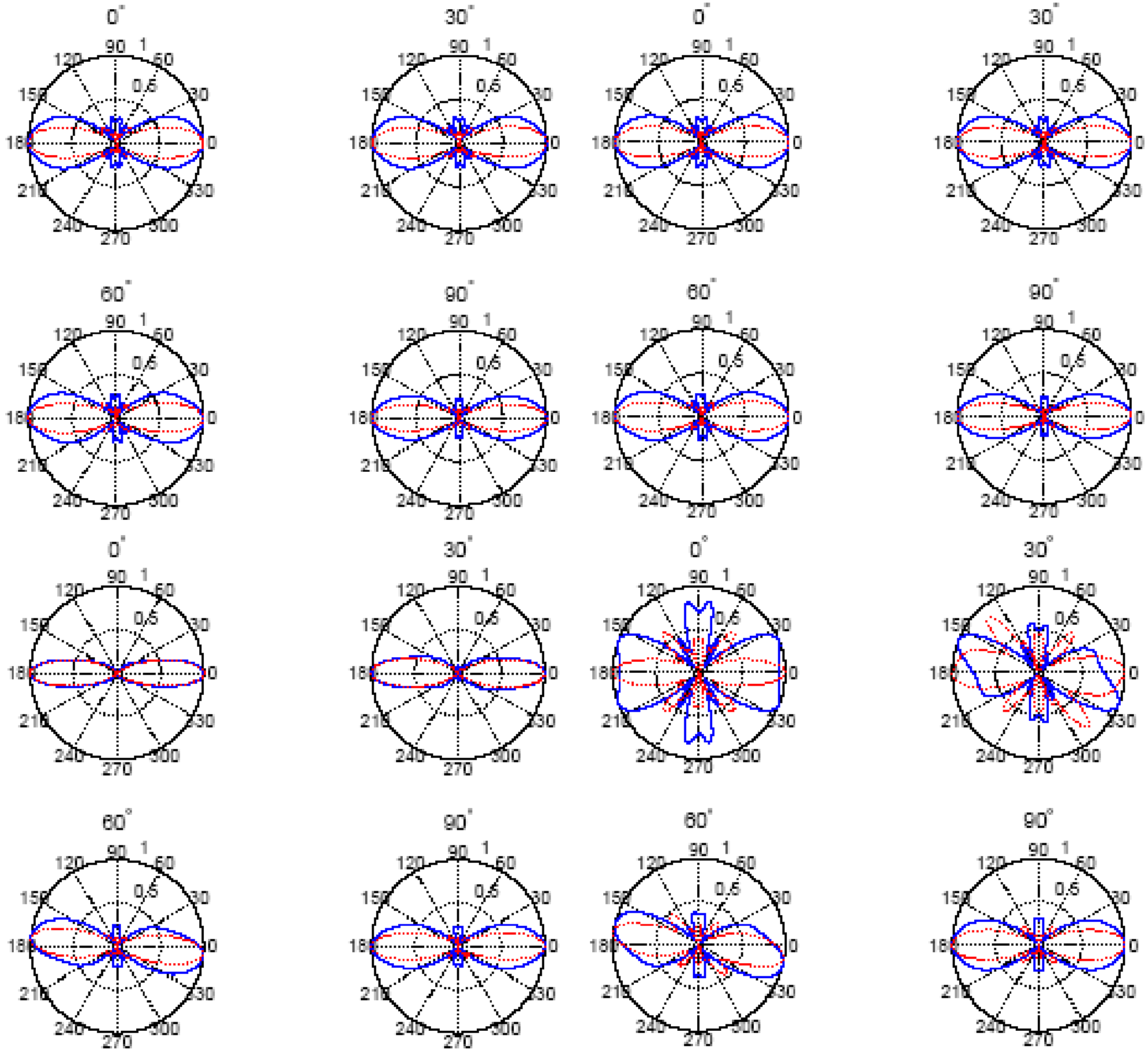

FIG. 6: Differential ionization rates of N_2 for different orientations of the molecular axis with respect to the polarization vector of the laser field (the value of the corresponding angle is denoted above each subpanel), and for two values of the laser field intensity: 10^{14} W/cm^2 (solid blue lines) and 2×10^{14} W/cm^2 (dotted red lines). The laser field is linearly polarized having the wavelength 800 nm. The results are obtained using: the standard molecular SFA in the length gauge, Eq. (51) (upper left panel); the modified molecular SFA with the undressed initial state, Eq. (53) (upper right panel); the modified molecular SFA with the dressed initial state, Eq. (52) (lower left panel); the standard velocity gauge molecular SFA, Eq. (54) (lower right panel).

$1\pi_g$ HOMO of O_2

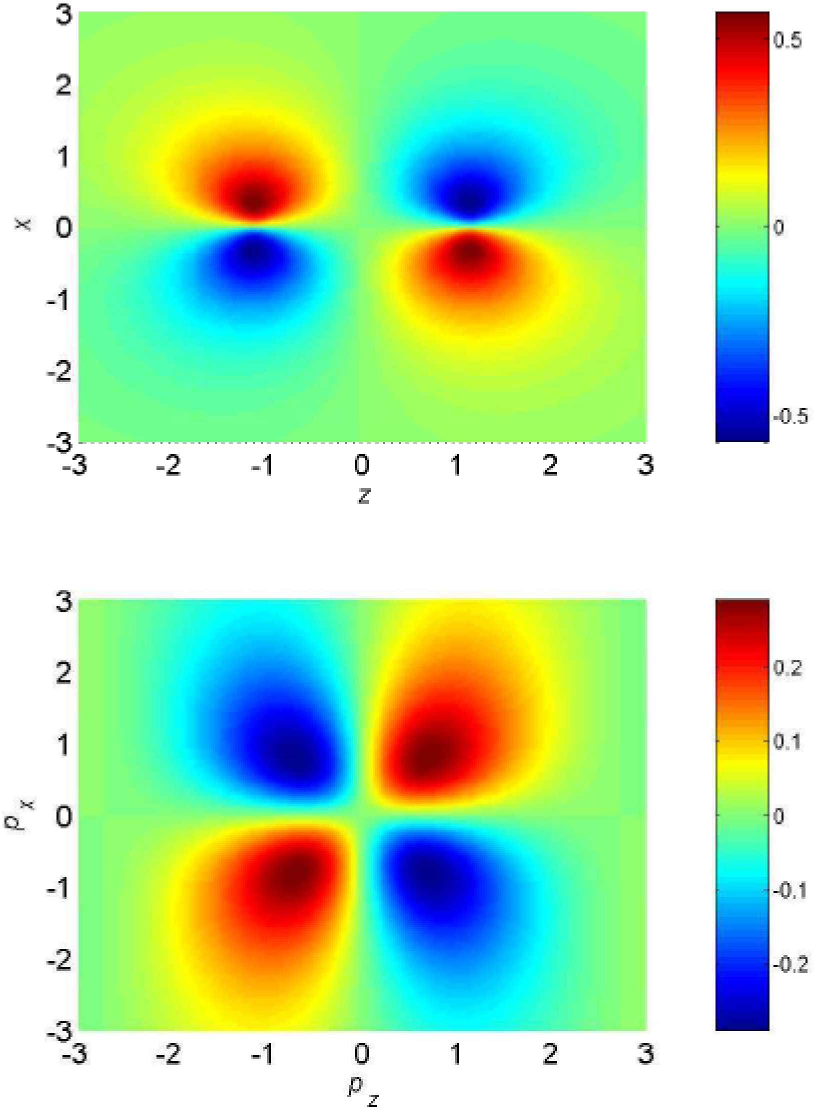

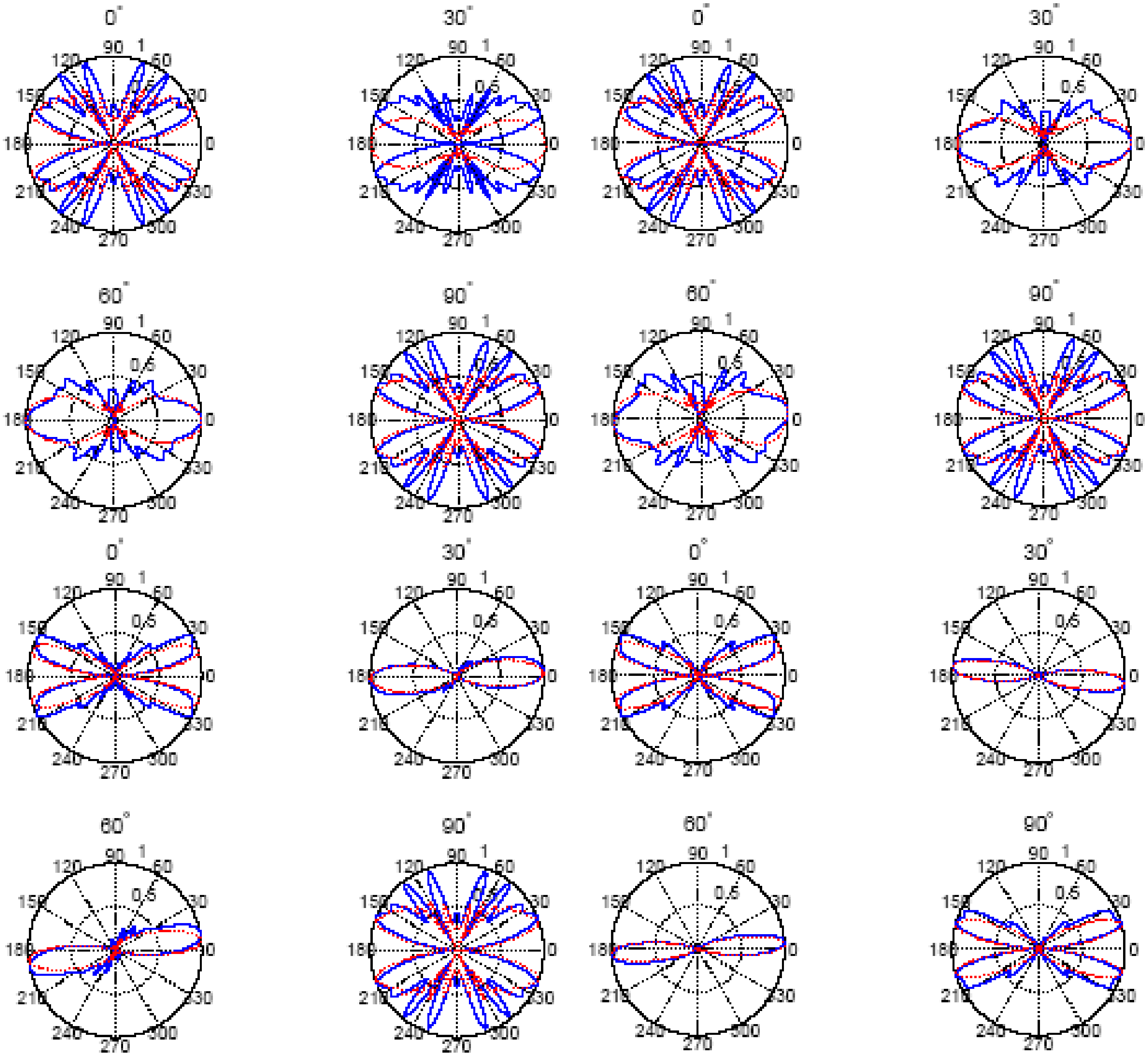

FIG. 7: Differential ionization rates of O_2 presented similarly as in Fig. 6 for the same laser parameters.

Imaging electron molecular orbitals via ionization by intense femtosecond pulses

G. Lagmago Kamta and A.D. Bandrauk

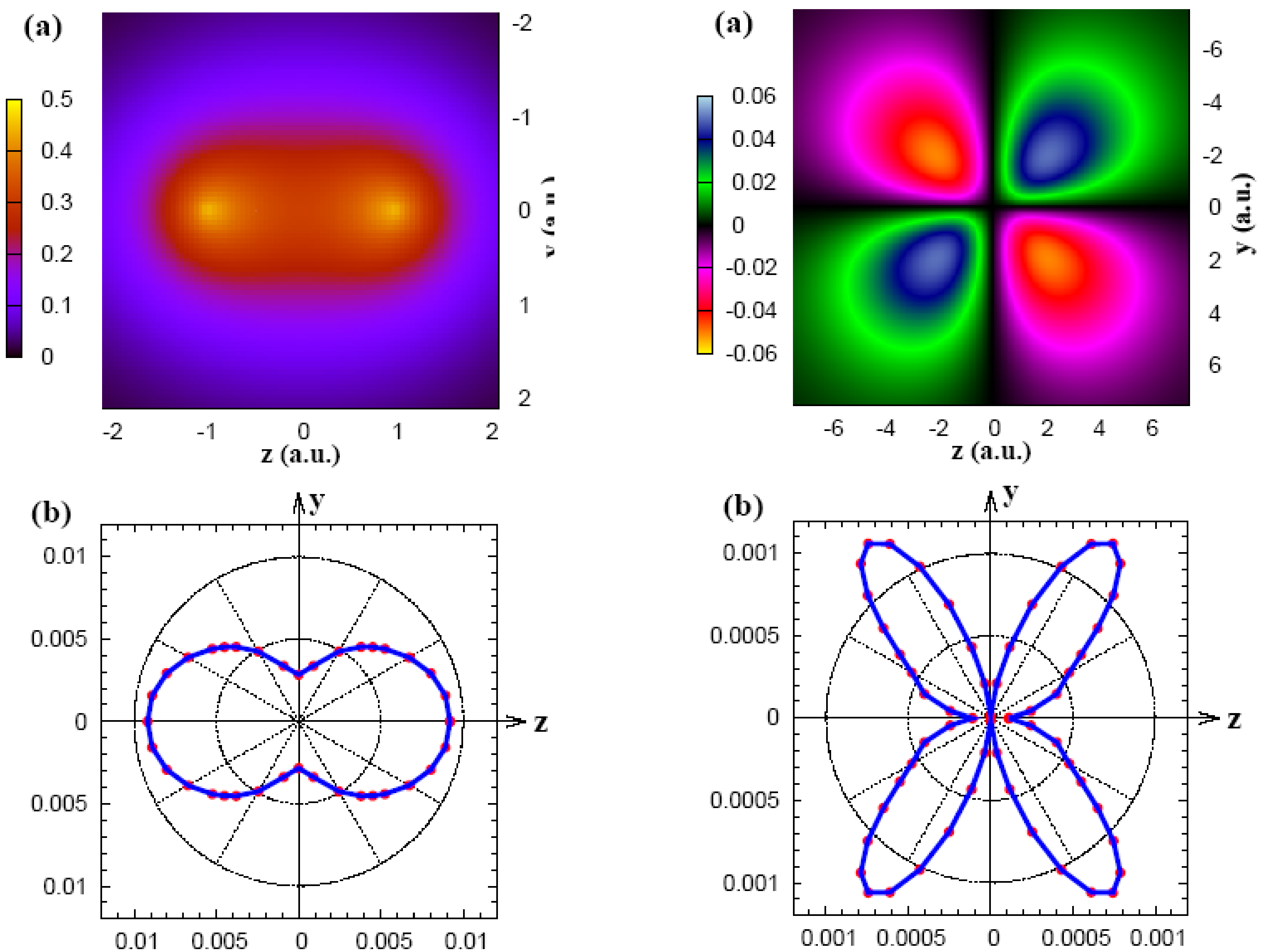

N_2

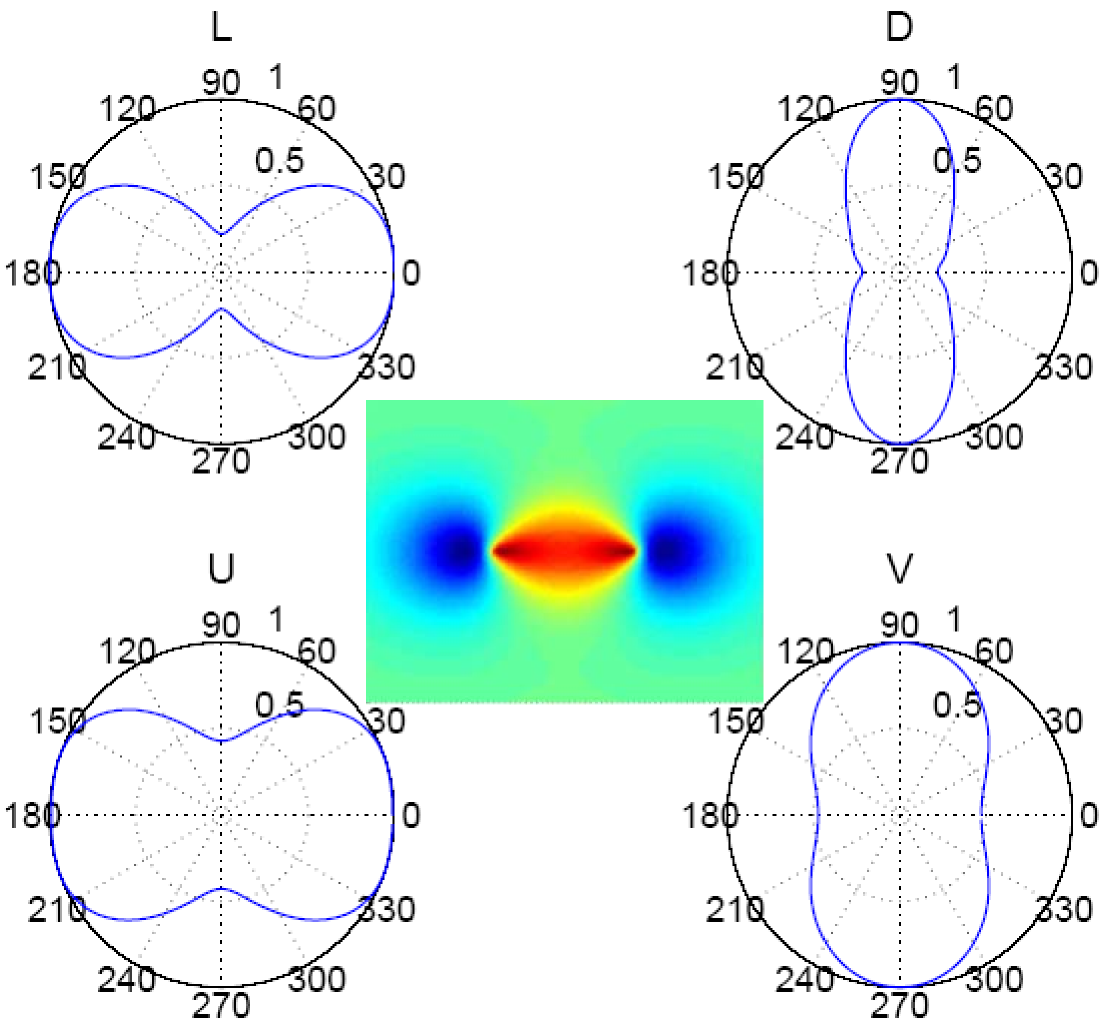

O_2

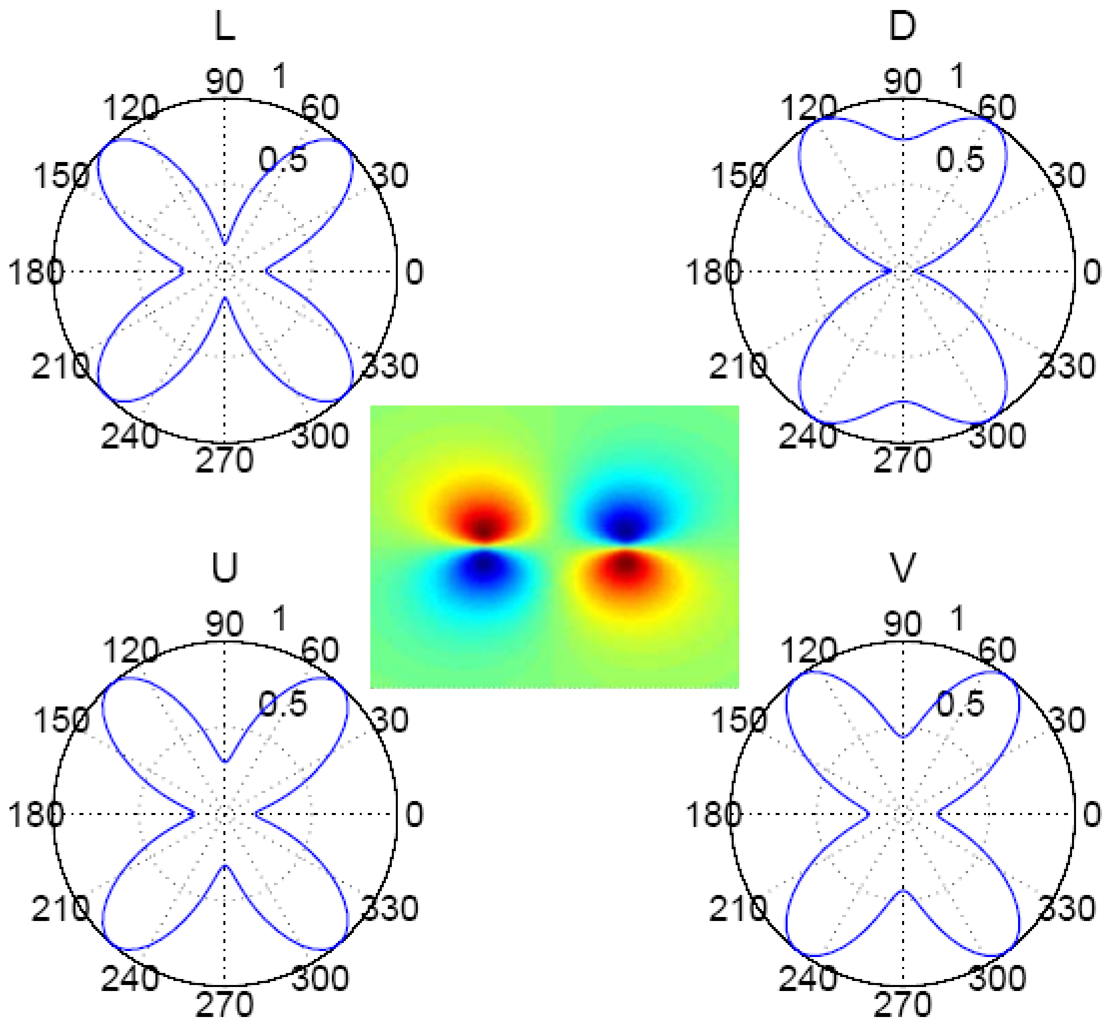

$1\pi_g$ HOMO of F_2 | $3\sigma_g$ HOMO of F_2